Department of Earth & Ocean Sciences
The University of Liverpool

THE BIOGEOCHEMISTRY OF NITROGEN IN THE ATLANTIC OCEAN

Thesis submitted in accordance with the requirements of the University of Liverpool for the degree of Doctor of Philosophy

By
Sarah Reynolds

July 2007

ABSTRACT

The biogeochemistry of nitrogen in the Atlantic Ocean

Sarah Reynolds

Nitrogen plays a fundamental role in limiting the primary productivity of the world's oceans. The Atlantic Ocean is characterised by N-starved oligotrophic gyres to the north and south of the equator, which arise from wind induced Ekman flux of surface waters over the subtropics, subsequent downwelling and the production of a depressed, thicker thermocline. Discrepancies exist between the traditional supplies of N to and the export production from the surface waters of the oligotrophic gyres.

This thesis focuses on the importance of N_2 fixation and the potential role that organic nitrogen has on fuelling export production in the Atlantic Ocean by examining the biogeochemistry of organic nitrogen. The study formed part of the Atlantic Meridional Transect (AMT) programme and involved three northbound cruises between the Falkland Islands or Cape Town and the U.K., where organic nitrogen was sampled from the euphotic zone of the various biogeochemical regimes of the Atlantic.

The spatial extent of N_2 fixation was assessed through the use of stable nitrogen isotope analysis of suspended particulate organic nitrogen (PON_{susp}). Consistently depleted signals (with respect to ^{15}N) extend over the centre of the northern subtropical gyre; this partly coincides with a region where the tracer N* increases westward following the gyre circulation. The non-conservative behaviour of N* implies that N_2 fixation is responsible for the depleted $\delta^{15}N$ PON_{susp}. A mixing model suggests that N_2 fixation over parts of the northern gyre provides up to 74% of the N utilised by phytoplankton. However, since the PON_{susp} represents only a small fraction of total N, N_2 fixation probably plays a minor role in supplying new N to the photic zone of the northern subtropical gyre.

The dynamics of organic nitrogen were investigated through the identification and quantification of dissolved free and hydrolysable, and particulate amino acids. Concentrations along AMT varied with biogeochemical regime; amino acids were depleted in the centres of both the northern and southern oligotrophic gyres and elevated in the higher productivity regions around the equator and temperate zones. The application of the *Dauwe and Middleburg* [1998] degradation index demonstrated that the 'age' of organic matter also varied, in that more degraded material was found in the gyres compared with the equator and temperate regions. These findings suggest that organic nitrogen can provide a source of N to primary producers.

Examination of the enantiomeric ratios of chiral amino acids revealed that bacteria make a minor contribution to dissolved organic nitrogen in the open ocean, contradicting previous claims of bacterial contributions of 45-80%. Bacteria make a more substantial contribution of the particulate organic nitrogen. Surprisingly, archaea dominated the particulate pool, which is consistent studies revealing they are the dominant prokaryote in the world's oceans.

ACKNOWLEDGEMENTS

This project was a challenging yet enjoyable experience. There are a number of people that I am indebted to, who with their help and encouragement have driven me forward enabling me to complete this thesis.

First and foremost I would like to thank my supervisors, Professors George Wolff and Ric Williams. George has been a fantastic supervisor who has provided guidance, encouragement and patience throughout. Ric's enthusiasm and belief in me has been greatly appreciated. I have learnt a great deal from you both.

Dr. Anu Thompson has been not only an invaluable help throughout this project but also a good friend. I also express by gratitude to Mrs. Paula Houghton, who's diligence and patience in organising both practical and academic activities has been outstanding. Thanks also extend to Mrs. Carmel Pinnington for assistance in the laboratory, and Dr. Kostas Kiriakoulakis for advice and useful discussions.

This project would not have been possible without the efficiency and excellent management of the Atlantic Meridonal Transect (AMT) programme. A huge thanks go to all the AMT scientists and personnel, in particular to Dr. Carol Robinson for excellent leadership and Dawn Ashby; a great project manager. I would also like to thank all the Masters, officers and crew of the RRS James Clark Ross, RRS Discovery and RV Celtic Explorer and the UKORS staff.

I am grateful to Dr. Martin White and Professor John Patching at the National University of Ireland, Galway, for providing me with the opportunity to participate on the October Survey, 2004 (RV Celtic Explorer). Thanks also to Dr. Richard Sanders of the National Oceanography Centre (NOC) for enabling me to use facilities for organic nutrient analysis and arranging desk space for me at NOC during my write up. Dr. Claudia Castellani at the British Oceanographic Data Centre has been valuable in providing almost instant access to other AMT data. With regards to use of data thanks goes to Dr's Alex Poulton and Xi Pan.

I would like to send out the biggest thank you to all my friends who have had to endure this rollercoaster of a ride with me...sorry! There are far too many to thank individually but most of all I would like to thank Rachel Sharp, Corallie Hunt and Rhiannon Mather. You have been brilliant. You have always believed in me and given me constant encouragement and support.

Thanks to my family, especially my brother Owen, my Nanna and my Na. Most of all my deepest gratitude goes to my parents to whom this thesis is dedicated. You have driven and inspired me throughout my life. You have shown love, support and enthusiasm, which without I would not be where I am today.

And finally to Edward. If it was not for this project we never would have encountered one another on the RRS Discovery and to that I owe a lot to the AMT programme! Over the past two years you have been my rock...thank you.

I certify that the work described in this thesis is my own, except where otherwise stated, and has not been previously submitted for a degree at this or any other university.

CHAPTER 1

CHAPTER 2

CHAPTER 3

CHAPTER 5

LIST OF FIGURES

List of Tables

CHAPTER 1

The marine nitrogen cycle and its present understanding in the biogeochemical dynamics of the Atlantic Ocean

1.1 Introduction

Nitrogen is a key element in the structures of nucleic and amino acids, porphyrins, and amino sugars [*Brandes, et al.*, 2007] and commonly limits primary production in the marine environment [*Dugdale and Goering*, 1967]. In turn this can control the short-term sequestration of atmospheric carbon dioxide into marine phytoplankton [*Falkowski*, 1997]. Nitrogen, in both inorganic and organic forms, is introduced into the marine environment via rivers, wet and dry atmospheric deposition, and biological molecular dinitrogen (N_2) fixation. The chemistry and biochemistry of nitrogen in the world's oceans are complex; in recent years, substantial discoveries have changed our perspectives of our simplified conventional

view. These new insights into the marine nitrogen cycle will be the focus of this chapter, as will the implications for the biogeochemistry of the Atlantic Ocean.

1.2 Marine nitrogen chemistry

The marine chemistry of nitrogen is largely controlled by redox reactions [*Libes*, 1992] where multiple transformations of nitrogenous compounds are catalysed primarily by microbes [*Zehr and Ward*, 2002]. This ability of marine organisms to transform the redox state of N leads to the direct removal or addition of N to the oceanic pool [*Hulth, et al.*, 2005]. Nitrogen is present in the marine environment in many oxidation states (Table 1.01) with N_2 being the most abundant. The inorganic species, nitrate (NO_3^-), nitrite (NO_2^-) and ammonium (NH_4^+), are referred to as dissolved inorganic nitrogen (DIN) [*Libes*, 1992], whilst the organic N is a far more complex mixture of compounds existing in both particulate and dissolved forms.

Species	Molecular Formula	Oxidation state of N	Size of reservoir (10^{15} g N)	% of total pool
Nitrate ion	NO_3^-	+ V	570	2.5
Nitrite ion	NO_2^-	+ III	0.5	0.002
Nitric oxide	NO	+ II	-	-
Nitrous oxide	N_20	+ I	0.2	0.0009
Dinitrogen	N_2	0	22 000	95.2
Ammonia	NH_3	- III	-	-
Ammonium	NH_4^+	- III	7	0.03
Organic N				
Plant biomass	$R\text{-}NH_2$	- III	0.30	0.001
Animal biomass	$R\text{-}NH_2$	- III	0.17	0.0007
Microbial biomass	$R\text{-}NH_2$	- III	0.02	0.00006
Dissolved organic matter	$R\text{-}NH_2$	- III	530	2.3
Particulate organic matter	$R\text{-}NH_2$	- III	3-240	0.01-0.1

Table 1.01 Oxidation states of the species of N found in the marine environment with corresponding size of reservoir where known (adapted and modified from *Libes* [1992]).

1.2.1 Assimilation of nitrogen

Marine microorganisms absorb DIN species through their cell membrane where NO_3^- is subsequently assimilated after reduction to NO_2^- (assimilatory nitrate reductase) and then to NH_4^+ (assimilatory nitrite reductase) (Fig 1.01; pathway 1) [*Zehr and Ward*, 2002]. These anabolic reactions provide the necessary N required for the formation of metabolites such as proteins [*Libes*, 1992]. The majority of primary producers preferentially take up NH_4^+ over NO_3^-, since less energy is expended during the assimilation of ammonium. However, the utilisation of NO_3^- rather than NH_4^+ has little effect on the organism's growth rate [*Thompson, et al.*, 1989]. Until recently, it was assumed that all primary producers could grow on nitrate or ammonium. However, the unicellular cyanobacteria *Prochlorococcus* spp., major primary producers of the surface ocean, do not have the ability to grow on nitrate alone and thus require NH_4^+ or urea as a source of nutrient [*Moore, et al.*,

2002]. The discovery of the ability of bacteria to utilise DIN species [*Kirchman*, 1994] as well as the established role they take in the recycling of organic matter (see section 1.2.2 for further details) [*Azam, et al.*, 1983] further highlights the complexity of the marine N cycle.

1.2.2 Remineralisation and ammonification

The term remineralisation strictly refers to the decomposition of particulate organic nitrogen (PON) and dissolved organic nitrogen (DON) to DIN (Fig 1.01; pathway 2) [*Libes*, 1992]. PON is mainly living or dead phytoplankton biomass, detritus and faecal pellets, where as DON is released either through cell lysis, or heterotrophic consumption of PON with exudation of DON. Sloppy feeding can also result in the release of DON from PON [*Fuhrman*, 1987a]. Through the process of ammonification the N is released from the DON by bacteria, where the carbon-nitrogen bonds are broken releasing ammonia (NH_3) which subsequently reacts with hydrogen ions (H^+) or water (H_2O) to form NH_4^+ (Fig 1.01; pathway 3) [*Libes*, 1992]. This form of N is termed 'regenerated N' [*Dugdale and Goering*, 1967].

Whilst the role of bacteria in the breakdown of organic N is important in providing biologically available N to primary producers, it has been revealed that a number of phytoplankton have the ability to utilise the labile DON (i.e. that which readily undergoes change or breakdown) as a N source without bacterial mediation [*Bronk*, 2002; *Flynn and Butler*, 1986; *Palenik and Morel*, 1990a]. These phytoplankton possess cell surface oxidases that can oxidise amino acids and primary amines, releasing extracellular NH_4^+ which is subsequently taken up for growth [*Palenik and Morel*, 1990b].

1.2.3. N_2 fixation

N_2 is the most abundant form of N in the world's oceans but due to the strength of the triple bond (945 kJ mol^{-1}) between the N atoms, this pool is biologically unavailable to the majority of primary producers. However, a diverse set of organisms known as diazotrophs are capable of reducing N_2 to NH_3 (Fig 1.01; pathway 4). Once thought of as rare organisms in the marine environment, N_2 fixation was deemed insignificant in the oceans [*Capone and Carpenter*, 1982; *Lipschultz and Owens*, 1996a]. However, over the past twenty years there has been increasing recognition that N_2 fixation is more important that previously thought. For example, the extensive occurrence of *Trichodesmium* spp., non-heterocystous colonial N_2 fixing cyanobacteria in oligotrophic subtropical waters [e.g. *Capone, et al.*, 2005], and the identification of a major role for unicellular diazotrophs [*Zehr, et al.*, 1998; *Zehr, et al.*, 2001] and heterocyst-forming cyanobacterial symbionts [*Villareal and Carpenter*, 1989] has led to estimates of global oceanic N_2 fixation increasing by an order of magnitude (~100 Tg N yr^{-1} [*Capone, et al.*, 1997; *Gruber and Sarmiento*, 1997; *Mahaffey, et al.*, 2005]; cf. [*Capone and Carpenter*, 1982; *Carpenter and Romans*, 1991]. For further discussion of N_2 fixation see Chapter 3.

1.2.4. Nitrification, denitrification and anammox

Nitrification is the biological oxidation of NH_4^+ to NO_2^- and then subsequently to NO_3^- by the marine bacteria *Nitrosomonas* spp. and *Nitrobacter* spp., respectively (Fig 1.01; pathway 5) [*Libes*, 1992]. Nitrification was once thought to only occur in the deep ocean where NO_3^- concentrations are high, but recent developments have revealed that the majority of water column nitrification occurs in

the lower regions of the euphotic zone [*Zehr and Ward*, 2002]. Since NO_3^- is depleted in the surface ocean, it was assumed that nitrification rates here were negligible however, direct ^{15}N rate measurements have shown that this is not the case [*Dore and Karl*, 1996; *Ward, et al.*, 1989] and that it can sustain 15 – 50% of primary production [*Wankel, et al.*, 2007; *Yool, et al.*, 2007].

Denitrification is a simple anaerobic heterotrophic process whereby NO_3^- is used as a terminal electron acceptor in the oxidation of organic matter after dissolved oxygen is exhausted (Fig 1.01; pathway 6) [*Brandes, et al.*, 2007]. It is often coupled with nitrification across oxic/anoxic interfaces in both sediments and suboxic waters [*Nielsen and Glud*, 1996], leading to the loss of fixed N via mineralisation, oxidation and denitrification to N_2O and N_2 [*Zehr and Ward*, 2002]. During denitrification the enzymes responsible for the reduction of more oxidised forms of N to N_2 are inhibited by the presence of oxygen [*Codispoti, et al.*, 2001]. Thus, denitrification is confined to anoxic/suboxic sediments and waters, such as those found in the Black Sea, Cariaco Basin and the oxygen minimum zones of the Eastern tropical Pacific and Arabian Sea [*Hulth, et al.*, 2005]. This process accounts for a global loss of 175 – 450 Tg fixed N yr^{-1} [*Codispoti, et al.*, 2001; *Gruber and Sarmiento*, 1997] in oxygen depleted regions in the marine environment.

As it is a heterotrophic process, denitrification should be accompanied by the liberation of NH_4^+ [*Brandes, et al.*, 2007], however *Richards* [1965] noticed that NH_4^+ does not accumulate in suboxic waters. It was not until the mid 1990's that an explanation was offered, following the discovery of a new pathway, **ana**erobic a**mm**onium **ox**idation, termed 'anammox' which was first detected in a fluidised bed reactor used in waster water treatment [*Mulder, et al.*, 1995]. NH_4^+ is oxidised to N_2, using NO_2^- as the oxidant [*Vandegraaf, et al.*, 1995], where N_2 is formed through the

pairing of one N atom from both NO_2^- and NH_4^+ (Fig 1.01; pathway 7) [*Thamdrup and Dalsgaard*, 2002] by specialised bacteria that appear to belong to *Planctomycetales* spp. [*Dalsgaard, et al.*, 2005]. This process clearly differs from denitrification which combines N from two NO_3^- molecules to form N_2 [*Arrigo*, 2005]. Anammox has been detected in anoxic continental shelf sediments where it accounted for 24-67% of the total N_2 production [*Thamdrup and Dalsgaard*, 2002]. Anammox also occurs in other environments, such as the anoxic waters of the Black Sea [*Kuypers, et al.*, 2003], the oxygen minimum zone of the Benguala upwelling [*Kuypers, et al.*, 2005] and in polar sea ice [*Rysgaard and Glud*, 2004]. Anammox explains not only the NH_4^+ deficiencies observed in anoxic waters and sediments [*Thamdrup and Dalsgaard*, 2002] but may also be responsible for up to 50% of the global removal of fixed N in oceanic waters [*Dalsgaard, et al.*, 2005].

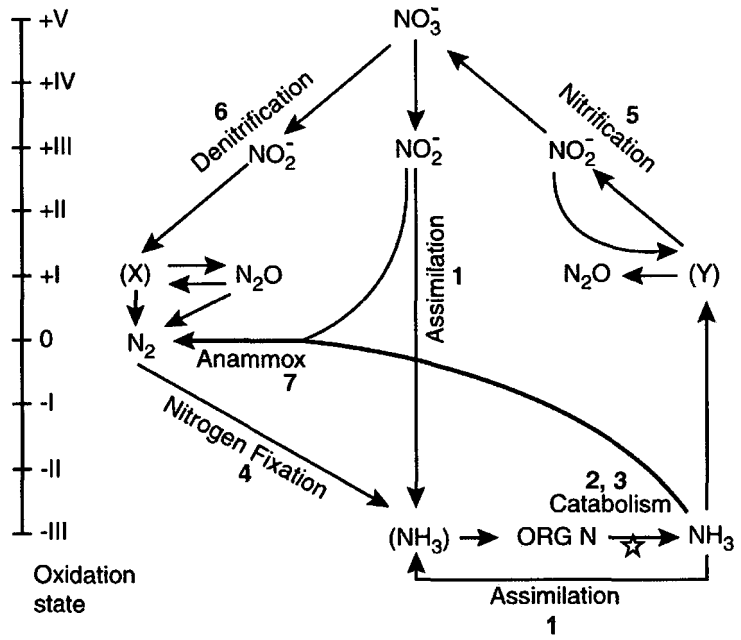

Figure 1.01 Marine nitrogen cycle involving redox reactions mediated by marine microorganisms. Oxidation states of the various N species shown on the left hand side. 'X' and 'Y' are intra-cellular intermediates that do not accumulate in water column. ☆ Catabolism includes remineralisation, whereby particulate N is reduced to DON and subsequently reduced to NH_3 through the process of ammonification. Figure from [*Codispoti, et al.*, 2001] adapted by [*Naqvi*, 2006]

1.3. Maintenance of primary production in the Atlantic Ocean

Primary production is a biological process whereby organic compounds are produced from carbon dioxide, water and nutrients (macro i.e. nitrogen and phosphorus; micro i.e. iron) through the process of photosynthesis. Photoautotrophic primary production in the open ocean is fuelled by two sources of N supply: (i) 'regenerated production', namely primary production maintained from recycled N i.e. NH_3, urea and DON derived from the excretory activities of animals and the metabolism of heterotrophic microorganisms; (ii) 'new production' which is supported by allochonthous N inputs i.e. the physical injection of NO_3^- from deep waters into the euphotic zone, the introduction of N through N_2 fixation, terrestrial run-off or the atmospheric deposition of N species [*Dugdale and Goering*, 1967; *Eppley and Peterson*, 1979]. If the oceans were an ideal closed system, primary production could be consistently maintained through the recycling of N through an enclosed food web, however, losses of PON from the euphotic zone to deeper waters preclude this. Losses of N from the surface ocean are replenished by allochthonous N fuelling export production, while recycled N is thought to sustain primary production [*Eppley and Peterson*, 1979].

Nitrogen in the deep ocean exists in a consistent stoichiometric ratio with phosphorus (P). This ratio of N to P lies at 16:1 and is termed the Redfield ratio [*Redifeld*, 1934] after Alfred C. Redfield. Redfield recognised that this stoichiometric relationship is similar to that of plankton and when this organic matter is remineralised N and P are released at equal rates to establish an analogous ratio in the deep ocean [*Arrigo*, 2005; *Tyrrell*, 1999]. This ratio between N and P can deviate from the Redfield stoichiometry from either exogenous nutrient delivery or by

microbial metabolism, which can include N_2 fixation, denitrification and anammox [*Arrigo*, 2005] (Fig 1.02).

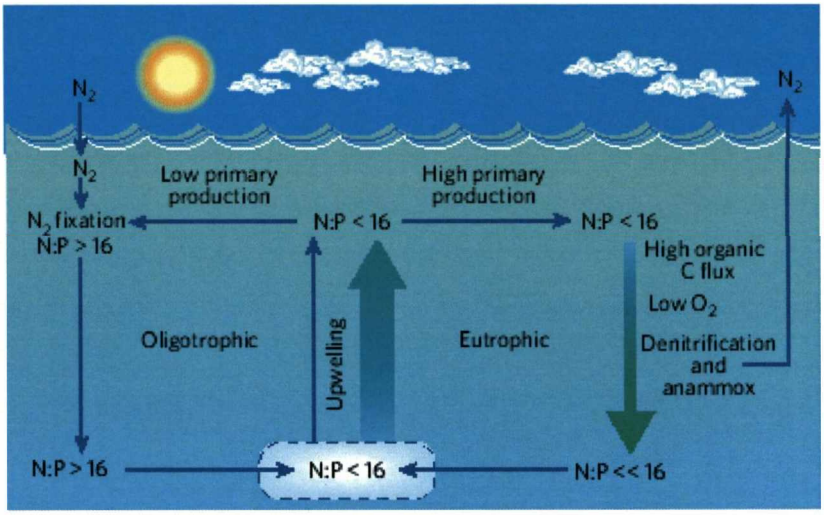

Figure 1.02 The global ocean balance between N_2 fixation and the loss of fixed N through anammox and denitrification. Perturbations in Redfield stoichiometry indicated [*Arrigo*, 2005].

In the surface Atlantic Ocean, rates of primary production are high around the equator and in the northern and southern temperate regions [*Poulton, et al.*, 2006a]. At the equator, NO_3^- is supplied to the euphotic zone through Ekman induced upwelling, whilst in the northern and southern temperate regions, convection is primarily responsible for the supply of new N to surface waters (Fig 1.03) [*Williams and Follows*, 2003]. To the north and south of the equator, large regions of the surface Atlantic Ocean are characterised by N deficient waters, where the winds induce downwelling over subtropical gyres. The restricted availability of N in these oligotrophic gyres limits phytoplankton production throughout most of the year with the exception of the late wintertime, when wind and convectively driven mixing introduces NO_3^- from below the thermocline to the euphotic zone [*McGillicuddy and Robinson*, 1997]. Nevertheless, due to extensive area of these gyres, they are

responsible for up to 2.0 mol C $m^{-2}yr^{-1}$ of organic carbon export flux. which could account for almost 50% of the global biological organic carbon pump [*Emerson, et al.*, 1997]. This drawdown of carbon to the deep ocean reduces the partial pressure of carbon dioxide in surface waters.

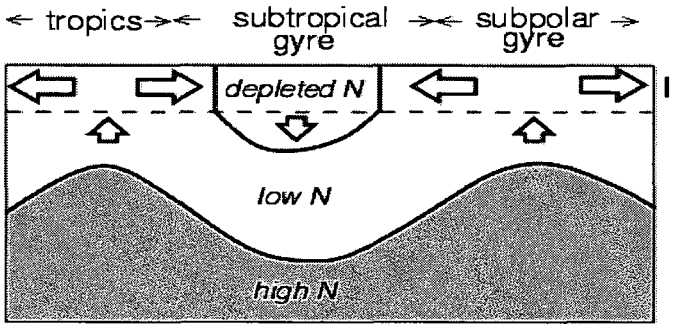

Figure 1.03 Ekman volume fluxes along a vertical meridional section [*Williams and Follows*, 2003]

Independent geochemical estimates of carbon export in the oligotrophic Sargasso Sea are between 0.42 and 0.56 mol N m^{-2} yr^{-1}[*Jenkins*, 1988; *Jenkins and Goldman*, 1985]. Traditional views of new N supply to the surface ocean include diffusion of NO_3^- from deep waters and atmospheric deposition. The diffusive flux of NO_3^- from the upper thermocline into the euphotic zone is an order of magnitude too small (0.01 mol N m^{-2} yr^{-1} [*Ledwell, et al.*, 1993]; 0.05 mol N m^{-2} yr^{-1} [*Lewis, et al.*, 1986]) to explain the estimated export production. Atmospheric inputs of N (0.005 – 0.03 mol N m^{-2} yr^{-1} [*Knap, et al.*, 1986]; 0.0014 – 0.05 mol N m^{-2} yr^{-1} [*Spokes, et al.*, 2000]) are also deemed to have a minor role in driving export production. Over the past decade extensive research has been conducted to try and account for the discrepancies that exist in the maintenance of export production over the north Atlantic subtropical gyre. These processes will now be briefly discussed.

1.3.1 Potential supplies of N to the surface Atlantic Ocean

Evidence suggests that physical processes such as lateral advection [*Williams and Follows*, 1998] and mesoscale eddies [*McGillicuddy, et al.*, 1998] could play an important role in sustaining export production over the north Atlantic subtropical gyre. Through Ekman upwelling, NO_3^- is supplied to the euphotic zone in the subpolar gyre, off the eastern boundary and over parts of the tropics. This NO_3^- can then be subsequently advected horizontally to the northern flanks of the subtropical gyre where climatological estimates suggest 0.06 to 0.12 mol N m^{-2} yr^{-1} is supplied [*Williams and Follows*, 1998]. Whilst this mechanism of NO_3^- transport is important across intergyre boundaries (supporting 0.4 to 0.8 mol C m^{-2} yr^{-1}), in the subtropical gyre interior the supply is insignificant [*Williams and Follows*, 1998].

Mesoscale ocean eddies are formed predominantly through baroclinic instability of boundary currents and density fronts [*Williams and Follows*, 2003] while a mesoscale front is characterised by contrasting dynamically active scalars (density or potential vorticity) associated with a jet [*Strass*, 1992]. Upwelling due to the formation of cyclonic eddies and their intensification caused by interaction with surrounding mesoscale features causes spatially and temporally intermittent fluxes of NO_3^- into the euphotic zone (Fig 1.04) [*McGillicuddy and Robinson*, 1997]. An unstable front can develop a geostrophic circulation that may upwell ribbons of high NO_3^- water along a front, subduct chlorophyll-rich features or spin-off NO_3^- rich eddies [*Garcon, et al.*, 2001]. In the summer of 1995 at the BATS site in the oligotrophic Sargasso Sea, an eddy event was observed, where cooling persisted for thirty days and NO_3^- concentrations increased from undetectable to1.4 mmol m^{-3}. Phytoplankton biomass and particulate material also increased during this period [*McGillicuddy, et al.*, 1998]. Model estimates of eddy induced NO_3^- flux to the

euphotic zone suggest that 0.19 to 0.35 mol N m^{-2} yr^{-1} is supplied to the euphotic zone at BATS, which is sufficient in closing the N budget for the Sargasso Sea [*McGillicuddy and Robinson*, 1997; *McGillicuddy, et al.*, 1998].

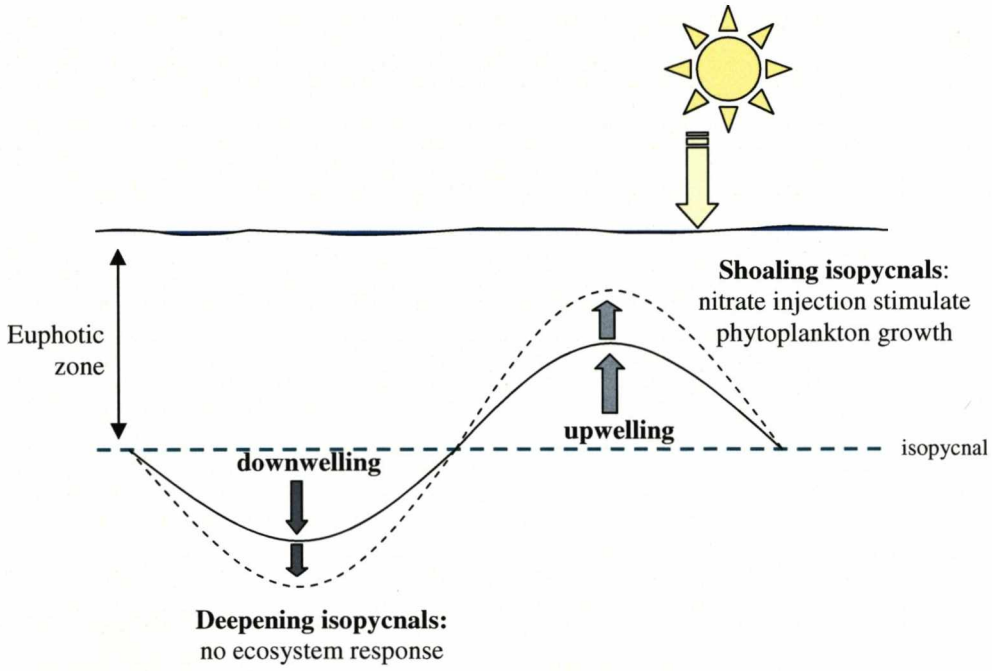

Figure 1.04 Fluctuations in the nutricline caused by eddy rectification and the observed biological response. The solid line depicts the vertical deflection of an individual isopycnal caused by the presence of two adjacent eddies of opposite sign. The dashed line indicates how the isopycnal might be subsequently perturbed by interaction of the two eddies.[*McGillicuddy and Robinson*, 1997]

However, model estimates of the central region of the subtropical gyre suggest that eddy upwelling events are insufficient (0.05 mol N m^{-2} y^{-1}) to maintain the export production and therefore alternative supplies of N are required [*Oschilles and Garcon*, 1998; *Oschlies*, 2002].

These alternative supplies include N_2 fixation [*Gruber and Sarmiento*, 1997] and the lateral advection of DON from neighbouring upwelling regions in the tropics and subpolar gyres [*Abell, et al.*, 2000; *Roussenov, et al.*, 2006; *Williams and Follows*, 1998]. DON is a heterogeneous mixture of compounds composed of biologically labile moieties, which turn over from days to hours, and refractory components,

which persist for months to hundreds of years [*Bronk*, 2002]. Examples of identified organic nitrogen compounds include urea, amino acids, proteins and nucleic acids [*Berman and Bronk*, 2003]. Whilst the refractory forms dominate the DON pool, it is the smaller labile and semi-labile pools which are more important due to their potential as N sources to primary producers [*Bronk*, 2002; *Flynn and Butler*, 1986; *Palenik and Henson*, 1997; *Palenik and Morel*, 1990a; b]. In the Atlantic Ocean DON dominates the total dissolved nitrogen pool (>60%) in near surface waters. At the flanks of the northern and southern subtropical gyre concentrations of DON are found to be ~5 μM whilst in the centre of the gyres concentrations were lower at ~4 μM [*Mahaffey, et al.*, 2004]. Model studies [*Roussenov, et al.*, 2006] show that semi-labile DON produced over the upwelling zones in the tropics, subpolar gyre and along the eastern boundary current of the subtropical gyre is transported into the subtropical gyre interior through wind-driven Ekman circulation and overturning circulation. This DON transport has been estimated to provide 0.05 mol N m^{-2} yr^{-1} to the export production in this oligotrophic region which is comparable with estimates of NO_3^- supply through diapycnic diffusion and atmospheric deposition [*Roussenov, et al.*, 2006]. However, while important, this supply is still insufficient to account for the export production observed over the subtropical gyre of the north Atlantic.

Estimates of N_2 fixation for the north Atlantic subtropical gyre vary greatly from 0.02 mol N m^{-2} yr^{-1} [*Hansell, et al.*, 2004] to 0.31 mol N m^{-2} yr^{-1} [*Capone, et al.*, 2005], implying either that N_2 fixation is insignificant as a source of N in fuelling export production or that is substantial enough to close the N budget of the north Atlantic subtropical gyre.

1.4 Summary

The marine N cycle is complex, involving an array of regulatory mechanisms, some of which are mediated by a metabolically diverse range of microorganisms [*Hulth, et al.*, 2005]. The recent discoveries of processes such as anammox have enabled us to account for inputs and losses of N to and from the system that were previously unexplained.

Nitrogen plays a fundamental role in the biogeochemical dynamics of the Atlantic Ocean, where in the northern and southern oligotrophic gyres, primary production is limited by the availability of N. Traditional views of N supply to the euphotic zone fail to account for the observed export production. The realisation of the potential role that DON could play in accounting for this discrepancy requires further investigation of the chemistry and reactivity of this source of N.

Whilst N_2 fixation has long been understood as a process which introduces new N to the euphotic zone, it is not until the last decade that this mechanism has been recognised as a potentially crucial N contributor. Uncertainties still exist in the estimates of this input and the impact N_2 fixation has on the surrounding planktonic community.

Our knowledge of the marine N cycle is constantly increasing through the application of new biological and chemical techniques employed in the field and in laboratory based experiments. However, despite extensive research including model studies, aspects of the marine N cycle remain unresolved due to the complexity of the processes involved.

In order to address the uncertainties that exist in our knowledge of the biogeochemical nitrogen dynamics of the Atlantic Ocean, the following questions are addressed in this thesis:

(i) What is the spatial extent of N_2 fixation in the Atlantic Ocean?

(ii) How important in N_2 fixation in closing the N budget?

(iii) What is the reactivity and composition of the labile and semi-labile compounds of organic N?

The following chapter discusses these goals in greater detail and also provides context of various other biogeochemical processes occurring in the Atlantic Ocean.

CHAPTER 2

Project overview: Atlantic Meridional Transect Programme

2.1 Introduction

The Atlantic Meridional Transect (AMT – www.amt-uk.org) programme is funded by the UK National Environmental Research Council (NERC). A time-series of oceanographic observations at stations along north-south transects through the various biogeochemical regimes of the Atlantic Ocean underpins the programme [*Robinson, et al.*, 2006]. To date, 17 cruises have taken place between autumn 1995 and autumn 2005. A series of 12 bi-annual transect cruises were conducted between 1995 and 2000 (see [*Aiken, et al.*, 2000b] for review), making measurements of hydrographical and bio-optical properties, plankton community structure and primary production [*Holligan, et al.*, 2004]. The present study formed part of the second phase of the AMT programme which involved six cruises between 2003 and 2005;

this thesis presents results from three of these, namely AMT-12, AMT-14 and AMT-16.

2.2 Objectives

2.2.1 AMT

The aims of the AMT programme are to quantify the nature and causes of ecological and biogeochemical variability in the planktonic ecosystems of the tropical and temperate Atlantic Ocean, and the effect of this variability on the biological C pump and on air-sea exchange of radiatively active gases and aerosols [*Jickells, et al.*, 2003a]. The collected data has been or will be used in the development of models to describe the interactions between the global climate system, plankton functional biodiversity and ocean/atmosphere biogeochemistry [*Robinson, et al.*, 2006]. The investigation has three major objectives incorporating nine inter-linked hypothesis (Fig 2.01), these are:

(1) How the structure, functional properties and trophic status of the major planktonic ecosystems vary in space and time (hypotheses 1 – 4)

(2) How physical processes control the rates of nutrient supply, including dissolved organic matter, to the planktonic ecosystem (hypotheses 5 & 6)

(3) How atmosphere- ocean exchange and photo-degradation influence the formation and fate of organic matter (hypotheses 7 – 9) [*Robinson, et al.*, 2006].

For full details of objectives and hypotheses of the AMT programme see appendix A.

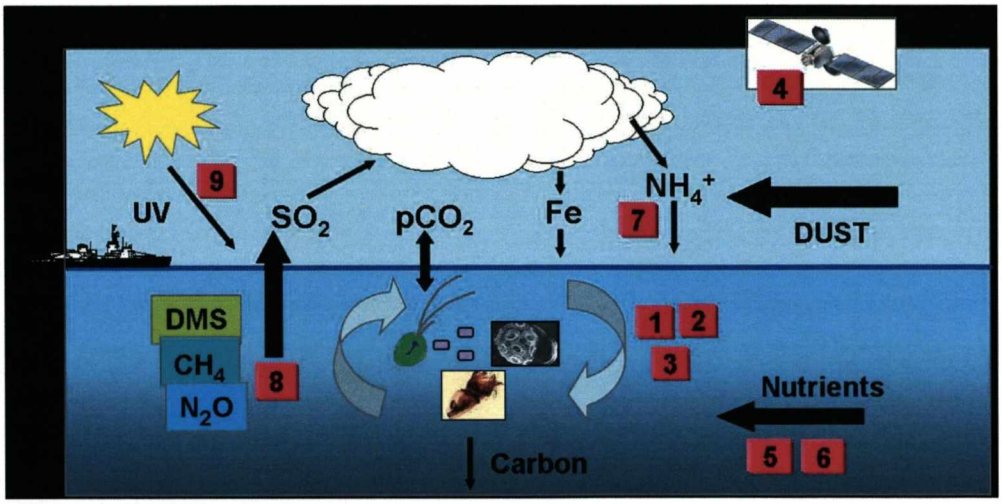

Figure 2.01 Schematic illustrating the nine inter-linked hypotheses of the second phase of the AMT programme (2002 – 2006) (http://web.pml.ac.uk/amt/research/amt_research.html)

2.2.2 Objectives of this study

The primary concern of this thesis was to determine the nature and source of the sustainable supply of N and P that drives export production over the oligotrophic regions. In order to address this problem, a series of questions were posed:

(i) What is the primary source of N to the surface Atlantic phytoplankton? Is there interannual variability? If so, what influences this?

- Achieved through the use of stable N isotopes in suspended PON

(ii) What are distributions of the labile and semi-labile components of DON? Do variations along the transect reveal the role that DON plays in the maintenance of primary production in the surface Atlantic Ocean.

- Achieved through the determination of free and hydrolysable dissolved amino acids.

(iii) What is the lability and nature of organic nitrogen along the AMT transect? What differences exist between the biogeochemical provinces and what does this suggest with regards to the biogeochemical cycling of the organic matter?

- Achieved by examination of the distributions of individual amino acids, with the use of the Dauwe degradation index to determine the 'age' of the organic matter.

(iv) What is the microbial role in the production and cycling of the DON and PON pools in the surface waters of the Atlantic Ocean?

- Achieved by examination of the D-amino acids and quantification of the microbial contribution to the relative pools.

The present study is included under objective two (section 2.2.1), hypothesis 5 of the AMT programme. Hypothesis 5 states: 'Net heterotrophy and export production in the subtropical gyre are partly sustained by lateral inputs of dissolved organic nutrients from neighbouring upwelling regions.'

2.3 Cruise Review

2.3.1 Protocol: transects, sampling & measurements

AMT 12, 14 and 16 were northbound gyre cruises which involved passage as far westwards into the northern gyre as possible, given the time constraints (Fig. 2.02). Full details of these cruises can be found in the appropriate cruise reports [*Bale, et al.*, 2005; *Holligan, et al.*, 2004; *Jickells, et al.*, 2003a]. During the cruises a wide range of measurements and samples were taken including carbon fixation rates [*Poulton, et al.*, 2006a], stocks of nano- and picoeukaryotic phytoplankton [*Tarran,*

et al., 2006], nutrients in the marine aerosol [*Baker, et al.*, 2006] and DMS production [*Bell, et al.*, 2006]. The sampling took place throughout the day with an average station time of ~4 hours involving deployments of a rosette sampler with an attached SeaBird 9/11 CTD and a Chealsea MKII Aquatracker fluorometer, stand alone pumps (SAPs) and bio-optic sensors (Table 2.1) [*Robinson, et al.*, 2006].

Time	Operation	Research area
Pre-dawn	Bongo nets (200 μm, 50 μm: 200-0 m, 50-0m)	Mesozooplankton abundance, diversity and size distribution
~03:00 GMT	CTD(s) (0-300 m) + fluorescence, oxygen, transmission, ADCP, FRFF	Plankton community structure, primary production and respiration, calcification, N_2 fixation, new and regenerated production, nutrients, CDOM, DOC/N, POC/N, PIC, BSi, climate reactive gases (DMS, N_20, CH_4), carbon species, oxygen
05:00 GMT	SAPs (~every 3rd day)	Export production, isotopic composition of particulate organic carbon
11:00 GMT	CTD (0-1000m) + fluorescence, oxygen, transmission, ADCP Optics rig + FRFF Single net (200 μm; 100-0 m)	Iron speciation, nutrients community structure, CDOM Optical properties, satellite algorithm development Mesozooplankton diversity and activity
Continuous	Thermosalinograph, fluorescence, pCO2	Province determination, source and sink regions of CO_2
Continual	Water sampling from the non-toxic supply	Alkalinity, TCO_2, ammonia, DMS, CDOM, calibration samples for salinity, HPLC pigments, POC/N, PIC, BS
Continual	Atmospheric sampling when wind conditions permit and rainfall when possible	Air-sea exchange

Table 2.01 Typical daily sampling schedule on AMT cruises [*Robinson, et al.*, 2006].

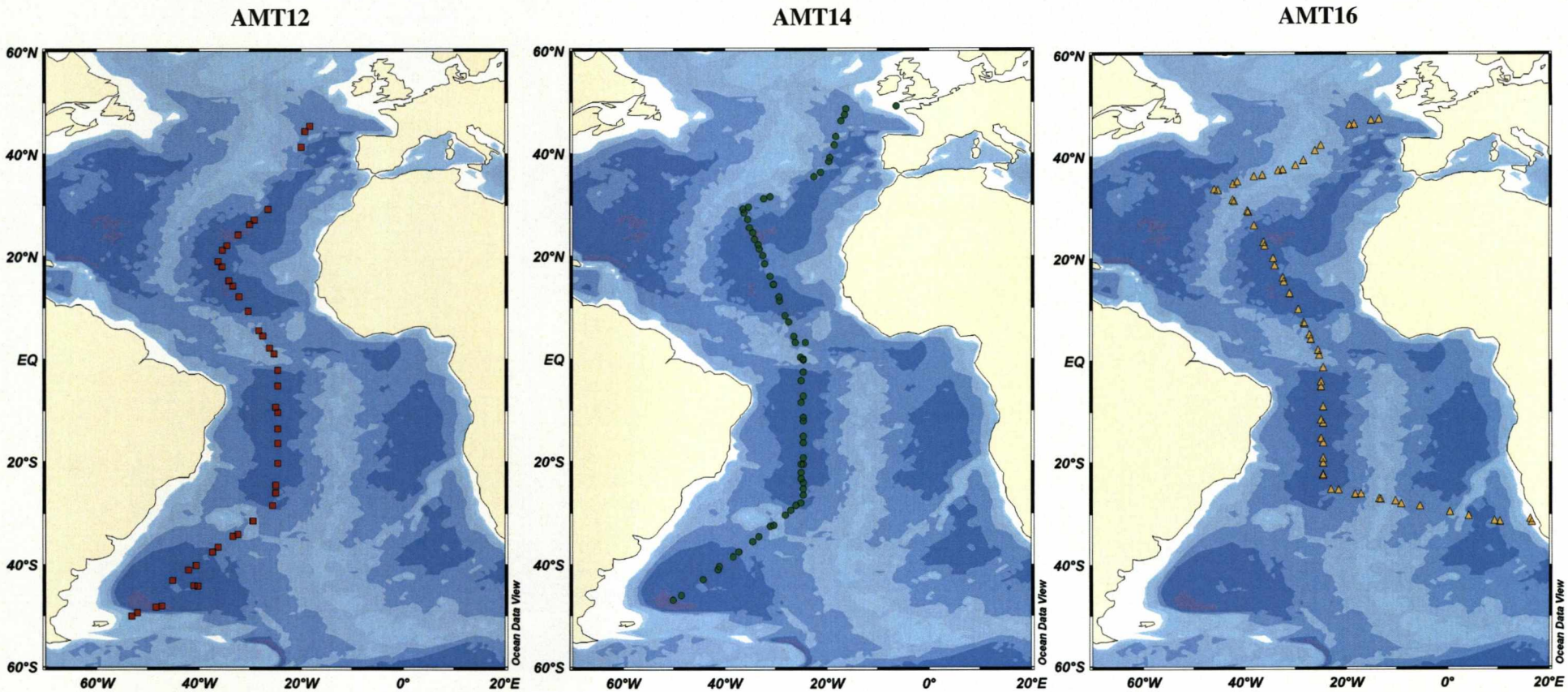

Figure 2.02 Northbound cruise tracks of AMT 12, 14 and 16, points showing stations. Shading denotes bathymetry of ocean floor.

To answer the questions posed at the outset of this study, a number of particulate organic matter samples were taken along the transects using CTDs and SAPs. Dissolved organic matter was also sampled from the CTDs, and on AMT-16 enzyme activity incubations were conducted on-board (Table 2.2). Full details of why and how these samples were taken will be given in later chapters.

2.3.2 Hydrographical and biological features of the Atlantic Ocean

2.3.2.1 Physical properties

Examination of the latitudinal sections (0-300 m) of density, salinity and temperature data (Fig. 2.03) collected from CTD casts over three years (AMT-12, 14 and 16) reveals the general physical structure of the surface Atlantic Ocean. Surface temperature is directly controlled by radiative heating, as well as by the exchange of sensible and latent heat with the atmosphere. The highest temperatures are observed in the upper 50 m of the water column at the equator. There is a pattern of decreasing temperature with increasing latitude due to a higher degree of insolation at the equator.

The highest salinities are found in the subtropical gyres of the Atlantic Ocean, where a deep halocline is observed mirroring that of the deep thermocline. At the equator, where much fresher waters are observed at the surface and where temperatures are at their highest, the relationship between salinity and temperature breaks down due higher rates of precipitation [*Aiken, et al.*, 2000a], and through the influence of the Amazon outflow [*Robinson, et al.*, 2006].

Cruise	Dates	Ship	From	To	Samples / Measurements taken
AMT12	12.05.03 – 14.06.03	RRS JCR†	Port Stanley, Falklands	Grimsby, UK	Stable N isotopes of PON_{susp} (SAPs) DON and DOP (CTD) POC and PON (SAPs & underway)
AMT14	26.04.04 – 02.06.04	RRS JCR†	Port Stanley, Falklands	Grimsby, UK	Stable N isotopes of PON_{susp} (SAPs) DON and DOP (CTD) POC and PON (SAPs & underway) Dissolved free amino acids (CTD)
AMT16	19.05.05 – 29.06.05	RRS Discovery	Cape Town, South Africa	Falmouth, UK	Stable N isotopes of PON_{susp} (SAPs) DON and DOP (CTD) POC and PON (SAPs) Dissolved free amino acids (CTD) Particulate phospholipids (SAPs) Amino peptidase and phosphatise activities (CTD)

Table 2.02 Details of cruises this Ph.D was involved with, plus samples and measurements made on board
† RRS James Clark Ross

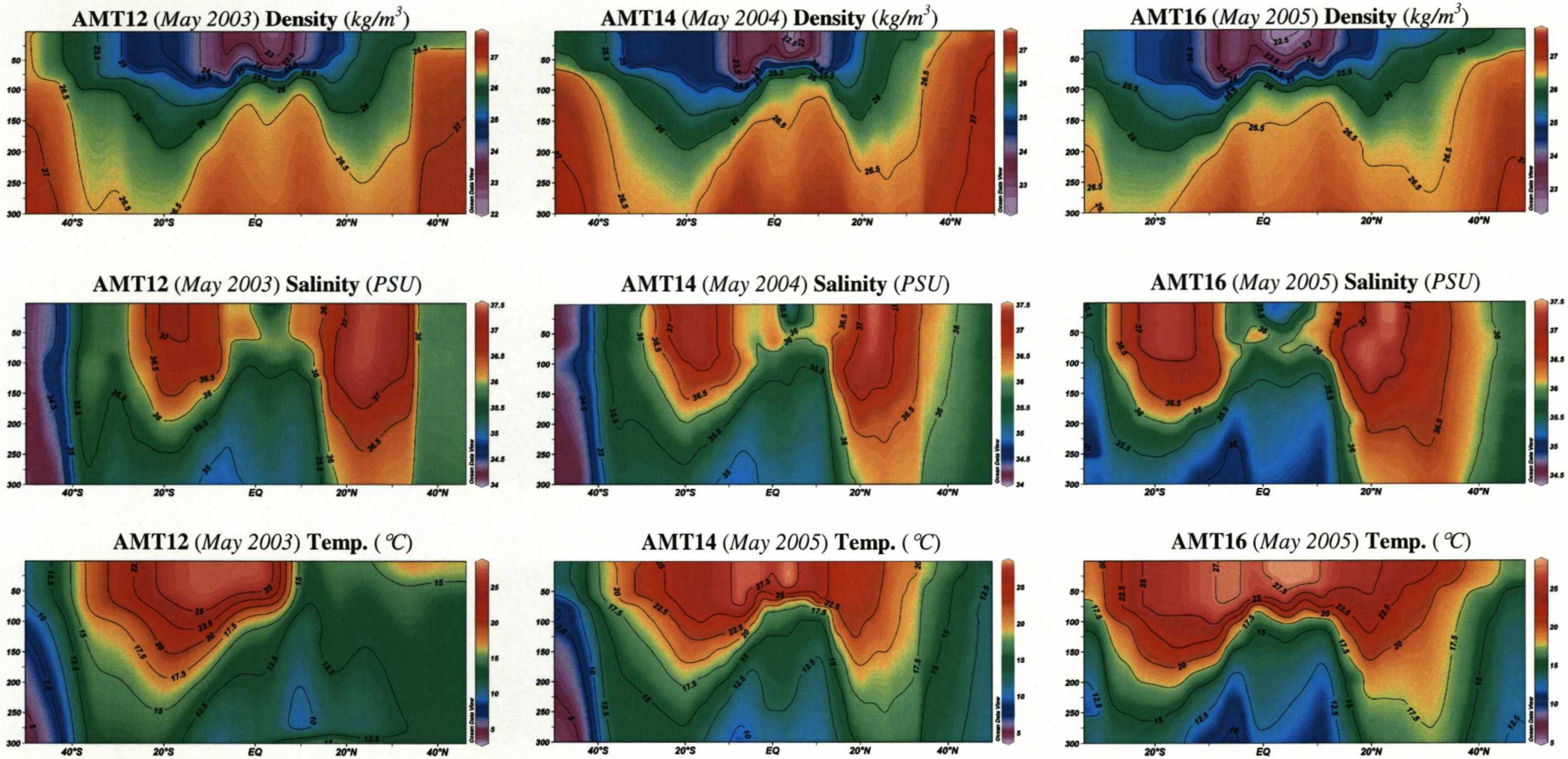

Figure 2.03 Density (km/m^3), salinity (PSU) and temperature (°) latitudinal sections of the Atlantic Ocean from the respective cruises. Data collected from each CTD (equipped with a Seabird 9/11 CTD and a Chealsea MKII Aquatracker Fluorometer) cast along the cruise transect

Density reflects the combined effects of temperature and salinity, where temperature is the dominant parameter, giving rise to the lowest densities at the equator.

The Atlantic Ocean is characterised by an undulating thermocline which is much thicker in the both the northern and southern subtropics than at the equator (Fig 2.03). Wind induced Ekman flux is responsible for this structure, since over the tropics westerly trade winds drive polewards Ekman transport on either side of the equator which drives a band of equatorial upwelling. Over the sub-tropics, anticyclonic gyres exist due to a convergence in Ekman flux of surface waters resulting in downwelling and a depressed, thicker thermocline [*Williams and Follows*, 2003].

2.3.2.2 Chlorophyll a

Chlorophyll *a*, the photosynthetic pigment of most phytoplankton, can be used as a proxy for phytoplankton biomass (e.g. [*Platt and Sathyendranath*, 1988]). SeaWifs composite images (Fig. 2.04 a-c) of the Atlantic Ocean for the periods of the AMT-12, 14, and 16 cruises demonstrate the surface patterns of chlorophyll *a*. High concentrations are observed at high latitudes of both the northern and southern hemisphere and at the upwelling zones of the equator and Mauritania. The images compiled for AMT14 and 16 clearly illustrate the highly productive Benguala current off the eastern coast of South Africa.

The latitudinal sections of chlorophyll *a* for AMT-12, 14 and 16 constructed from data collected from the Aquatracker Fluorometer attached to the CTD (corrected with shipboard measurements) (Fig. 2.04 d-f), reveal the undulating gyre structures to the north and south of the upwelling waters at the equator. The highest

(a) AMT12 (*May 2003*)

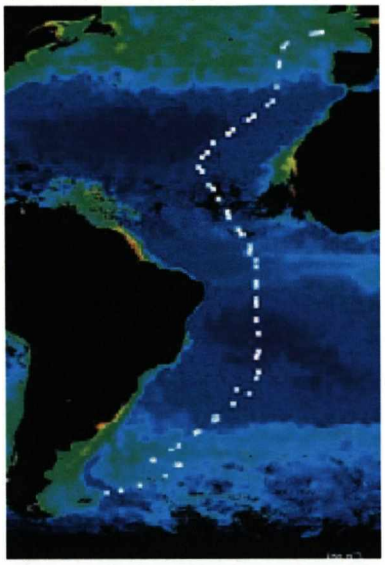

(b) AMT14 (*May 2004*)

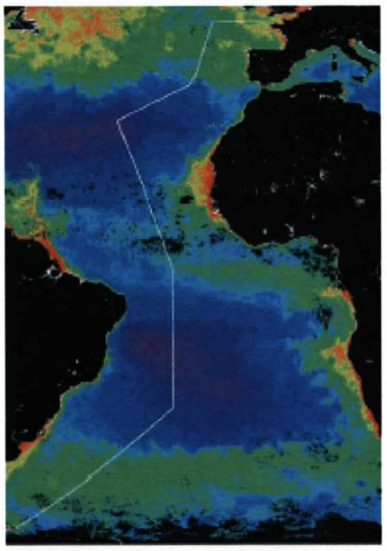

(c) AMT16 (*June 2005*)

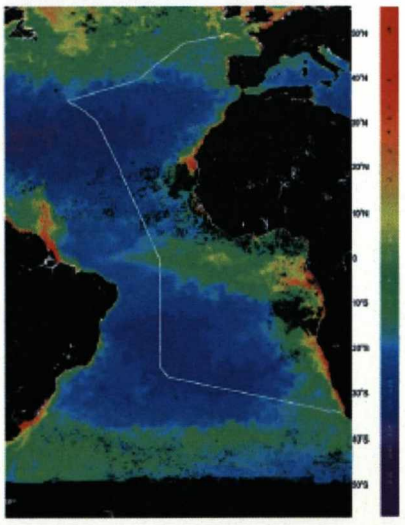

(d) AMT12

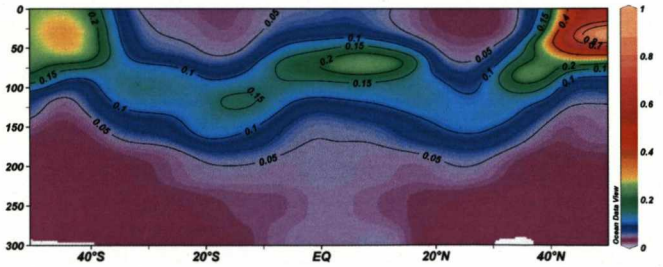

(e) AMT14

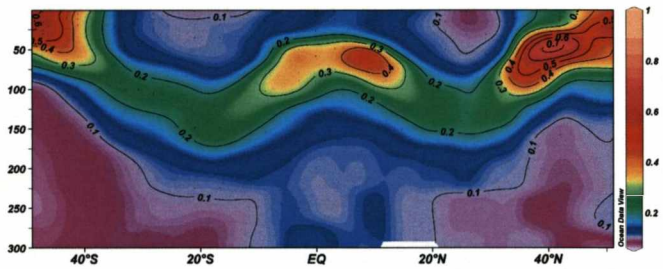

(f) AMT16

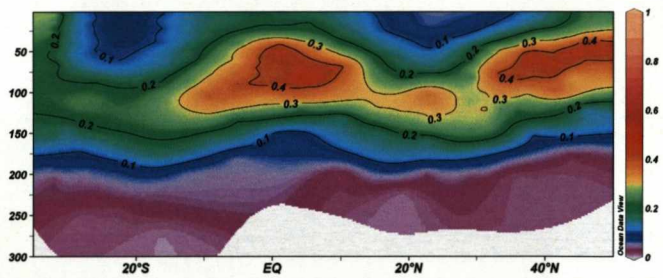

Figure 2.04 Composite chlorophyll a images (SeaWifs) of the Atlantic Ocean (a-c) with corresponding chlorophyll a (mg m^{-3}) latitudinal sections (d-f).
(a) taken from AMT12 cruise report [*Jickells, et al.*, 2003a], (b) and (c) [*Robinson, et al.*, 2006].

levels of chlorophyll *a* are observed in the temperate waters at high latitudes in the southern and northern points of the transect and at the equator. The surface waters (<50 m) of both subtropical gyres are characterised by chlorophyll *a* concentrations >0.1 mg m^{-3}. A deep chlorophyll maximum (DCM) exists along the entire AMT transect, where chlorophyll *a* concentrations lie between 0.2 – 0.3 mg m^{-3} in the gyres whilst at the equator they are often above 0.4 mg m^{-3}. The depth of this DCM changed with latitude according to variations in the structure of the water column [*Maranon, et al.*, 2001] and is closely related to the depth of the nitricline [*Poulton, et al.*, 2006a] (see section 3.4.1 for further description of the nitricline). *Marañón et al.* [2000] found that the DCM makes a relatively minor contribution to the total integrated biomass and productivity of the euphotic zone, being formed through mechanisms including the accumulation of cells from overlying waters, differential sinking rates, and physiological photoacclimation.

2.3.2.3 Primary productivity

Photoautotrophic primary production is the synthesis of organic compounds from inorganic compounds through the process of photosynthesis. Rates of primary production measured through the incorporation of inorganic ^{14}C (in the form of sodium bicarbonate) into organic matter [*Nielsen*, 1951] along the AMT transect reveal variations relating to depth and biogeochemical regime. Daily rates of C fixation are highest in surface waters and decrease with depth as irradiance decreases [*Poulton, et al.*, 2006a] and the DCM does indeed make a minor contribution to water column C fixation [*Maranon, et al.*, 2000]. Along the AMT transect the highest rates of C fixation were observed in the equatorial and northern and southern temperate regions (>0.3 – 0.5 mmol C m^{-3} d^{-1}), whilst the lowest rates were found in

the northern and southern oligotrophic subtropical gyres (<0.2 mmol C m^{-3} d^{-1}) [*Poulton, et al.*, 2006a]. The varying rates of primary production in the Atlantic Ocean are related to the undulating nitricline structure (see section 3.4.1 for further description of the nitricline) the supply of NO_3^- to the surface waters is greater in the equatorial region than in the oligotrophic gyres. However, *Poulton et al* [2006] found that NO_3^- concentrations at the DCM are significantly higher than those estimated to be required to support the rates of C fixation observed and have attributed this to light limitation of primary production at the DCM.

2.3.3.4 Metabolic balance

The metabolic balance of the worlds oceans i.e. the balance between plankton autotrophic and heterotrophic processes, is termed net community respiration [*Robinson and Williams*, 1999]. This measurement determines the amount of biologically fixed C available for export to the deep ocean, or for return to the atmosphere [*Gist, et al.*, 2007]. Since oceans are open systems, a degree of imbalance between biological production and consumption can, in principle, be sustained by the import or export of organic matter [*Williams*, 1998]. In situations where an accumulation of DOC develops in surface waters, and net consumption occurs concurrently with low primary production, a net heterotrophic metabolism can develop [*Serret, et al.*, 2001].

Rates of productivity and respiration are determined from on-deck incubations, where changes in dissolved oxygen concentrations over 24 hours are measured using Winkler titrations. Incubations conducted in the dark are a measurement of respiration as no photosynthesis occurs, while incubations carried out in the light are representative of net production. To determine gross production,

the rates from the dark incubations are subtracted from those obtained in the light incubations.

Measurements of production and respiration made on recent AMT cruises (AMT12 – 17) revealed that overall, the northern oligotrophic gyre was net heterotrophic while the southern gyres is more balanced [*Gist, et al.*, 2007]. However, *Gist et al* [2007] report that the metabolic balance of the oligotrophic gyre changed with season, where both gyres were net heterotrophic in the autumn and more balanced in the spring. They also reported an apparent decrease in respiration from the eastern edge of the northern gyre towards its centre, which could possibly be indicative of an allochthonous organic carbon source to the east of the gyre.

2.3.3.5 Community structure

Understanding the community structure in the Atlantic Ocean is of fundamental importance because of the role that the biota play in the dynamics of the various biogeochemical cycles and ultimately in the drawdown of carbon. Along the AMT transect, size fractionated Chl *a* measurements and flow cytometry analysis has revealed that prokaryotic picophytoplankton (<2 μm) make up 50-80% of the autotrophic biomass, with the exception of highly productive waters, where larger eukaryotes such as diatoms and dinoflagellates dominate [*Robinson, et al.*, 2006]. *Prochlorococcus* sp., unicellular cyanobacteria, dominate the picophytoplankton community in the northern and southern oligotrophic gyres, the biomass integrated above the nitricline (± standard error) being 173 (±21) mg C m^{-2} in the northern gyre,190 (±14) mg C m^{-2} in the southern gyre and 141 (±15) mg C m^{-2} in the equatorial region [*Heywood, et al.*, 2006].

In the temperate and upwelling regions of the Atlantic Ocean eukaryotic plankton abundances were greater than in the oligotrophic gyres, with integrated carbon biomass values ranging between 160 to 320 mg C m^{-2}. Of this, picoeukaryote phytoplankton dominated contributing 25-60% of the total [*Tarran, et al.*, 2006].

Through the use of phytoplankton diagnostic pigments further information on the phytoplankton community structure can be revealed [*Poulton, et al.*, 2006a]. Alloxanthin, 19'-hexanoyloxyfucoxanthin and 19'-butanoyloxyfucoxanthin, which are the primary pigments found in nanoplankton, made up <50% of the total diagnostic pigments in the surface waters of the tropics and subtropics. Microphytoplankton, markers for which include fucoxanthin and peridinin, made up a much smaller fraction of less than 10% in the same waters. In the northern regions of the north Atlantic subtropical gyre, diagnostic pigments for nanoflagellates (peridinin) dominated the surface waters whist in the deeper waters in the DCM of the tropics and subtropics, pigments were evenly distributed revealing cyanophytes (zeaxanthin) and nanoflagellates [*Poulton, et al.*, 2006a].

Measurements of other prokaryotic phytoplankton, i.e. heterotrophic bacteria, along the AMT transect show that abundances were greatest in the surface waters around the equator and at the high latitudes of the northern and southern points of the transect [*Heywood, et al.*, 2006]. Integrated carbon biomass values above the nitricline were greatest in the northern oligotrophic gyre (~750 mg C m^{-2}; average of values for AMT12 and AMT14), values being slightly lower in the southern gyre (~625 mg C m^{-2}; average of values for AMT12 and AMT14) and lower again at the equator (~500 mg C m^{-2}; average of values for AMT12 and AMT14) [*Heywood, et al.*, 2006].

2.4 Summary

The biogeochemical regimes of the Atlantic Ocean are clearly observed from hydrographical features such as salinity and temperature. The bi-annual transect obtained through the AMT programme, where the different provinces are extensively sampled, provide an ideal platform from which to determine the major sources of N to the surface phytoplankton of the oligotrophic regions and to examine the dynamics of organic nitrogen.

CHAPTER 3

Assessing the role and importance of nitrogen fixation within the Atlantic Ocean

3.1 Introduction

The supplies of nitrogen to primary producers in the surface waters of the world's oceans and its subsequent reworking are complex (Fig 3.01) In recent years the process of N_2 fixation which involves the conversion of N_2 to biologically available ammonium [*Lipschultz and Owens*, 1996b], has been recognised as globally significant in providing a source of 'new' N [*Dugdale and Goering*, 1967] to primary producers of surface waters and drawing down organic N and C from the euphotic zone to the deep ocean interior [*Capone, et al.*, 1997; *Karl, et al.*, 1997]. However, the extent and importance of N_2 fixation remain a matter of debate due to

difficulties in the measurement of *in situ* rates of N_2 fixation and differences in the methods used.

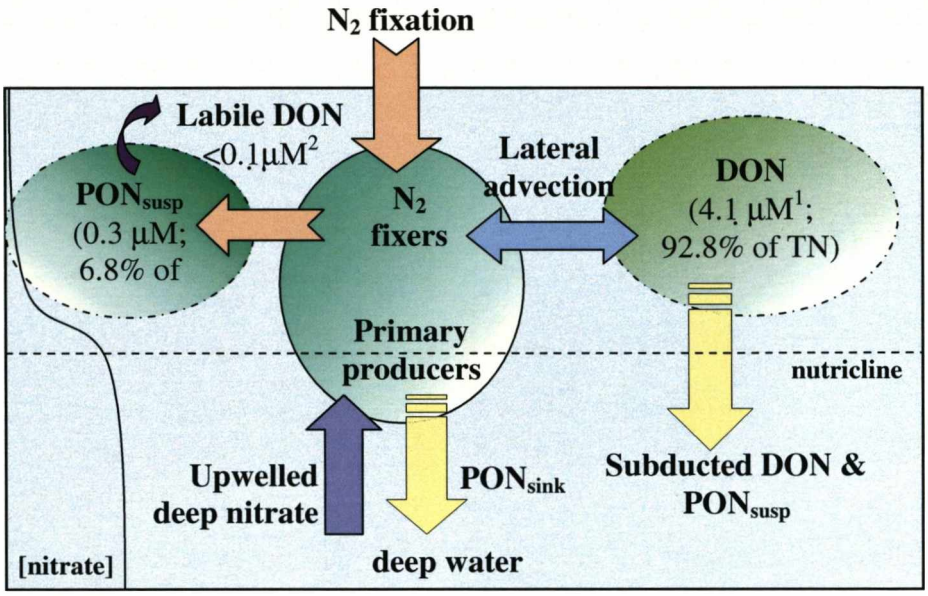

Figure 3.01 Pathways of N through the oligotrophic ocean. Proposed mechanisms fuelling primary production include upwelling of deep NO_3^-, advection of DON and N_2 fixation. Subsequent re-workings of this sequestered N are shown. Concentrations and size of pools given where known. [1][*Torres 2006*, pers comm], [2][*Mahaffey, et al.*, 2004].

This Chapter focuses on N_2 fixation in the Atlantic Ocean utilising the stable N isotopic signature of particulate organic nitrogen (PON) collected during three cruises over a three year period. The importance and distribution of these signals in providing a new source of N to the euphotic waters of the oligotrophic regions of the Atlantic Ocean will be discussed.

3.1.1 Marine nitrogen fixation

The biological fixation of inert atmospheric N_2 into ammonium is governed by the nitrogenase enzyme (3.1).

$$N_2 + 8H^+ + 8e^- + 16MgATP \rightarrow 2NH_3 + H_2 + 16MgADP + 16P \quad (3.1)$$

The microorganisms that are responsible for N_2 fixation in the oceans are prokaryotic and include both bacteria and archaea [*Karl, et al.*, 2002], the most studied of these being the filamentous cyanobacteria *Trichodesmium* sp. [*Capone, et al.*, 1997; *Orcutt, et al.*, 2001; *Tyrrell, et al.*, 2003]. *Trichodesmium* sp. are non-heterocystous colonial cyanobacteria [*Capone, et al.*, 1997] which, due to their positive buoyancy, high light-adapted photosynthetic apparatus and ability to grow in waters with unusually high N:P and C:P ratios, plus their high capacity for N_2 fixation, make them remarkably adaptive for survival within oligotrophic waters [*Karl, et al.*, 2002]. The most common species in the north Atlantic is *T. thiebautii* (Fig 3.02a) which occurs as macroscopic aggregates containing from 100 to over 200 trichomes (filaments) [*Capone, et al.*, 2005]. Concentrations of filaments within the upper mixed layer of the Atlantic Ocean have been conservatively estimated at ~8.5 $\times 10^6$ filaments m^{-2} [*Tyrrell, et al.*, 2003].

(a)

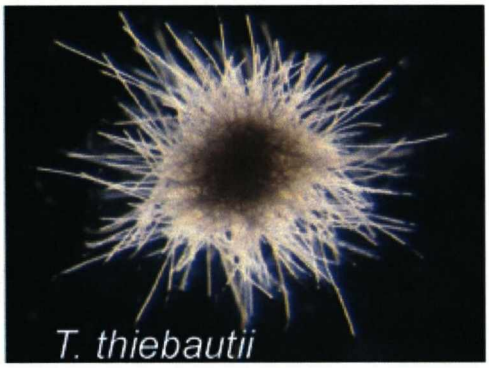

(b)

Figure 3.02 (a) *T. thiebautii*, the most abundant species of *Trichodesmium* sp. in the north Atlantic (www.whoi.edu/science/B/people/ewebb/Tricho.html) **(b)** Bloom of *Trichodesmium* sp. in surface waters as seen from space (www.aims.gov.au/pages/research/trichodesmium/tricho-01.html)

When *Trichodesmium* sp. is in such high numbers in surface waters, extensive blooms can be observed from space (Fig 3.02 b). Various estimates have been made of the contribution of new N that *Trichodesmium* sp. can supply to primary producers in oligotrophic waters (Table 3.1), which range from 4 – 267% of N export.

However, despite the importance of *Trichodesmium* sp. it has become apparent in recent years that much smaller diazotrophs may also play a role in contributing new N to the euphotic zone of the subtropical oceans. For example N_2 fixing unicellular cyanobacteria (3 – 10 μm in diameter) may be widely distributed in marine environments [*Zehr, et al.*, 2001], which even at low densities over the open ocean could contribute significant quantities of new N (Table 3.1) [*Zehr, et al.*, 1998], that might equal or exceed the contribution made by *Trichodesmium* sp.[*Zehr, et al.*, 2001].

3.1.2 What regulates N_2 fixation?

N_2 fixation is dependent on the expression of the enzyme system nitrogenase, which is a complex of highly conserved proteins [*Karl, et al.*, 2002]. Two major factors influence nitrogenase synthesis; the availability of fixed N and the presence of O_2. Since the presence of fixed N averts the need of N_2 fixation [*Paerl and Zehr*, 2000], the diazotrophs do not suffer N limitation. However, nitrogenase is extremely sensitive to O_2 in that it is rapidly and permanently inactivated by exposure to O_2 [*Gallon*, 1992], which considering that the world's oceans are either in equilibrium, or hold higher concentrations of O_2 than found in the atmosphere [*Karl, et al.*, 2002] is surprising. Nonetheless diazotrophs have evolved a variety of strategies to maintain active nitrogenase in the presence of ambient O_2 and that generated through photosynthesis [*Gallon*, 1992]. Such mechanisms include temporally separating photosynthetic activity (daylight) from the process of N_2 fixation (night-time) [*Gallon*, 1992] and in the case of *Trichodesmium* sp. confinement of nitrogenase to certain trichomes [*Bergman and Carpenter*, 1991], which may contain one or more consecutively arranged cells containing nitrogenase in differentiated cells [*Janson, et al.*, 1994]. This compartmentalisation of nitrogenase effectively separates the activities of photosynthesis and N_2 fixation.

The availability of non-nitrogenous nutrients (P and Fe), temperature and the quality and quantity of light can all affect *Trichodesmium* sp. growth rates and N_2 fixation [*Mulholland and Bernhardt*, 2005]. With regards to light limitation, photosynthesis supplies the energy and C skeletons for N uptake and assimilation, thus the availability of light and low photosynthetic rates can constrain N_2 fixation at depth [*Mulholland and Bernhardt*, 2005].

Fe plays an important role in the electron transfer reactions of the enzyme nitrogenase [*Howard and Rees*, 1996]. *Sanudo-Wilhelmy et al* [2001] revealed that N_2 fixing bacteria may have iron requirements 2.5 – 5.2 times greater than NH_4^+ assimilating phytoplankton. Since iron limitation controls the rates of phytoplankton productivity and biomass in the ocean [*Martin and Fitzwater*, 1988], the higher demand for Fe by diazotrophs suggests that they too are limited by Fe. Laboratory cultures of *Trichodesmium* sp. grown under Fe limiting conditions revealed that no only did rates of N_2 fixation decline but also the photochemical quantum yields and the relative abundance of photosystem I to photosystem II reaction centres [*Berman-Frank, et al.*, 2001]. Seasonal maps of aeolian Fe fluxes and model derived maps of surface water total dissolved Fe demonstrate that large areas of the sub tropical Atlantic and Indian Oceans are more favourable for N_2 fixation by *Trichodesmium* sp. while Fe appears to be limiting to diazotrophs in the eastern Pacific [*Berman-Frank, et al.*, 2001]. The limitation in the eastern Pacific could be attributed to the degree in difference of aeolian dust inputs to the surface waters between the northern sub tropics of the Atlantic (202 Mt yr^{-1}) and Pacific (72 Mt yr^{-1}) [*Duce and Tindale*, 1991; *Jickells, et al.*, 2005] which introduces Fe to the water. However, even with high inputs of Fe from dust deposition, N_2 fixation can still be limited by Fe, as not all Fe is bioavailable [*Mahowald, et al.*, 2005]. In a study by [*Achilles, et al.*, 2003] the bioavailability of Fe to *Trichodesmium* sp. colonies was altered by its complexation with various organic ligands. The most bioavailable forms were found to be inorganic Fe and Fe bound to the dihydroxamate siderophore.

Studies have revealed that N_2 fixation is also controlled by the availability of P [*Mills, et al.*, 2004; *Mulholland and Bernhardt*, 2005; *Wu, et al.*, 2000]. In the central Atlantic Ocean, N_2 fixation rates were found to have a strong positive

correlation with P concentrations [*Sanudo-Wilhelmy, et al.*, 2001]. Furthermore culture experiments with residual P concentrations resulted in higher N_2 fixation rates than those with depleted P levels [*Mulholland and Bernhardt*, 2005]. Mills et al., [2004] proposed that due to the high deposition of dust to the surface waters of the North Atlantic Ocean that it was P and not Fe that limited N_2 fixation here. However, they went on to show through bio-assay addition experiments, that combined additions of P and Fe enhanced N_2 fixation, whereas individual additions of P or Fe alone, did not stimulate N_2 fixation. Thus, in the North Atlantic, Fe and P apparently co-limit the N_2 fixation capabilities of marine diazotrophs. It has also been suggested that N_2 fixation in the North Atlantic appears to be P-limited rather than Fe-limited, while the North Pacific, which holds higher levels of P, is Fe-limited due to lower dust inputs [*Wu, et al.*, 2000].

3.1.3 Rates of N_2 fixation

N_2 fixation can be measured indirectly, by assessing the activity of the nitrogenase enzyme complex using acetylene reduction assay, or directly by $^{15}N_2$ assimilation or the accumulation of fixed N into microbial biomass [*Paerl and Zehr*, 2000]. Estimated rates derived from different methods show a wide range of values (Table 3.1). There are many problems with the areal estimates because in the case of N_2 fixation, neither spatial nor temporal uniformity can be assumed as much of the total N_2 fixation in the sea occurs during stochastic, heterogeneous blooms that are not easily predicted or resolved by marine expeditionary field work [*Karl, et al.*, 2002]. Furthermore the rates are reported for the amount of N fixed over a period of a year, when at BATS it is known that N_2 fixation occurs only during the spring/summer months [*Orcutt, et al.*, 2001]. It is not clear whether this is the case

for the entire Atlantic Ocean. Therefore the values quoted in Table 3.1 could be an underestimate or an overestimate. In an attempt to resolve the mismatch between the known supplies of N to the surface Atlantic and the observed N export, the percentage of N export that could be supported by N_2 fixation has been calculated (Table 3.1). The values vary greatly (4% to 267%), but this is a crude estimate as it has been assumed that all the N introduced to the surface waters via N_2 fixation is exported to deeper waters, when actually a large proportion of the new N will remain in the euphotic zone and be remineralised. However, despite the assumptions made in table 3.1, the range of estimates highlights the on going debate regarding the importance of N_2 fixation in the Atlantic Ocean and demonstrates the need for further work in understanding its role in the N budget.

Location	Comment	Average areal Estimates mol N m^{-2} y^{-1}	N_2 fixation supporting percentage of N export[§]	Reference
Sargasso Sea, N. Atlantic	***Trichodesmium*** extrapolation	0.26 – 1.31	53 – 267%	[*Carpenter and Romans*, 1991]
N. Atlantic	***Trichodesmium*** extrapolation	0.06 – 0.16	12 – 37%	[*Lipschultz and Owens*, 1996a]
Sargasso Sea, N. Atlantic	N*, residence time	0.18 – 0.91	37 – 186%	[*Michaels, et al.*, 1996]
N. Atlantic (10°-50°N, 25°-90°W)	Integrated N*, N:P	0.07 (0.11)[†]	14% (22%)[†]	[*Gruber and Sarmiento*, 1997]
BATS	C_I inventory	0.38	75%	[*Gruber, et al.*, 1998]
Atlantic (40°N - 40°S)	C_I inventory	0.04	10%	[*Lee, et al.*, 2002]
BATS	C_I inventory	0.18	36%	[*Anderson and Pondaven*, 2003]
N. Atlantic (15°-22°N, 25°-75°W)	Excess nitrate	0.02 – 0.08 (0.04 – 0.11)[†]	5 – 15% (8 – 23%)[†]	[*Hansell, et al.*, 2004]
N. Atlantic (10°-40°N, 35°-75°W)	Excess nitrate	0.02 – 0.09	4 – 19%	[*Bates and Hansell*, 2004]
N. Atlantic	^{15}N isotope mass balance	0.31	63%	[*Capone, et al.*, 2005]
All N. Atlantic	***Trichodesmium*** extrapolation	0.07	15%	[*Capone, et al.*, 2005]
N. Atlantic	**Unicellular bacterioplankton** extrapolation	0.02	4%	[*Falcon, et al.*, 2004]

Table 3.01 Average areal estimates of the amount of N that N_2 fixation introduces to the Atlantic Ocean based on various geochemical and direct approaches (Adapted from *Capone, et al.*, 2005 and *Mahaffey, et al.*, 2005) [§]Average N export of 0.49 mol N m^{-2} y^{-1} [*Jenkins and Goldman*, 1985; *McGillicuddy, et al.*, 1998] [†]Assuming an N:P ratio of 45 for diazotrophs rather then 125 as originally computed by Gruber and Sarmiento [1997] (N:P ratio of 125 based on observations by Karl et al. [1992]. N:P ratio of 45 of the prominent N_2 fixer, *Trishodesmium* sp. [*Mahaffey et al.*, 2005 and references therein]).

3.2 Approach

3.2.1 Stable nitrogen isotopes as a tool in identifying N pathways

The study of $\delta^{15}N$ in water has revealed how the phototrophic assimilation of nitrogen operates and its dynamics in aquatic ecosystems [*Fogel and Cifuentes*, 1993]. While the two stable isotopes, ^{14}N and ^{15}N (99.634% and 0.366% by atoms respectively) behave chemically in a similar way to one another [*Owens*, 1987] , during uptake of inorganic N by marine microorganisms, ^{14}N is preferentially consumed relative to the heavier ^{15}N isotope leading to biological fractionation in favour of the lighter isotope in the organisms cell [*Montoya and McCarthy*, 1995]. However, in environments such as the oligotrophic regions of the Atlantic Ocean where nitrogen is limiting, nitrogen is completely sequestered by the autotroph, there is no fractionation and the isotopic composition of the source-N is reflected within the organism [*Altabet and McCarthy*, 1985] (Fig 3.03).

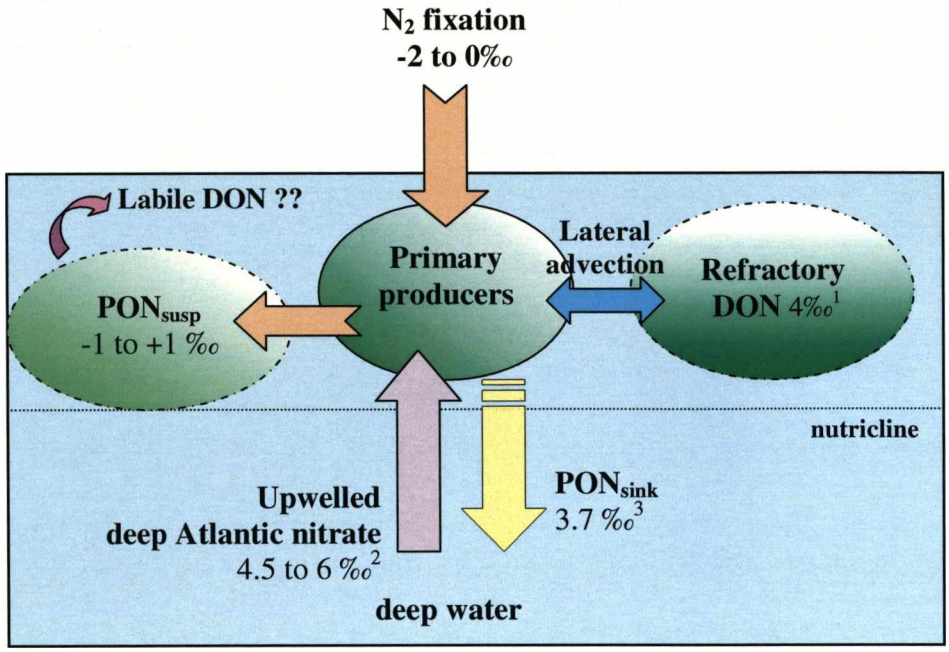

Figure 3.03 Pathways of N with corresponding $\delta^{15}N$ values of the N pools in the oligotrophic Atlantic Ocean. $\delta^{15}PON_{sink}$ taken from sediment trap at 100m depth [1][*Knapp, et al.*, 2005], [2][*Knapp, et al.*, 2005; *Liu and Kaplan*, 1989] [3][*Altabet*, 1988].

The key sources of N are now briefly discussed in terms of their isotopic signal. The sources of N that can lead to a depleted signal in the $\delta^{15}N$ PON_{susp} include atmospheric N_2 (0‰) [*Minagawa and Wada*, 1986], the wet deposition of NO_3^- (-2.1‰ to -5.9‰) [*Hastings, et al.*, 2003], marine derived atmospheric NH_4^+ (-5‰ to –8‰) [*Jickells, et al.*, 2003b] and remineralised N (primarily NH_4^+; -2‰) [*Checkley and Miller*, 1989].

In contrast, deep nitrate is isotopically enriched with values in the Atlantic Ocean ranging between 4.5‰ and 6‰ [*Knapp, et al.*, 2005; *Liu and Kaplan*, 1989; *Sigman, et al.*, 1997]. The enriched signal of nitrate reflects the remineralisation of PON, principally from the PON_{susp} rather than the sinking pool (PON_{sink}). The more abundant PON_{susp} pool becomes isotopically enriched with depth through progressive decomposition and removal of dissolved N species depleted in ^{15}N [*Altabet*, 1988]. The

$\delta^{15}N$ PON_{sink} is also initially enriched with depth [*Altabet*, 1996], although $\delta^{15}N$ PON_{sink} then becomes isotopically depleted deeper in the ocean interior, either due to a loss of an enriched N fraction or by sorption of ^{14}N rich compounds [*Altabet, et al.*, 1991; *Nakatsuka, et al.*, 1997; *Voss, et al.*, 1996]. The isotopic signature of dissolved organic nitrogen (DON) is also important, since aside from molecular N_2, it is the largest available nitrogen pool in the surface waters of the oligotrophic gyres (Fig. 2 a) [*Berman and Bronk*, 2003; *Jackson and Williams*, 1985; *Roussenov, et al.*, 2006]. At BATS, $\delta^{15}N$ values for DON were consistently found to be in the range of 3.5‰ to 4.5‰ in the upper 100 m over 12 months. However, the stability in both concentrations and the N isotopic composition of DON suggests that this DON pool is mainly recalcitrant and not assimilated by phytoplankton [*Knapp, et al.*, 2005].

3.2.2 Stable isotopes – Theory

Natural variations in stable isotopic ratios occur when the specific reaction rates vary for chemical species containing different isotopes of an element [Altabet, 1996]. This chemical fractionation occurs because a chemical bond, which involves a heavier isotope, has a lower vibrational frequency and is thereby stronger than the equivalent bond involving a lighter isotope. Thus, the probability of a ^{14}N-X bond breaking is greater than for compounds containing ^{15}N-X [Owens, 1987].

In the reporting of the isotopic composition of biological materials the δ (‰) notation is used since natural variability is small (3.2),

$$\delta = \frac{R_{sample} - R_{standard}}{R_{standard}} - 1 \times 1000 \qquad (3.2)$$

where R is the ratio of the light isotope to the heavier isotope of the sample or the standard. This isotopic ratio or fractionation (3.3) is defined as

$$\alpha = \frac{X_{h.p} / X_{h.s}}{X_{l.p} / X_{l.s}} \qquad (3.3)$$

where X_h is the heavy isotope, X_l is the light isotope, *s* is the substrate and *p* is the product [Fogul and Cifuentes, 1993]. Fractionation factors (ε) are often transformed to the same units as 'δ' notation (3.4) [Altabet, 1996]

$$\varepsilon = (\alpha - 1) \times 1000 \qquad (3.4)$$

Mass balance dictates that the isotopic ratio of the substrate increases as a function of depletion of the heavy isotope (3.5) as governed by Rayleigh fractionation

$$\delta_{substrate\,(f)} = \delta_{substrate\,(f=1)} - \varepsilon \times \ln (f) \qquad (3.5)$$

where f is the fraction of unutilised substrate (Fig 3.04) [Altabet, 1996]. If the product is in a closed system, its observed δ as it accumulates is given by the integral of the combination of equations 3.3 and 3.4 with respect to f (3.6)

$$\delta_{product\,(f)} = \delta_{substrate\,(f=1)} + f / (1-f) \,.\, \varepsilon \,.\, \ln (f) \qquad (3.6)$$

Here mass balance requires that the δ of the substrate at f = 1 equals the δ of the product at f = 0 (Fig 3.4) [Altabet, 1996].

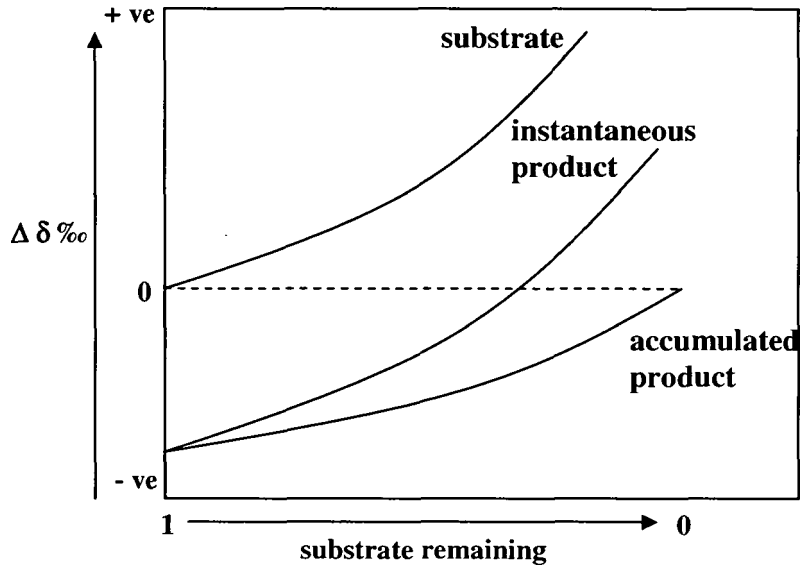

Figure 3.04 Diagram illustrating the changes in δ of a substrate, instantaneous product and accumulated product during a simple one step substrate to product reaction. Adapted from Owens [1987] and Altabet [1996].

3.3 Methods

3.3.1 Sampling protocol

Suspended particulate organic nitrogen samples on AMT 12, 14 and 16 were collected using Stand Alone Pumps (SAPs; Challenger Oceanic; see Chapter 2 for cruise details and Fig. 2.02 for cruise tracks; see Appendix B for list of stations). Two GF/F filters (293 mm diameter; Whatman; pre-combusted at 400°C, >4 hours) were placed on the filter bed with the top filter being used for the analysis. The SAPs were deployed to

depths of 50, 100 and 150 m and pumped ~1000 L seawater in 90 minutes. The filters were removed and wrapped in pre-combusted (400°C >4 hours) aluminium foil and frozen (-20°C) until further analysis in the laboratory. Prior to analysis, filters were lypholised (-60°C; 10^{-2} Torr, 24 h).

3.3.2 Determination of PON, POC and chlorophyll a

Concentrations of particulate organic carbon (POC) and particulate nitrogen (PN) were determined as described by Kiriakoulakis et al [2004]. Briefly, analyses of freeze-dried SAPS filters were carried out in duplicate (analytical error < 10 %; CE Instruments NC 2500 CHN analyser), on aliquots of known area (~130 mm^2), using the HCl vapour method of Yamamuro and Keyanne [1995]. Chlorophyll *a* concentrations were determined from Niskin water bottle samples and the underway non-toxic water supply by Dr. Alex Poulton (National Oceanography Centre, UK) using a fluorometric assay of the acetone extract of particulate material collected on a GF/F filter [*Welschmeyer*, 1994]. Chlorophyll *a* concentrations were also obtained from an *in situ* fluorometer fitted on the CTD rosette sampler frame, data being calibrated against the field samples.

3.3.3 Determination of $\delta^{15}N\ PON_{susp}$

Isotopic analyses of PON_{susp} were conducted at the Marine Science Institute Analytical Lab, University of California by Robert Petty. Analyses were carried out directly on filter aliquots (314 mm^2) without decarbonation. The samples were analysed using a Thermo Finnigan Delta-Plus Advantage isotope ratio mass spectrometer (IRMS),

coupled to a Costech Instruments ECS 4010 elemental combustion system ("EA") via a Thermo Finnigan Conflo III open-split interface. The EA was equipped with a Costech Zero Blank autosampler, utilizing a 32-position, large-capacity sample wheel. Sample $\delta^{15}N$ ratios were measured relative to atmospheric nitrogen, where

$$\delta^{15}N = \left[\frac{(^{14}N/^{15}N)_{sample}}{(^{14}N/^{15}N)_{standard}} - 1 \right] \times 100\% \quad , \qquad (3.7)$$

with the samples calibrated against a variety of primary standards, and normalized for weight-to-δ bias and calibration offset using a secondary isotope ratio standard (acetanilide).The samples were analysed in duplicate (i.e. two separate aliquots of the filter were analysed) and the precision can be obtained by taking the variation of the mean of the two measurements made. The average of this mean was found to be ±0.95 ‰. The accuracy of the analysis was determined by combining errors associated with measuring both the primary standards and the acetanilide standard, which gave the accuracy to be ± 0.4‰.

3.3.4 Determination of Inorganic Nitrate and Phosphate

Inorganic nitrate and phosphate concentrations in seawater samples collected on all cruises and were analysed on board by Malcolm Woodward and Katie Chamberlain (Plymouth Marine Laboratory, UK) using a Technicon segmented flow colorimetric autoanalyser [*Woodward and Rees*, 2001]. Analytical precision was ± 2 - 4% with reproducibility errors in the same range.

3.3.5 *Validity of data - trophic tests*

PON_{susp} is derived from phytoplankton, but may also be modified by organisms from higher trophic levels by grazing and the microbial loop. When N is assimilated by zooplankton, there is an enrichment of ~ 3‰ [*Minagawa and Wada*, 1986], which is significant when using isotopic data to infer N sources to the phytoplankton. In order to determine if higher trophic particulate material has affected the measured $\delta^{15}N$ in the present study, the relationships between POC and PON:$\delta^{15}N$ PON_{susp} with chlorophyll *a* were examined. Organisms of higher trophic levels feeding on suspended particles significantly alter both POC and PON_{susp}, leading to enhanced values of POC/Chlorophyll *a* and PON/Chlorophyll *a* [*Waser, et al.*, 2000]. If the PON_{susp} material measured is principally derived from heterotrophs rather than autotrophs, a positive relationship would be expected between these ratios and $\delta^{15}N$ PON_{susp}. At a confidence level of 95% ($P< 0.05$; T-test), no statistically-significant positive or negative relationship was found in the individual or collective cruise data sets, which implies that the measured $\delta^{15}N$ PON_{susp} is representative of autotrophic PON (Fig 3.05).

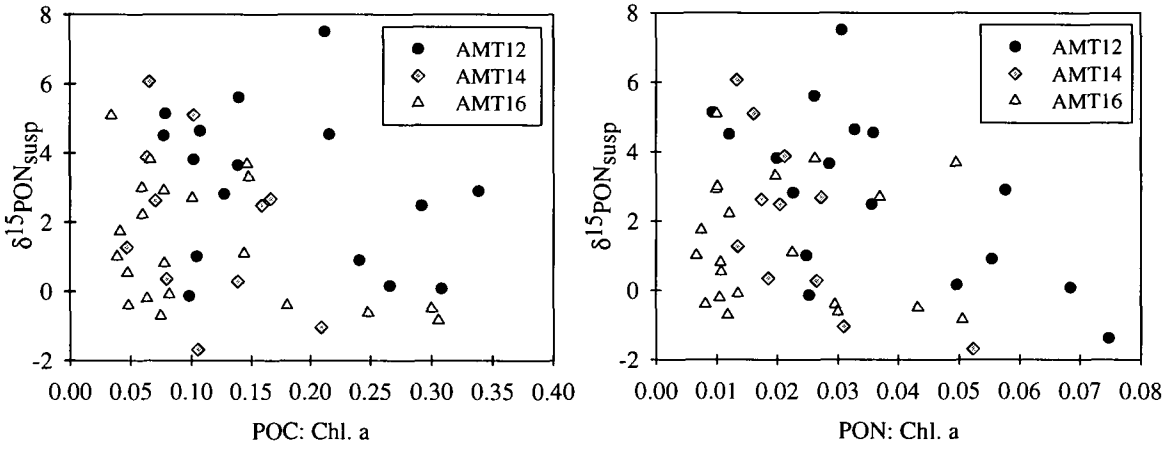

Figure 3.05 Trophic tests to determine if δ^{15}Nmeasured in the PON_{susp} represents principally autotrophic derived material as opposed to a major heterotrophic influence. The lack of any significant positive relationship demonstrates that the PON_{susp} predominantly comprises of lower trophic level particulate material

3.4 Nitrate and Isotopic N Distributions

3.4.1 Nitricline structure of the Atlantic Ocean

The AMT cruise transects pass through distinct biogeochemical regimes of the Atlantic Ocean as revealed by the nitrate concentrations of the upper 300 m of the water column (Fig 3.06). The nitricline varies meridonally, reflecting the background gyre structure and pattern of convection. The nitricline is deepest at 30°N and 25°S over the central parts of the subtropical gyres where there is downwelling and subduction, and is shallowest from 10°S to 15°N in the tropics where upwelling occurs. The nitricline also shallows polewards from the subtropical gyres, typically outcropping at 40°S in the south Atlantic and north of 45°N in the northern subpolar gyre.

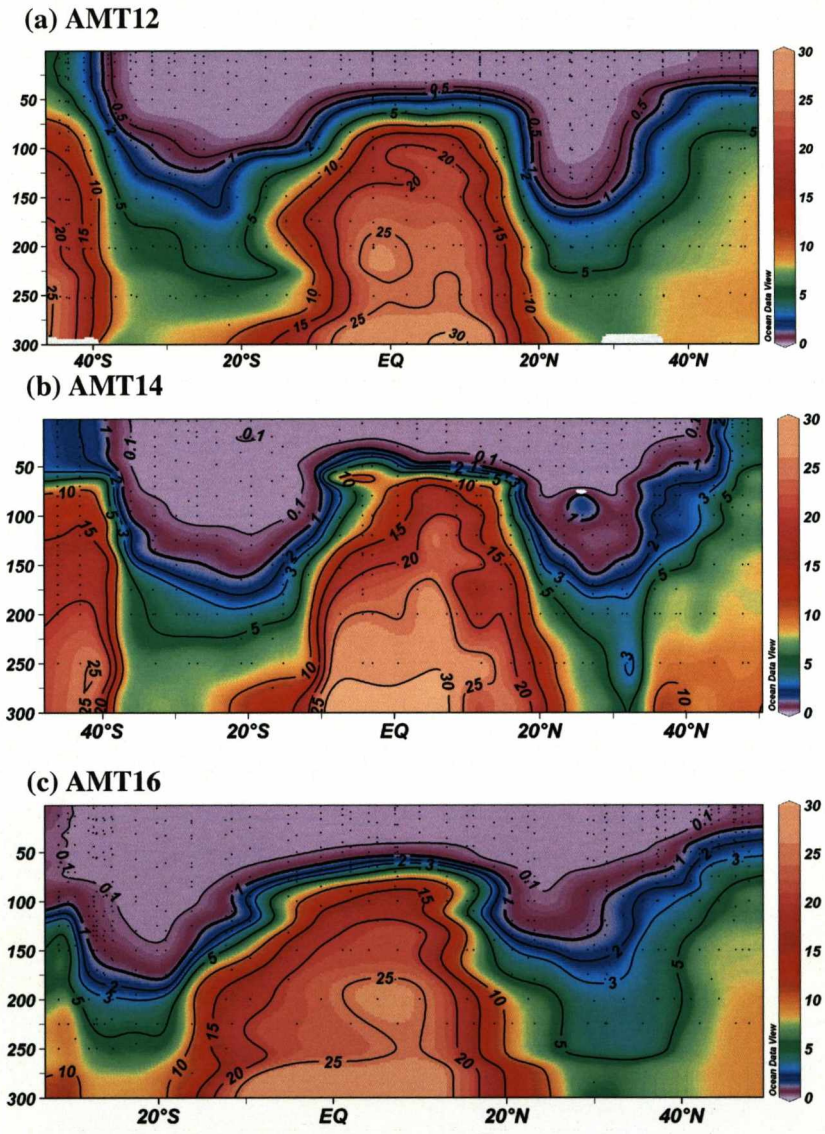

Figure 3.06 Meridonal nitrate (μM) sections, with the nitricline defined at 1 μM. The nitricline varies in a consistent manner annually. Strong upwelling is observed at the equator while there is a characteristic deep nitricline witnessed to the north and south of the equator, which characterises the oligotrophic gyres.

3.4.2 Spatial variability of the $\delta^{15}N$ PON_{susp} in the Atlantic

The $\delta^{15}N$ PON_{susp} has been measured in the Atlantic Ocean between 45°S and 50°N (AMT12, 14 & 16). In order to consider the general variations in the $\delta^{15}N$ PON_{susp}, the data have been averaged separately above and below the nitricline (previously defined at 1 μM).

3.4.2.1 Spatial variability above the nitricline

For all three transects a consistently depleted signal (-1 to 0‰) is observed in the northern basin between 7°N and 31°N, compared with an enriched signal of 4 - 7‰ at the equator and further north at 40°N (Fig 3.07 a). With regards to the AMT12 and 14 transects, enriched values of 5‰ are found at 40°S which become depleted (0‰) at 33°S and then subsequently enriched towards the equator. Signals along the AMT16 transect show a different pattern in the South Atlantic in that between 27°S and 12°S the $\delta^{15}N$ PON_{susp} gradually depletes from 3.2‰ to 1.6‰.

3.4.2.2 Spatial variability below the nitricline

Meridonal sections of the $\delta^{15}N$ PON_{susp} reveal a more enriched signal, as expected, below the nitricline (Fig. 3.07 b) compared with above the nitricline. The southern gyre (3.7 – 5.5‰) is slightly more enriched than the northern gyre (3 – 4‰), with even greater enrichment (6 – 8‰) being observed at the equator, at the southern flanks of the southern gyre and at the northern flanks of the northern gyre.

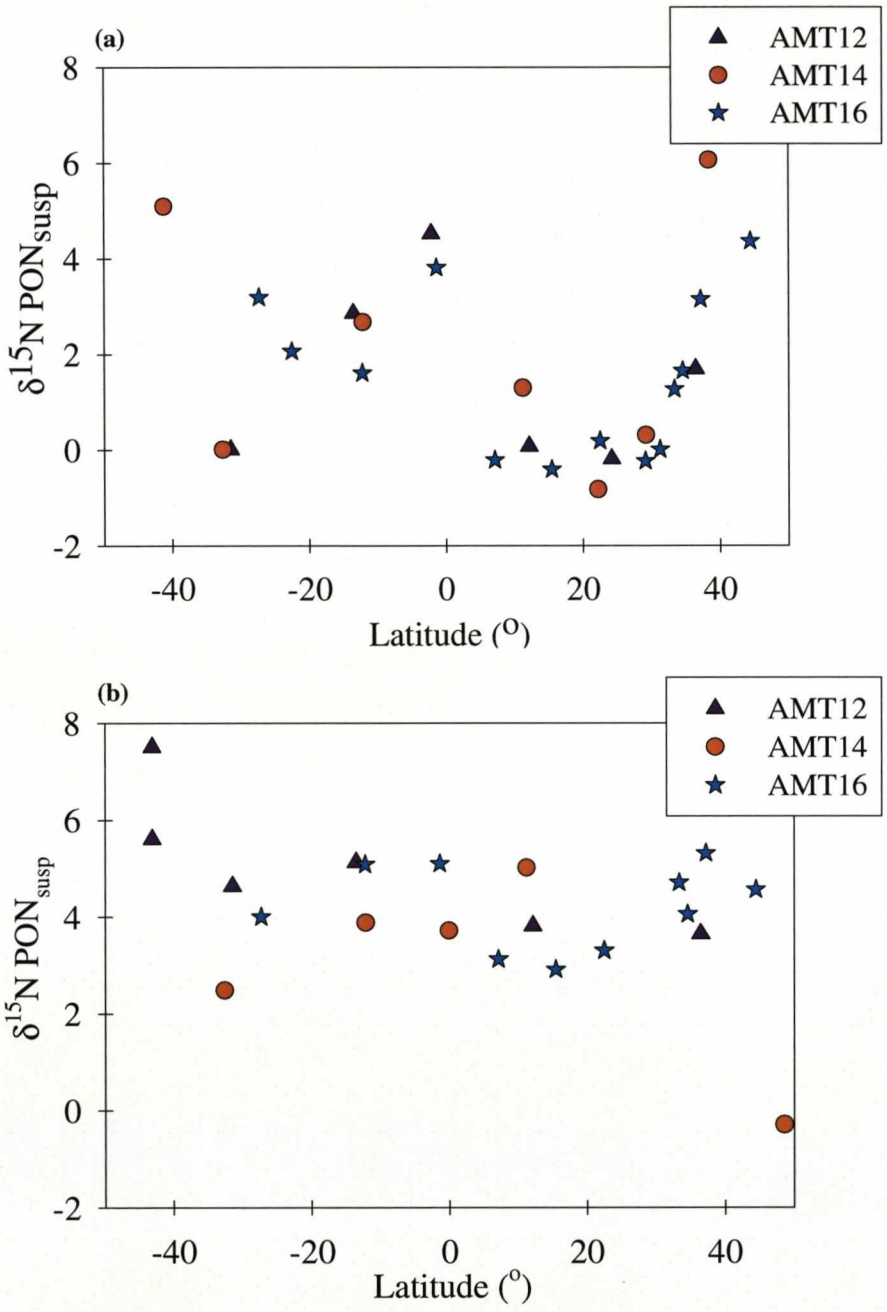

Figure 3.07 Meridonal variations in $\delta^{15}N$ PON_{susp} for data averaged (a) above the nitricline and (b) below the nitricline.

3.5 How are the $\delta^{15}N$ PON_{susp} signals controlled?

3.5.1 Enriched signals

At the equator, the enriched $\delta^{15}N$ PON_{susp} signal coincides with the nitricline (>1μM) shoaling to depths as shallow as 40m and is attributed to the wind-induced upwelling of nitrate rich waters. Deep Atlantic nitrate has a $\delta^{15}N$ range of 4.5‰ to 6‰ [*Knapp, et al.*, 2005; *Liu and Kaplan*, 1989]. On the northern flank of the northern gyre, isotopic enrichment might result from deep NO_3^- supplied by convection at the end of the winter. On the southern flank of the southern gyre the enriched $\delta^{15}N$ PON_{susp} implies a source of deep NO_3^-; this NO_3^- is probably supplied as part of the northern transport of intermediate waters from the Southern Ocean.

The enrichment in isotopic values with depth in the oligotrophic gyres shows a strong relationship with the nitricline. Phytoplankton lying at or below the nitricline utilise the deep nitrate providing enriched isotopic N and leading to enrichment of PON_{susp}. The dominant phytoplankton at the base of the euphotic zone, are thought to be primarily responsible for particulate export in the oligotrophic gyres, while smaller lower protists dominate surface waters where they are involved in an efficient microbial loop [*Azam, et al.*, 1983; *Poulton, et al.*, 2006a]; This may explain the isotopic gradient in the photic zone. If the deeper-dwelling phytoplankton are indeed enriched in $\delta^{15}N$ as suggested by the present data set, and if they are the main contributors to export production, then this could explain the enriched values of PON_{sink} at the base of the euphotic zone [*Altabet*, 1996], which subsequently deplete isotopically with depth [*Altabet, et al.*, 1991; *Nakatsuka, et al.*, 1997; *Voss, et al.*, 1996]. Alternatively, the

enrichment of $\delta^{15}N$ PON_{susp} with depth may simply reflect its greater degree of degradation [*Altabet,* 1988].

3.5.2 Depleted signals

The low values of $\delta^{15}N$ PON_{susp} within the northern and southern oligotrophic gyres of the Atlantic Ocean might reflect three distinct N sources:

(i) The uptake of remineralised compounds excreted by zooplankton, principally NH_4^+ [*Biggs*, 1977; *Corner and Davies*, 1971], which are depleted in ^{15}N. In oligotrophic regions, where phytoplankton take up and assimilate all nitrogen excreted by zooplankton, there is little or no overall isotopic fractionation [*Checkley and Miller*, 1989] and thus, $\delta^{15}N$ PON_{susp} is depleted.

(ii) Direct fixation of dissolved N_2 by marine diazotrophs gives rise to depleted $\delta^{15}N$ of PON [*Carpenter, et al.*, 1997; *Mahaffey, et al.*, 2003; *Minagawa and Wada*, 1986].

(iii) Uptake of isotopically light N supplied to the surface ocean by atmospheric deposition could give rise to depleted $\delta^{15}N$ PON_{susp} [*Hastings, et al.*, 2003].

Modelled atmospheric fluxes of N to the surface North Atlantic Ocean are only in the range of 0.003 – 0.007 mol N m^{-2} yr^{-1} [*Dentener, et al.*, 2006; *Galloway, et al.*, 2004; *Prospero, et al.*, 1996]. *In situ* aerosol measurements along the AMT transect showed a dry N deposition flux of ~0.01 mol N m^{-2} yr^{-1} [*Baker, et al.*, 2003] in the same region where there is the depleted signal of $\delta^{15}N$ PON_{susp} in the northern subtropical gyre. These estimates of atmospheric deposition appear to be relatively unimportant in sustaining export production, since they are much smaller than the export flux of 0.42

and 0.56 mol N m^{-2} yr^{-1} determined for the western subtropical North Atlantic [*Jenkins and Goldman*, 1985].

Hence, N_2 fixation or the uptake of regenerated N are the most likely processes responsible for the depleted $\delta^{15}N$ PON_{susp}. To distinguish between the two processes, the relative size of the NO_3^- and PO_4^{3-} pools can be considered. Redfield stoichiometry [*Redfield*, 1958] is perturbed by N_2 fixation in favour of NO_3^- relative to PO_4^{3-}. A quasi-conservative tracer, N*, which utilises a linear combination of NO_3^- and PO_4^{3-} (3.8) has been used to define the distribution of N_2 fixation and denitrification at the basin scale [*Gruber and Sarmiento*, 1997],

$$N^* = (N - 16P + 2.90\ \mu mol\ kg^{-1})\ 0.87\ . \qquad (3.8)$$

Gruber and Sarmiento [1997] suggest that high values of N* are due to the remineralisation of N-rich organic matter from diazotrophic organisms (see Section 4.32 for further analysis). Meridional sections of the upper 300m of the Atlantic over 3 years reveal that high N* values consistently lie below the photic zone in the northern gyre (Fig. 3.08). These signals are in accord with the climatological analysis of *Gruber and Sarmiento* [1997].

The localised region of depleted $\delta^{15}N$ PON_{susp} at 32°S found in the austral autumn might be due to a localised patch of N_2 fixation or through uptake of remineralised N, since N* values lie between 1 and -1 over the entire southern basin (Fig. 3.08). However, the data set for the South Atlantic is rather limited and it is difficult to provide a reliable explanation for the depleted $\delta^{15}N$ PON_{susp} signal there.

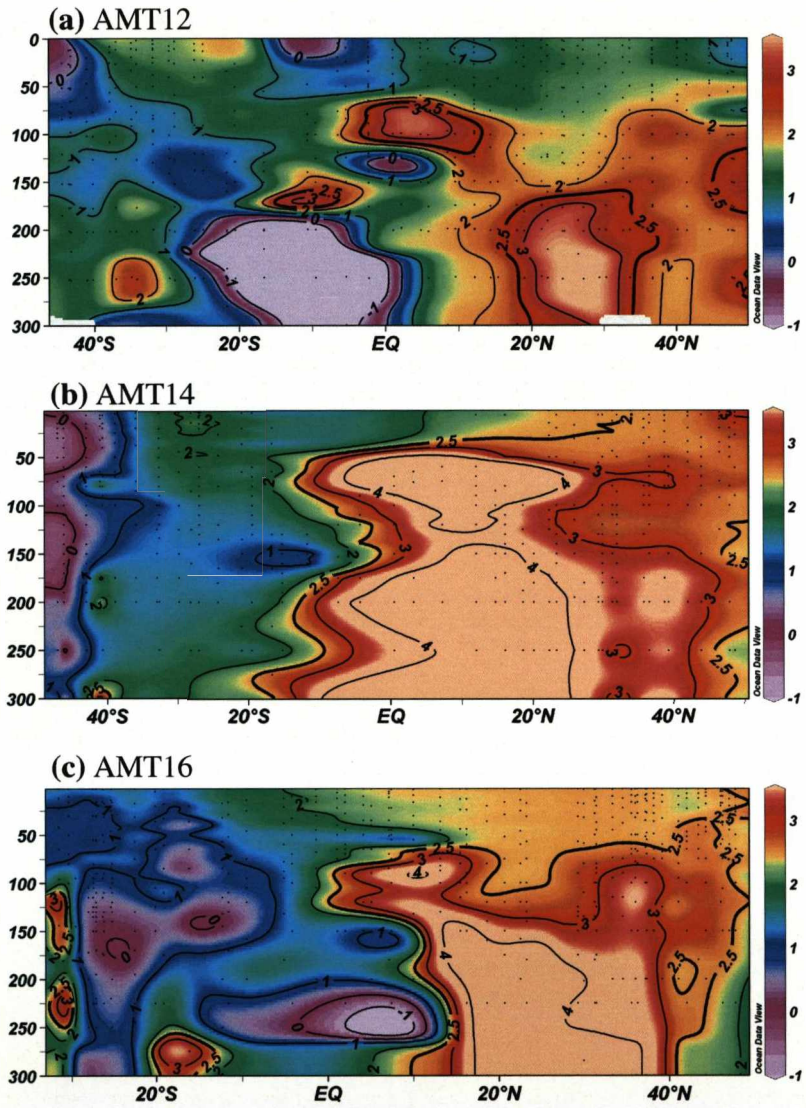

Figure 3.08 Plotted latitudinal sections of N* in the upper 300m of the Atlantic Ocean (a) AMT12, (b) 14, (c) 16. The difference in N* between the northern and southern gyre is noticeable and the elevated N* in the northern gyre is a consistent feature.

3.6 Synthesis of the Atlantic Ocean

3.6.1 Spatial extent of the depleted isotopic N signal

A synthesis of $\delta^{15}N$ PON_{susp} data for samples collected above the nitricline has been made by collating data from the present study and from AMT10 surveyed [*Mahaffey, et al.*, 2004; *Mahaffey, et al.*, 2003] (Fig. 3.09 a). In the northern gyre between 25°W and 55°W, there is an extensive region of depleted $\delta^{15}N$ PON_{susp}, while elevated values occur in the more temperate waters of the Northeast Atlantic and off the west coast of Africa. In the South Atlantic, there are low values of $\delta^{15}N$ PON_{susp} in the centre of the subtropical gyre, with more enriched values off the east coast of South America and at the equator.

The robustness of these signals is assessed by calculating the standard deviation (σ) and the standard error ($\sigma / \sqrt{n}$) based upon the number of independent data points (n) (Fig. 3.09 c, d). Within the northern gyre, the zone of depleted $\delta^{15}N$ reveals little variability and low standard errors are implied from the independent data points. Thus, the extensive region of depleted $\delta^{15}N$ PON_{susp} appears to be a robust signal. However, on the eastern side of the north Atlantic basin, there is a large standard deviation and standard error, reflecting how conditions are more variable there with upwelling off the west coast of Africa and convection in the north east Atlantic. The variability of the signals in the South Atlantic is small where there is data, but the data coverage is too limited to infer any robust signals.

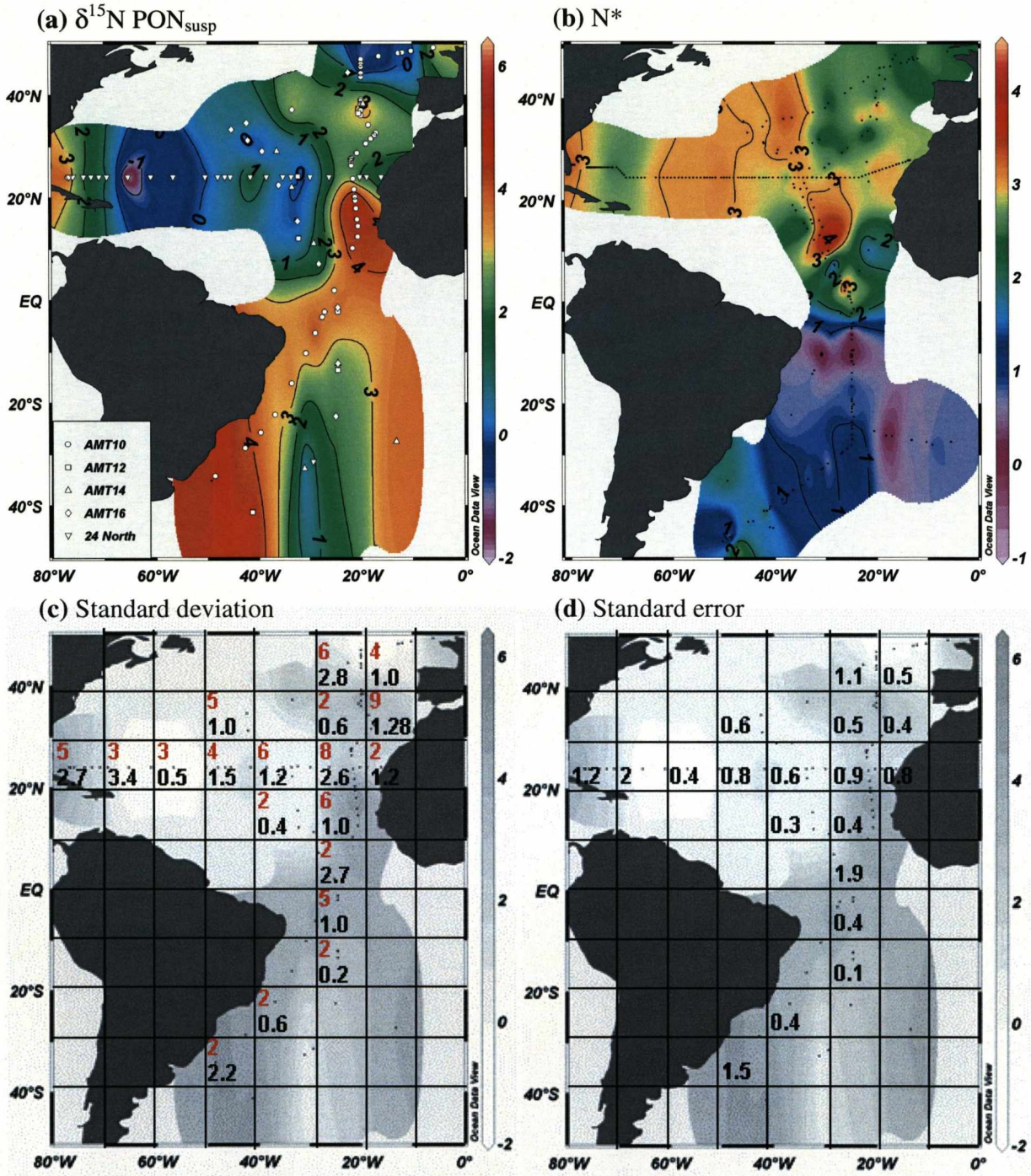

Figure 3.09 Horizontal structure of (a) $\delta^{15}N$ PON_{susp} above the nitricline demonstrating local patches of inferred N_2 fixation. (b) Widespread elevated N* values over entire northern basin, values averaged from below the nitricline to 300m. (c) Standard deviation of $\delta^{15}N$ PON_{susp} (black) along with the number of data points (red.). (d) Standard error of $\delta^{15}PON_{susp}$.

3.6.2 *Spatial extent of elevated N**

The depleted $\delta^{15}N$ PON_{susp} signal in the northern subtropical gyre coincides with N* having a local maximum between 10°N and 30°N in the centre of the gyre (Fig. 3.09 a & 3.10 a, b). N_2 fixation is only reliably implied from N* when this tracer increases following the flow [*Deutsch, et al.*, 2001], i.e. N_2 fixation leads to enhanced N:P ratios in the underlying thermocline following a moving water mass. Thus, elevated N* over the North Atlantic only provides a crude bulk measure of N_2 fixation occurring in the basin, instead, it is the gradient in N* created by horizontal transport which is a more accurate indicator of the source region. Comparing our N* signals (Fig. 3.10 b) and the latest drifter data (Fig. 3.10 c) [*Lumpkin and Pazos*, 2006] suggests that the local maximum in N* occurs where there is westward flow on the southern flank of the subtropical gyre. Thus, in our view, the most likely region of N_2 fixation in the North Atlantic is between 35°W – 50°W and 15°N – 30°N, where there is both depleted $\delta^{15}N$ PON_{susp} and a westward increase in N* following the gyre circulation.

This region of potential N_2 fixation is subject to enhanced dust inputs from the Saharan Desert, which provide the limiting nutrients (P and Fe) for marine diazotrophs [*Mills, et al.*, 2004] and creates an ideal niche for N_2 fixation to occur. In support of this view, *Mahaffey, et al* [2003] reported a natural fertilisation event in the North Eastern Atlantic with coincident signals of depleted $\delta^{15}N$ PON_{susp}, phytopigments indicative of cyanobacteria and prochlorophytes, and elevated N:P ratios in the thermocline.

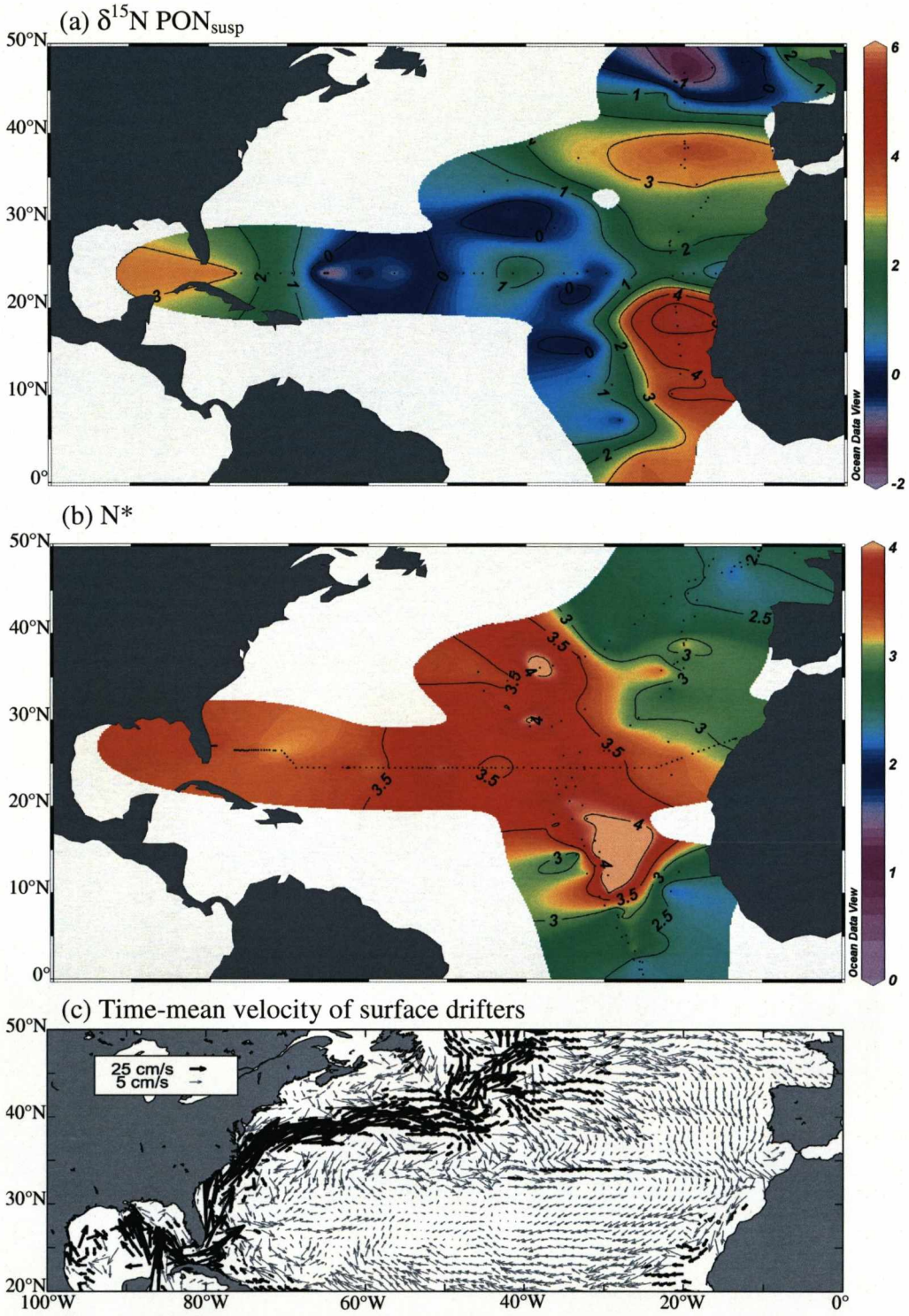

Figure 3.10 (a) $\delta^{15}N$ PON_{susp} above the nitricline for the North Atlantic, depleted signal seen over much of the central subtropical gyre; (b) N* (values averaged below the nitricline down to 300 m) for the North Atlantic; (c) Time-mean velocity of surface drifters [*Lumpkin and Pazos*, 2006], westward flow of 5 cm s^{-1} at 20°N coincides with elevated N*, revealing the non-conservative behaviour of N*, thus the most likely region of N_2 fixation in the North Atlantic is between 30°W – 50°W and 15°N – 30°N.

3.6.3 N_2 fixation – local or far-field signatures?

The region of depleted $\delta^{15}N$ PON_{susp} appears to be more confined than the N* signal, which extends over much of the North Atlantic. This mismatch poses the question of whether these signals reflect local or far field control? It has been previously suggested that the N* signal could be advected around the northern basin with the gyre circulation [*Hansell, et al.*, 2004]. Whilst at the surface, NO_3^- and PO_4^{3-} have very short residence times due to their rapid uptake by photoautotrophs, below the euphotic zone these nutrients are not utilised rapidly. Therefore, the NO_3^- and PO_4^{3-} can be advected within the thermocline without much modification and, thus, distribute the N* signal around the northern gyre. In turn, the isotopic signal might partially reflect the effect of advection. However, the lifetime of PON_{susp} is only 30 to 60 days in the euphotic zone [*Charette, et al.*, 1999] suggesting that PON_{susp} might be advected 150 to 300km, assuming a typical surface velocity of 5cm s^{-1} in the gyre interior. Therefore, the different extent of the N* and depleted N isotopic signals reflects their different lifetimes.

3.7 Significance of N_2 fixation within the North Atlantic.

3.7.1 Role of N_2 fixation in providing new N to PON_{susp}

There has been some controversy surrounding the importance of N_2 fixation as a source of new N to the oligotrophic regions of the North Atlantic. At BATS in the Sargasso Sea, the percentage contribution of new N from N_2 fixation [*Knapp, et al.*, 2005] determined both from direct *in situ* rate measurements and geochemical estimates

varies from 2% [*Orcutt, et al.*, 2001] to 8% [*Gruber and Sarmiento*, 1997]. A simple 2-end member mixing model (3.9) is applied to the present North Atlantic data set in order to estimate the percentage contribution of new N supplied via N_2 fixation through the PON_{susp} pool (Table 3.2).

The domain is separated into a region on the western side of the north Atlantic subtropical gyre (65°W - 80°W, 20°N - 40°N), the centre of the oligotrophic gyre (30°W - 65°W, 7°N - 32°N) and also the eastern side of the gyre (5°W - 32°W, 7°N - 40°N). Within these regions, the average $\delta^{15}N$ PON_{susp} was identified, and the percentage contribution of new N that N_2 fixation contributes to the PON_{susp} pool was then estimated using three boundary $\delta^{15}N$ values for deep nitrate (4‰, 4.5‰ and 5‰) and a value of -1‰ for N_2 fixation:

$$\left(\frac{\delta^{15}N\ PON_{susp} - \delta^{15}N\ N_2}{\delta^{15}N\ NO_3 - \delta^{15}N\ N_2}\right)\times 100\% \qquad (3.9)$$

Given the three choices for the boundary values of deep NO_3^-, the percentage contribution of N from N_2 fixation to the PON_{susp} pool within the central part of the subtropical gyre is estimated to range between 72% (±4%) and 77% (±3%) (Table 3.2), with the errors representing the standard error of the $\delta^{15}PON_{susp}$ signals. On the western side of the gyre, the contribution of N_2 fixation was found to be lower in the range of 48% (±25%) to 57% (±21%) and lower again on the eastern side of the basin from 25% (±8%) to 37% (±7%). Hence, N_2 fixation is clearly important over the central part of the northern subtropical gyre in providing new N to the PON_{susp} pool, but less important on

the western and eastern sides of the subtropical gyre. This difference suggests that other processes become important on the western and eastern sides of the gyre: on the western side, eddy transfer of nitrate close to the western boundary current is likely to be important [*Williams and Follows*, 2003] and, on the eastern side, the lateral transfer of nitrate and DON from coastal upwelling [*Roussenov et al.*, 2006].

Northern subtropical gyre	Western side (65°W - 80°W, 20°N - 40°N)	Centre (30°W - 65°W, 7°N - 32°N)	Eastern side (5°W – 30°W, 7°N - 40°N)
Average $\delta^{15}PON_{susp}$	**1.6‰**	**0.4‰**	**2.8‰**
n	8	21	28
Standard deviation	3.5	1.1	2
Standard error	1.3	0.2	0.4
	% contribution of N from N_2 fixation to PON_{susp} ± Standard Error[4]		
4‰[1] for deep NO_3^-	48% ± 25%	72% ± 5%	25% ± 8%
4.5‰[1] for deep NO_3^-	53% ± 23%	75% ± 4%	31% ± 7%
5‰[1] for deep NO_3^-	57% ± 21%	77% ± 4%	37% ± 6%
	Nutrient concentrations and % of total N		
$[PON_{susp}]$[3] % to total N pool	0.1μM 1.9%	0.3μM 6.8%	0.2μM 4.7%
$[NO_3^-]$[2] % to total N pool	0.1μM 1.9%	0.02μM 0.4%	0.08μM 1.9%
[DON][2] % to total N pool	5.1μM 96.2%	4.1μM 92.8%	4.0μM 93.4%
	% contribution of N from N_2 fixation through PON_{susp} to total N pool ± Standard error[4]		
4‰[1] for deep NO_3^-	**0.9%** ± 0.5%	**4.8%** ± 0.3%	**1.2%** ± 0.4%
4.5‰[1] for deep NO_3^-	**1.0%** ± 0.4%	**5.1%** ± 0.3%	**1.5%** ± 0.3%
5‰[1] for deep NO_3^-	**1.1%** ± 0.4%	**5.2%** ± 0.2%	**1.7%** ± 0.3%

Table 3.02 Estimates of the percentage contribution of new N that N_2 fixation provides to the PON_{susp} pool and subsequently to the total N pool over separate regions of the northern subtropical gyre. [1][*Knapp, et al.*, 2005; *Liu and Kaplan*, 1989; *Sigman, et al.*, 1997]. [2]Mean concentration (averaged above 1 μM nitricline) over region. [3]Typical concentrations (averaged above 1 μM nitricline) for each region. [4]Standard error associated with the $\delta^{15}N$ PON_{susp}, based upon ($\sigma / \sqrt{n}$) where σ is the standard deviation and n is the number of independent data points.

3.7.2 Role of N_2 fixation in providing new N to the total N pool.

The isotopic calculation is now extended to estimate the percentage contribution of new N that N_2 fixation introduces via PON_{susp} to the total N pool. The total N pool is defined here by DON, NO_3^- and PON_{susp}; while PON_{sink} is important in the export of N out of the euphotic zone, PON_{sink} makes only a minor contribution to the total N pool [*Wakeham and Lee*, 1989]. Within the centre of the northern gyre, the PON_{susp} pool represents only ~6.8% of the total N (Fig 3.01, Table 3.2). Thus, the average contribution of new N supplied from N_2 fixation via PON_{susp} to the total N pool is 5.0% (±0.3%) again with the errors representing the standard error of the $\delta^{15}PON_{susp}$ signals for the region (Table 3.2) At the western and eastern sides of the gyre the contribution of new N supplied from N_2 fixation via the PON_{susp} are even smaller and only typically reach 1.0% (±0.4%) and 1.5% (±0.3), respectively.

The contributions of NO_3^- and DON now need to be considered in the total N pool. DON dominates the total N pool in surface waters accounting for 93 – 96% across the northern basin, while surface NO_3^- represents only 0.4 – 1.9% of the total N pool. While no measurements of $\delta^{15}N$ NO_3^- or $\delta^{15}N$ DON were made in the present study, data are available from BATS with typical values of 3.5‰ for surface NO_3^- and 4‰ for DON (Table 3) [*Knapp, et al.*, 2005]. Using these data, applying the 2-end member mixing model (3) to the western side of the northern subtropical gyre suggests that the new N supplied to the total N pool from N_2 fixation via DON is 8.2% (±8%) and via NO_3^- is 0.3% (±0.1%) with the error range now representing the standard deviation of the estimates obtained from the choice of three boundary $\delta^{15}N$ values for deep NO_3^-. Thus, our estimate of the total supply of new N from N_2 fixation reaches 9.2% (±4.5%) over

the western side of the northern subtropical gyre. If the same calculations were applied to the central and eastern regions of the North Atlantic including the DON and NO_3^- pools there (Table 3.3), the total supply of new N from N_2 fixation would be 13.7% and 9.2% respectively. However, since it is unlikely that $\delta^{15}N$ DON or $\delta^{15}N$ NO_3^- are the same across the entire northern basin, these estimates are speculative. Further work is necessary to determine the stable N isotopic composition of components of the N pool in order to understand the different sources of N utilised by phytoplankton.

Northern subtropical gyre	**Western side** (65°W - 80°W, 20°N - 40°N)			
	4 ‰ for deep NO_3^-	4.5‰ for deep NO_3^-	5‰ for deep NO_3^-	**Mean ± Standard Deviation[2].**
$[PON_{susp}]^+$ and % to total N pool	0.1μM 1.9%	0.1μM 1.9%	0.1μM 1.9%	
% contribution of N from N_2 fixation through PON_{susp} to total N pool	0.9%	1.0%	1.1%	**1.0%** ±0.1
$[NO_3^-]^1$ and % to total N pool	0.1μM 1.9%	0.1μM 1.9%	0.1μM 1.9%	
% contribution from N_2 fixation through surface NO_3^- to total N pool	0.2%	0.3%	0.5%	**0.3%** ±0.1
$[DON]^1$ and % to total N pool	5.1μM 96.2%	5.1μM 96.2%	5.1μM 96.2%	
% contribution from N_2 fixation through DON to total N pool	0%	8.7%	16.1%	**8.2%** ±8.0
	Total % contribution from N_2 fixation to total N pool			**9.2%** ±4.5

Table 3.3 2 end-member mixing model (4) applied to surface NO_3^- and DON to gain an estimate for the percentage contribution of new N that N_2 fixation makes via surface PON_{susp}, NO_3^- and DON over the western side of the northern subtropical gyre. $^+$ See table 3.2 for details ^{1}Typical concentrations (averaged above 1 μM nitricline) for region. Range of boundary values used for deep NO_3^- whilst δ^{15}DON is 4‰ and $\delta^{15}N$ surface NO_3^- is 3.5‰ (average at 100m at BATS) [*Knapp, et al.*, 2005]. ^{2}Standard deviation of the estimates obtained from the three boundary values chosen for deep NO_3^-

3.8 Wider context

The isotopic mass balance method employed in this study reveals that nitrogen fixation varies over the northern subtropical gyre, accounting for 72% to 76% of the PON_{susp} in the central region (30°W - 65°W, 7°N - 32°N) and 27% to 40% in the western region of the gyre (65°W - 80°W, 20°N - 40°N). In comparison, using the same method, *Montoya, et al.* [2002] estimates the contribution of nitrogen fixation to PON_{susp} of 30 – 40% over the tropics (25°W - 60°W, 0° - 15°N) and the western side of the gyre (42°W - 80°W, 7°N - 28°N); likewise, *Capone, et al.* [2005] estimates a similar contribution of 36% over the western side of the gyre (42°W - 80°W, 7°N - 28°N). These estimates of *Montoya et al* [2002] and *Capone et al* [2005] are consistent with our estimates over our western region, but are lower than our estimates over the central region of the subtropical gyre. *Montoya et al* [2002] and *Capone et al* [2005] used the same 2-end member mixing model (3), but with a more depleted $\delta^{15}N$ value for N_2 fixation of -2‰, rather than our boundary value of -1‰. Our estimates for nitrogen fixation for the central region only decrease to 60 – 65% when this lower boundary value of -2‰ is instead used. Thus, the contrasting estimates of nitrogen fixation over the central part of the subtropical gyre could reflect differences in the precise location and timing of each survey.

On previous AMT cruises (1 – 8), the nitrogen fixing cyanobacteria *Trichodesmium* spp. was found to be most abundant to the north of the equator (0 – 15°N). *Tyrrell et al.* [2003] estimated that nitrogen fixation provided >20% of total new N input in these tropical waters. This estimate is greater than this studies estimates of nitrogen fixation providing ~9% of the total N pool in the western North Atlantic and the

speculative 14% in the central part of the subtropical gyre, but these differences might easily be accounted for by the different regions, timing and uncertainties in the studies.

In our view, N_2 fixation leads to the extensive depleted $\delta^{15}N$ PON_{susp} over the North Atlantic subtropical gyre, as well as the westwards increase in N* following the gyre circulation along 20°N. This view is in accord with independent studies suggesting that N_2 fixation occurs in the Atlantic Ocean and provides a significant source of N phytoplankton to the subtropical Northern gyre [*Capone, et al.*, 2005; *Gruber and Sarmiento*, 1997; *Michaels, et al.*, 1996]. However, the importance of N_2 fixation in providing an area-integrated flux is uncertain, since estimates range from 0.03 – 0.3 mol N m^{-2} y^{-1} (see *Capone, et al.*, 2005 for full details). This uncertainty reflects the difficulty of providing area-averaged estimates for a process associated with blooms, which are spatially heterogeneous and often short lived.

3.9 Conclusions

A unique data set of stable isotopic data for $\delta^{15}N$ PON_{susp} is presented for the Atlantic Ocean. Over the central part of the subtropical northern gyre, there was an extensive signal of depleted $\delta^{15}N$ PON_{susp}. This signal was persistent and robust, being observed over 3 years. The PON_{susp} signal was primarily autotrophic rather than heterotrophic, based upon interpretation of the isotopic signals, particulate organic carbon, nitrogen and chlorophyll *a* levels.

The extensive depleted isotopic signal might be formed either by N_2 fixation or recycling. N_2 fixation appears to be the more plausible explanation, since the depleted

signals occur in a region where there is a westwards increase in the quasi-conservative tracer N* following the gyre circulation along 20°N.

Estimates of the percentage contribution of new N that N_2 fixation introduces via the PON_{susp} pool to the total N pool have been calculated using a two-end member mixing model. This estimate typically reaches ~ 74% in the centre of the oligotrophic gyre. Since the phytoplankton are included in the PON_{susp} pool, this underlines the importance of N_2 fixation as a source of new N to the primary producers. However, PON_{susp} accounts for only ~ 6.8% of total N in the centre of the gyre, so the contribution to the total N pool of new N from N_2 fixation is only 5%. If this estimate is repeated at the western side of the gyre including isotopic values for NO_3^- and DON [*Knapp et al.*, 2005], then ~9% of new N can be accounted for by N_2 fixation. This estimate is likely to be only slightly higher over the central part of the subtropical gyre, but further isotopic values are needed for DON and surface NO_3^- to provide a reliable estimate. It seems, therefore, that N_2 fixation can be an important source of N to the phytoplankton, but is unlikely to account for the mismatch in the supply of N and the observed export production for the subtropical gyre.

There is clearly a need for further work in obtaining measurements of $\delta^{15}N$ NO_3^- and DON in the North Atlantic in order to identify the relative importance of the different pathways of N through the marine system.

CHAPTER 4

The distributions and processes affecting amino acids in the Atlantic Ocean

4.1 Introduction

Amino acids are the building blocks of proteins; peptide chains of amino acids are formed through bonding between the amino and carboxylic acid functional groups. (Fig. 4.01). There are twenty protein amino acids, with glycine being the simplest.

In the marine environment, amino acids are the most abundant forms of N in phytoplankton [*Nguyen and Harvey*, 1997] and occur in particulate (e.g. [*Lee and Cronin*, 1984]) and dissolved (e.g. [*Hubberten, et al.*, 1994]) material. The dissolved amino acids are operationally separated into fractions, namely dissolved free amino

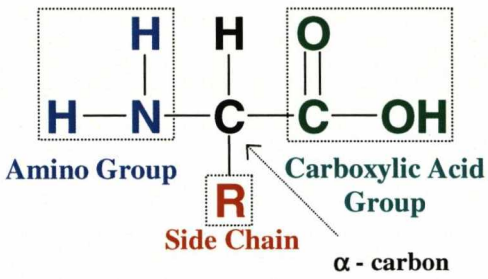

Figure 4.01 General structure of an amino acid, with the amine, carboxylic acid group and R group labelled. For each of the 20 amino acids the R side chain is different.

acids (DFAA) which are considered labile [*Fuhrman and Ferguson*, 1986] and the total hydrolysable amino acids (THAA) which are semi-labile [*Keil and Kirchman*, 1993]. Whilst dissolved amino acids are primarily products of protein hydrolysis by bacterial proteases [*Flynn and Butler*, 1986], they can also be released by phytoplankton [*Andersson, et al.*, 1985; *Hammer and Brockmann*, 1983; *Hellebust*, 1965; *Nagata and Kirchman*, 1991], representing 9 – 45% of total phytoplankton exudate [*Carlucci, et al.*, 1984]. Zooplankton also excrete dissolved amino acids [*Carlson*, 2002] as do bacteria [*Ogawa, et al.*, 2001]. Other sources of dissolved amino acids arise through sloppy feeding of microplankton by zooplankton [*Fuhrman*, 1987a] and the viral lysis of bacteria [*Middelboe and Jorgensen*, 2006].

Particulate amino acids (PAA) can make upto 25-50% of particulate organic carbon in surface waters [*Lee and Cronin*, 1984] and 50% of particulate organic nitrogen [*Lee*, 1988]. The major source of particulate amino compounds in the marine environment is by photosynthetic production of phytoplankton [*Lee*, 1988].

With the exception of glycine, amino acids exist in two enantiomeric forms, where the molecules are exact mirror images of one another i.e. they are non-superimposable. The enantiomers rotate the plane of polarised light in opposite

directions in equal amounts and are assigned to either the D- or L- form. This designation was once related to the Latin *levorotatory* (*l*), rotating the plane of polarised light to the left and *dextrorotatory* (*d*), rotating the plane of polarised light to the right. However, some molecules have been found not to correctly rotate the plane of polarised and the Fischer convention of labelling molecules is now more commonly used. Using the Fischer convention, molecules are named by the spatial configuration of its atoms. With regards to amino acids, if the R-side chain is placed below the α or chiral carbon, the amine acid group is to the left for L-amino acids and to the right for D-amino acids (Fig 4.02). Like most organisms, marine phytoplankton almost exclusively produce L-amino acids [*Jorgensen, et al.*, 1999]

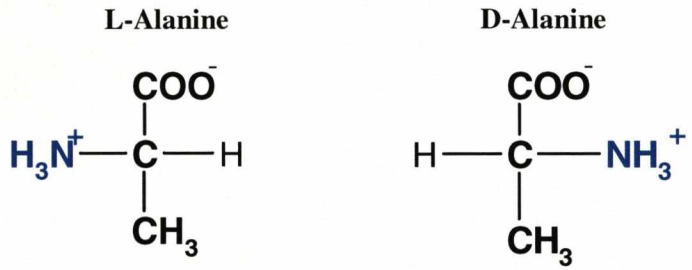

Figure 4.02 Structures of L-alanine and D-alanine drawn using the Fischer convention where the amine group (in blue) for L-alanine is to the left of the chiral carbon and for D-alanine is to the right of the chiral carbon.

D-amino acids in marine samples are thought to be primarily derived from bacterial cell walls e.g. [*Dittmar, et al.*, 2001; *Jorgensen, et al.*, 1999; *Lee and Bada*, 1977; *McCarthy, et al.*, 1998], where peptidoglycan is a major source of D-alanine, D-aspartic acid and D-glutamic acid [*Schleife.Kh and Kandler*, 1972] (Fig, 4.03).

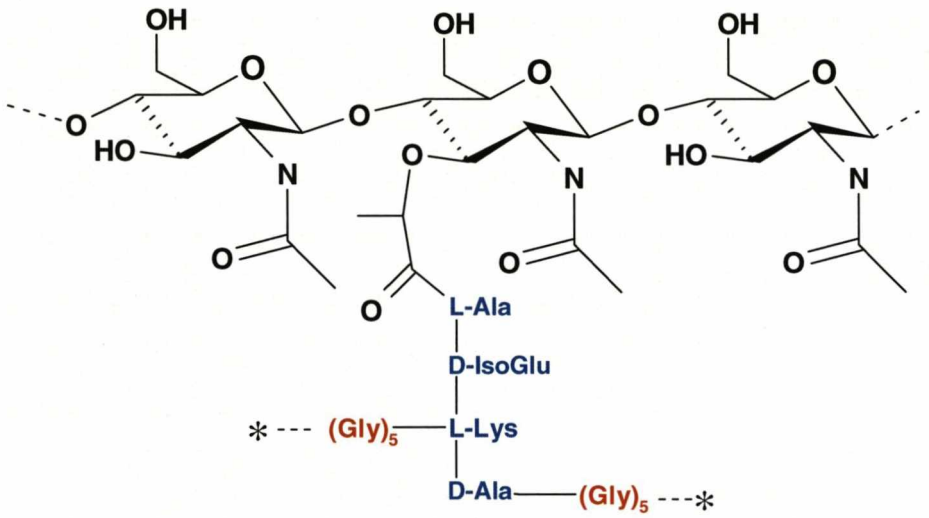

Figure 4.03 Structure of peptidoglycan, a component of bacteria cell walls. The D-amino acids occur in the peptide chains through bonding with *N-Acetyl muramic acid.

Examination of the D/L ratios of dissolved organic nitrogen (DON) has revealed that bacteria are a significant source of N to the dissolved pool in many marine environments [*Dittmar, et al.*, 2001; *Grutters, et al.*, 2002; *Jones, et al.*, 2005; *Jorgensen and Middelboe*, 2006; *Jorgensen, et al.*, 1999; *McCarthy, et al.*, 1998].

4.1.1 Objectives of this study

Identifying and quantifying dissolved and particulate amino acids in the marine environment can be a valuable tool in gaining further understanding of the marine N cycle.

The major objectives of this study were:

(i) To determine the DFAA, THAA and PAA concentrations along the AMT transect;

(ii) To determine the relative 'age' of the organic N along the AMT transect;

(iii) To assess the role of bacteria and archaea in the production and recycling of DON and PON.

If amino acids are utilised by autotrophs/heterotrophs as a source of N in the Atlantic Ocean, then amino acid concentrations would be expected to decrease towards the centres of the oligotrophic gyres away from neighbouring upwelling regions. Furthermore the relative 'age' of the organic N might be expected to be greater in the oligotrophic gyres with respect to the highly productive upwelling zones since the organic N would be scavenged by primary producers and thus subjected to a higher degree of degradation.

4.2 Methodology

4.2.1 Sampling regime

On AMT14 (28th April 2004 – 1st June 2004) seawater samples for analyses of DFAA and THAA were collected daily (11:00, local time) from the chlorophyll maximum using a Sea-Bird CTD Rosette sampler fitted with Go-Flo bottles. Depths of the chlorophyll maximum ranged from ~50 m near the equator to ~150 m in the centre of the northern sub-tropical gyre. On AMT16 seawater was collected in the same way (0300, local time; see Appendix C for station positions and depths). A Pyrex bottle (1L; rinsed with Milli-Q 18.2 MΩ water) was used to recover the seawater from the GoFlo bottle. The samples were then filtered through a GF/F filter (25 mm diameter; Whatman; pre-combusted at 400°C, >4 hours) using a glass syringe (100 ml; acid rinsed, 10% HCl and rinsed with Milli-Q water) and stainless steel filter holder into glass vials (2 x 7 ml;

pre-combusted at 400°C, > 4 hours). The samples were then stored (-20°C) until analysis in the laboratory.

Samples for the determination of particulate amino acids were collected on AMT16 using large volume Stand Alone Pumps (SAPs; Challenger Oceanic). Two GF/F filters (293 mm diameter; Whatman; pre-combusted at 400°C; >4 hours) were placed on the filter bed with the top filter being used for the analysis. The SAPs were deployed to depths of 50, 100 and 150m and pumped ~1000 L seawater in 90 minutes. The filters were wrapped in pre-combusted (400°C; >4 hours) aluminium foil and frozen (-20°C) until further analysis in the laboratory. Prior to analysis, filters were lypholised (-60°C; 10^{-2} Torr; 24 h).

4.2.2 Sample Preparation

4.2.2.1 Dissolved free amino acids (DFAA)

For the analysis of DFAA no further preparation was required apart from the addition of an internal standard. In this instance, of L-homoarginine (150μL of 100 μM) was added to the sample (850 μL), which resulted in a final internal standard concentration of 15 nM.

4.2.2.2 Hydrolysis of dissolved fraction

In order to measure THAA, water samples were hydrolysed under acidic conditions following a method modified from *Jones* [2003]. The sample was defrosted and an aliquot (850μL) was taken and placed in a glass culture tube. To this L-

homoarginine (internal standard; 150µL of 100 µM) was added to give a final internal standard concentration of 15 nM. Oxygen-free nitrogen gas was bubbled through the sample (1 minute) before and after the addition of hydrochloric acid (1ml; 6 M). The tubes were sealed with Teflon lined lids and placed in an oven (6 hours; 110°C). Once cooled, the samples were freeze dried (-60°C; 10^{-2} Torr) overnight to remove the acid and then resuspended into 1ml HPLC grade water and frozen until analysis.

4.2.2.3 Particulate amino acids

Preparation of particulate amino acid samples also involved acid hydrolysis. Four filter aliquots of known diameter and area (20mm diameter, 314 mm^2) were removed with a punch from the GF/F SAP filters and subsequently cut into smaller pieces and placed into a glass culture tube for extraction. L-homoarginine (0.1 - 0.4 mL; 89.79 µM) was added to the tube. Oxygen-free nitrogen was bubbled through the solution (1 minute) prior to and after the addition of hydrochloric acid (1 ml; 6 M). The tube was subsequently sealed with a Teflon lined screw top and placed in an oven (110°C; 6 hours). Once cooled, the sample extract was filtered through extracted glass wool. The extract was freeze-dried (-60°C; 10^{-2} Torr; 12 h) and then re-suspended in HPLC grade water (1 – 2 mL) and centrifuged. The supernatant was removed and filtered through a cellulose nitrate filter (0.45 µm) using a glass syringe prior to HPLC analysis.

4.2.3 HPLC analysis

4.2.3.1 HPLC equipment

An Agilent 1100 Series high performance liquid chromatography system was employed for the analysis of amino acids. The system comprises of a quaternary pump with solvent cabinet, vacuum degasser and a four channel gradient pump; an automated sampler and injector; a thermostated column compartment set at 25°C fitted with a Thermo Electron Corporation BDS Hypersil C18 column; a fluorescence detector set with an excitation wavelength of 330 nm and an emission wavelength of 445 nm and the photomultiplier tube (PMT) gain was at position 12. Agilent Chem Station software was utilised for instrument control, data acquisition and data evaluation.

4.2.3.2 Solvent and Reagent Preparation

All solvents used: water, methanol and acetonitrile were of HPLC (HiPerSolv) grade. However to reduce the contamination of the HPLC system, methanol was redistilled prior to use.

4.2.3.2.1 Sodium acetate buffer

A solution of buffer (23 mM) was prepared by dissolving 3.13 g of sodium acetate-3-hydrate (AnalaR) in of HPLC grade water (1 L). The pH was adjusted to 6.00 ± 0.01 with 10% glacial acetic acid. This solution was then filtered through a cellulose nitrate membrane filter (47 mm diameter; Whatman) and collected into a clean glass

flask. The sodium acetate buffer was made fresh at the beginning of every sequence set up.

4.2.3.2.2 Borate Buffer

Borate solution (1 M) was made by dissolving 6.183 g of boric acid in HPLC grade water (70 mL). The pH was adjusted using a solution of potassium hydroxide (10 M) solution prepared by dissolving 14.028 g of potassium hydroxide pellets in HPLC grade water (25 mL). 8.9 mL of this solution was required to adjust the pH to 10.5. This solution was then finally made up to 100 mL with HPLC grade water. The buffer was stable for two to three months (4°C; dark).

4.2.3.2.3 Derivatising Reagent

N-Iso-L-butyryl-L-cysteine (IBLC; 6.21 mg) and *o*-phthaldialdehyde (OPA; 2.85 mg) were weighed out and dissolved in HPLC grade water (375 μL) and 1.0 M borate buffer (125 μL). This resulted in a derivatising solution of the IBLC (260 mM) and OPA (170 mM) which remained stable for two days (4°C; dark)

4.2.3.3 Sample run

Amino acids were analysed for D- and L- amino acids following a method developed by *Kaufman and Manley* [1998]. A programmed injector performed pre-column derivatisation (Fig. 4.04) of the sample before introduction onto the column.

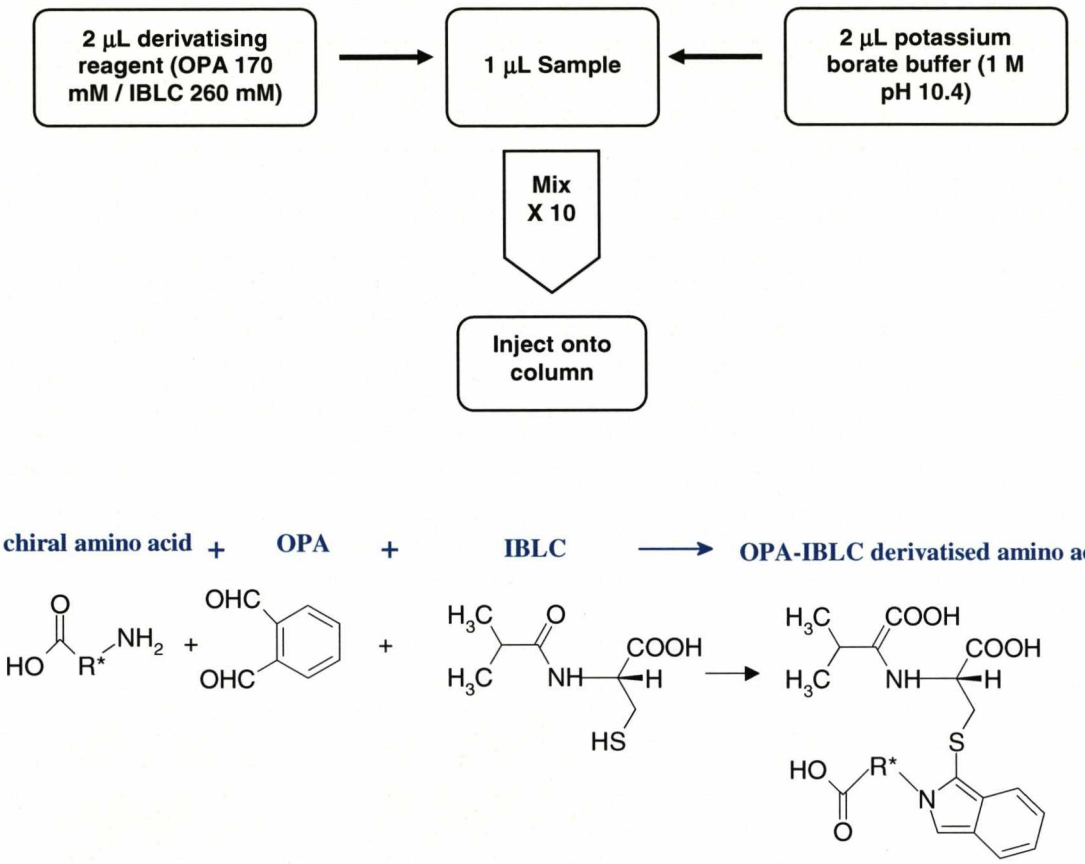

Figure 4.04 Reaction between a chiral amino acid and derivatising reagents *o*-phthaldialdehyde (OPA) and *N*-Iso-L-butyryl-L-cysteine (IBLC)

The sample was subjected to a stepped linear solvent gradient programme where water (A), methanol (B), acetonitrile (C) and 23 mM sodium acetate buffer (D) are the mobile phases (see Table 4.01). The flow was constant and ran at 0.5 mL/min with a total sample run lasting 120 minutes.

	Solvent B	Solvent C	Solvent D
Time (mins)	**% Methanol**	**% Acetonitrile**	**% Sodium acetate buffer**
0	5.0	0.0	95.0
2	5.0	0.0	95.0
31	23.0	0.4	76.6
75	50.0	2.0	48.0
85	95.0	5.0	0.0
95	95.0	5.0	0.0
105	5.0	0.0	95.0
120	5.0	0.0	95.0

Table 4.01 Solvent gradient programme for analysis of dissolved free and total hydrolysable D- and L- amino acids in seawater samples

The reproducibility of samples as a percentage of standard error was 29.6% (±5.8%) where blanks were typically 22.9% (± 5.2; standard error) of the sample concentration.

4.2.3.4 Quantification

4.2.3.4.1 Amino acid standards – preparation

In order to quantify amino acids, a suite of D- and L- amino acids of known concentration were analysed at the beginning of each sequence run (Fig. 4.04). Stock solutions of 10 mM (stored at -20°C) were made by dissolving χ mg (see table 4.02) of the required amino acid in HPLC grade water (1 mL). From the stock solutions, an amino acid standard working solution (50 µM) was made, by diluting stock solution (50 µL) of each amino acid (with the exception of L-homoarginine) with HPLC grade water in a volumetric flask (10 mL; pre-cleaned in a 10% nitric acid and thoroughly rinsed

with Milli-Q water; 18.2 $M\Omega cm^{-1}$ resistivity). This was subsequently separated into two equal aliquots, one being frozen (-20°C), while the other that was used daily was stored in a fridge (4°C), where it was stable for at least one month.

Amino acid	Molecular Weight	weight required
L-Alanine	89.09	0.8909 mg
D-Alanine	89.09	0.8909 mg
L-Arginine	210.67	2.1067 mg
D-Arginine	210.67	2.1067 mg
L-Aspartic Acid	133.10	1.331 mg
D-Aspartic Acid	133.10	1.331 mg
L-Glutamic Acid	147.13	1.4713 mg
D-Glutamic Acid	147.13	1.4713 mg
Glycine	75.06	0.7506 mg
L-Isoleucine	131.17	1.3117 mg
D-Isoleucine	131.17	1.3117 mg
L-Leucine	131.17	1.3117 mg
D-Leucine	131.17	1.3117 mg
L-Methionine	149.20	1.4920 mg
D-Methionine	149.20	1.4920 mg
L-Phenylalanine	165.19	1.6519 mg
D-Phenylalanine	165.19	1.6519 mg
L-Serine	105.09	1.0509 mg
D-Serine	105.09	1.0509 mg
L-Threonine	119.12	1.1912 mg
L-Valine	117.15	1.1715 mg
D-Valine	117.15	1.1715 mg
L-Homoarginine (IS)	224.69	2.2469 mg

Table 4.02 Amino acids with their corresponding molecular weights and the weight required to make a 10 µM/ml standard stock solution.

An amino acid standard of 2 nM concentration with an internal standard concentration of 10 nM was adequate for quantifying open ocean seawater samples (Fig. 4.05).

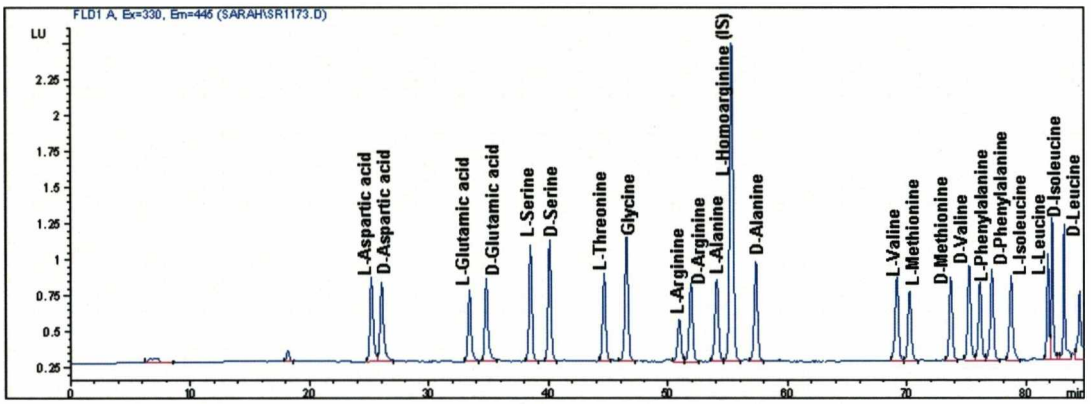

Figure 4.05 HPLC chromatogram of a 2 nM amino acid standard with 10 nM of internal standard (L-homoarginine) used to quantify open ocean samples.

4.2.3.4.2 Calculations

D- and L- amino acids concentration were calculated using response factors (see Appendix E for typical values) calculated from the amino acid standard (see equation 4.01).

$$Rf = \frac{A_A / A_{IS}}{[A] / [IS]} \qquad (4.01)$$

Where:
Rf = response factor

A_A = peak area of individual amino acid

A_{IS} = peak of internal standard

[A] = amino acid concentration (nM)

[IS] = internal standard concentration (nM)

The amino acid concentration in the seawater samples is then calculated using equation 4.02.

$$[A] = \left[\frac{A_S}{A_{IS}}\right] \times \left(C_{IS} \times \left[\frac{1}{Rf}\right]\right) \quad (4.02)$$

Where:

[A] = amino acid concentration in the sample (nM)

$\mathbf{A_S}$ = peak area of the amino acid within sample

$\mathbf{A_{IS}}$ = peak area of the internal standard added to sample

$\mathbf{C_{IS}}$ = concentration of internal standard added to sample (nM)

Rf = response factor

4.2.4 Total organic nitrogen

Total organic nitrogen was measured on samples from AMT14 and 16, however different methods were employed for the two cruises. AMT14 samples were taken from CTD casts and were subsequently analysed using the UV digestion technique following the method described by *Sanders and Jickells* [2000] by Dr. Sinhue Torres (National Oceanography Centre, Southampton).

Samples collected for TON analysis during AMT16 were analysed by high temperature catalytic oxidation following the method described by *Pan et al* [2005] by Mr. Xi Pan (National Oceanography Centre, Southampton).

4.2.5 Particulate organic nitrogen

Concentrations of particulate nitrogen (PN) were determined as described by [*Kiriakoulakis, et al.*, 2004]. See Chapter 3, section 3.3.2 for full details.

4.3 Results

4.3.1 Dissolved amino acids

4.3.1.1 Total Dissolved Amino Acids

Meridonal sections of total dissolved amino acids (DFAA + THAA) at the chlorophyll maximum along the Atlantic basin show variability along the transect and between the two cruises; AMT14 and AMT16. Concentrations of total dissolved amino acids (TDAA) differ mostly along the AMT14 (Fig 4.06 a) transect with greatest variability being found in the southern gyre (30°S - 10°S), where levels are in the range of 1 – 24 nM. At the equator concentrations of ~18 nM subsequently decrease towards the northern gyre (15°N - 43°N) where levels are less variable than in the southern gyre, ranging between 1 – 7 nM increasing to 9 nM at the northern flanks. Concentrations of TDAA along the AMT16 (Fig 4.06 b) transect are generally lower than for AMT14, nevertheless the general trends are similar. The greatest variability was once again in the southern gyre with values between 0.5 – 12 nM, whilst the northern gyre appears less variable with concentrations between 0.5 – 6.5 nM. In the equatorial region (10°S - 15°N) TDAA concentrations were between 2 - 4 nM.

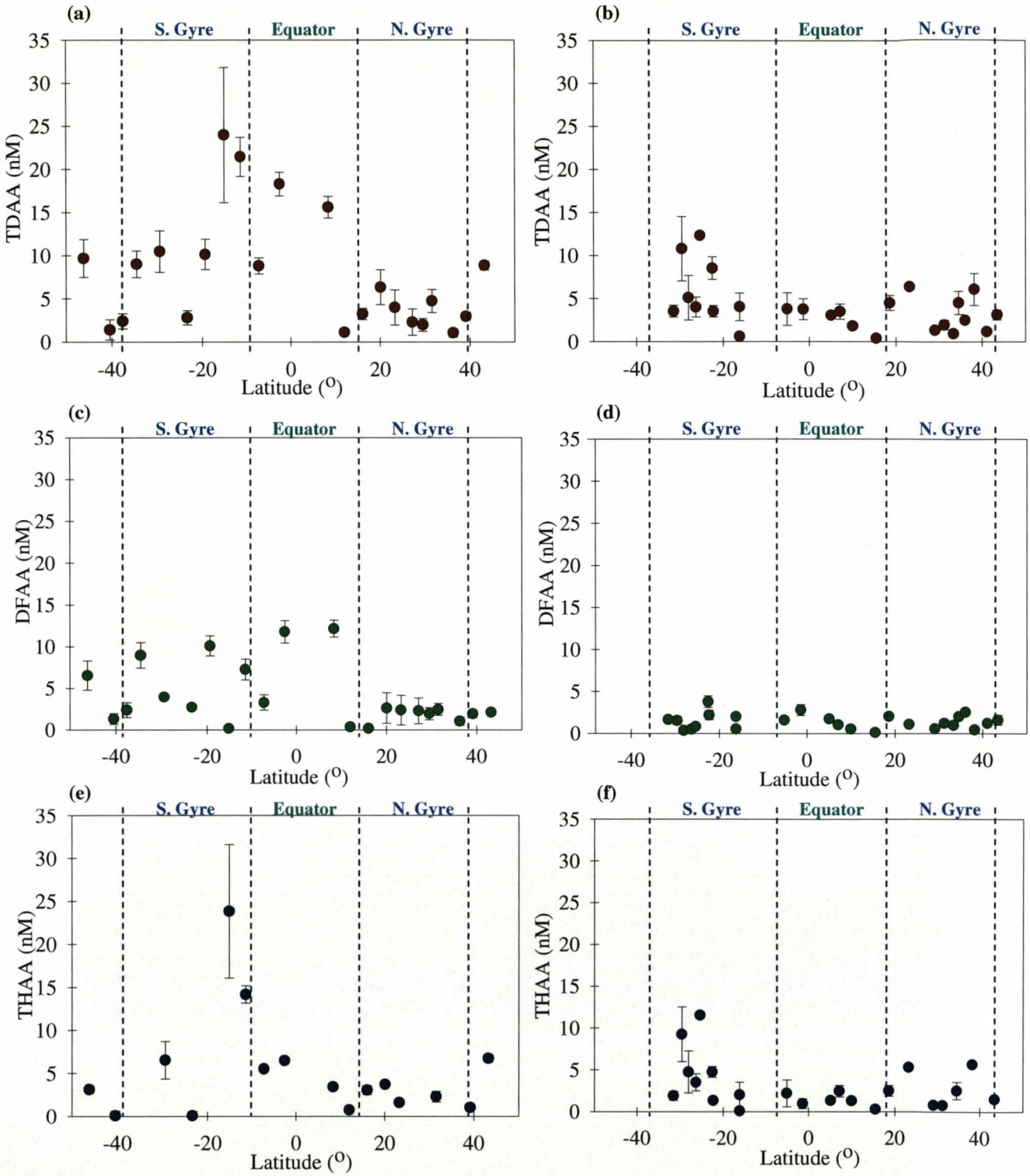

Figure 4.06 Total dissolved amino acids (a) AMT14 (b) AMT16; total dissolved free amino acids (c) AMT14 (d) AMT16; total hydrolysable amino acids (e) AMT14 (f) AMT16 at the chlorophyll maximum. Error bars represent the range of values (n=2). Biogeochemical regimes labelled.

4.3.1.2 Dissolved free amino acids

Concentrations of DFAA at the chlorophyll maximum along the AMT14 (Fig 4.06 c) transect ranged between 0.1 – 12 nM but were much lower, 0.2 – 4 nM along the AMT16 (Fig 4.06 d) transect. There was variability in the DFAA concentrations in the southern gyre (0.1 – 10 nM) during AMT14, which initially decreased towards the northern flanks of the southern gyre, and then increased to the greatest values found along the transect at the equator (12 nM). At the southern flanks of the northern gyre, levels of DFAA decrease dramatically to 0.4 nM, rise to 3 nM at 12°N, then remaining fairly stable in the northern gyre (1 – 3 nM). A similar pattern was observed for AMT16 despite concentrations being lower, with values ranging between 0.5 to 4 nM in the southern gyre, decreasing steadily at the southern flanks of the northern gyre to 0.2 nM. In the northern gyre DFAA showed little variation with concentrations ranging 0.2 – 2.5 nM.

4.3.1.3 Total hydrolysable amino acids

Total hydrolysable amino acids along the AMT14 (Fig. 4.06 e) transect at the chlorophyll maximum range between 0.2 and 23 nM with the highest concentrations being in the southern gyre. At the equator, levels are ~7 nM, decreasing in the northern gyre, where they range between 0.7 – 4 nM, then increasing slightly at the northern flanks of the northern gyre. Concentrations along the AMT16 (Fig. 4.06 f) transect again are lower than those found for AMT14. On the southern flanks of the southern gyre concentrations are at 10 nM which decrease to 0.6 nM in the gyre interior. Low levels

(0.8 – 2.5 nM) are observed at the equator, whilst in the northern gyre concentrations vary between 0.6 to 5 nM.

4.3.1.4 Contribution of Amino acids to TON

The molar percentage contribution of TDAA to total organic nitrogen (TDAA-N) is small (Fig. 4.07 a & b), with values ranging between 0.001 – 0.07%. AMT14 had higher TDAA-N than AMT16 with the highest percentage contribution at the equator (0.07%). In the southern gyre, values were variable with no apparent trend. To the north of the equator values initially decrease to 0.02% (6°N) and then subsequently increase to 0.05% at the southern flanks of the northern gyre. TDAA-N in the northern gyre are lower than the southern gyre ranging between 0.006 – 0.02%, however there is an increase in the contribution of TDAA to total organic nitrogen at the northern flanks of the northern gyre. Whilst the percentage contributions of TDAA-N to the TON are lower along the entire AMT16 transect when compared with AMT14, a similar pattern is observed, in particular to the north of the equator and the northern gyre. Values increase at the southern flanks of the northern gyre and subsequently decrease in the northern gyre interior where values are analogous with AMT14. Variability is observed in the southern gyre; however the highest molar percentage is at the southern flanks of the southern gyre and not at the equator.

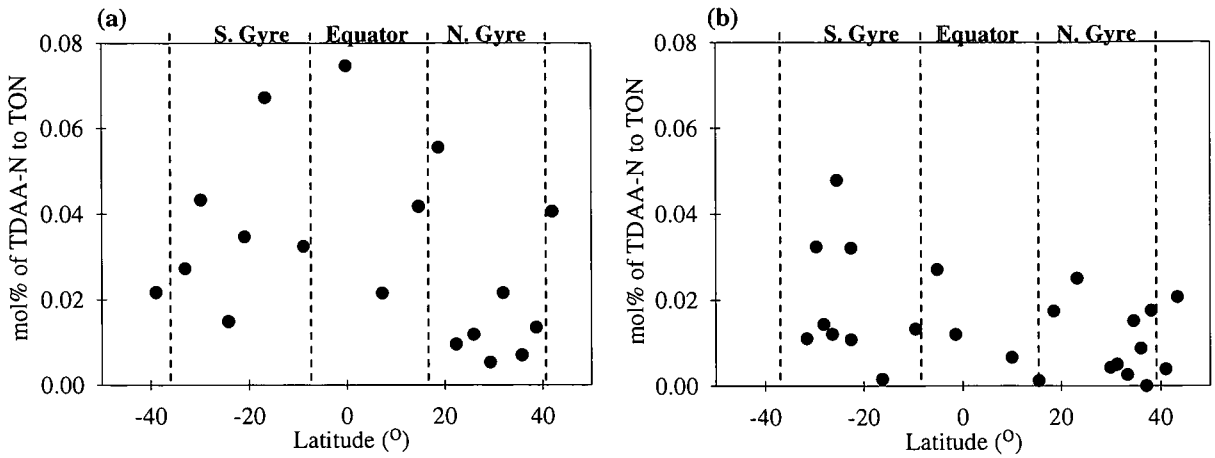

Figure 4.07 Molar percentage contribution of TDAA-N to the TON pool (a) AMT14 (b) AMT16. Biogeochemical provinces labelled.

4.3.1.5 Individual dissolved amino acids

The distributions of the individual protein amino acids along the AMT14 and 16 transects are similar. Serine is the dominant amino acid (33±1.4%) along the AMT14 transect with glycine (18±0.6%) and glutamic acid (17±0.8%) also being major compounds (Fig. 4.07). Glycine (18±0.9%) is the most abundant amino acid of the TDAA along the AMT16 transect followed by serine (16±0.4%) and alanine (16±0.5%) (Fig. 4.08).

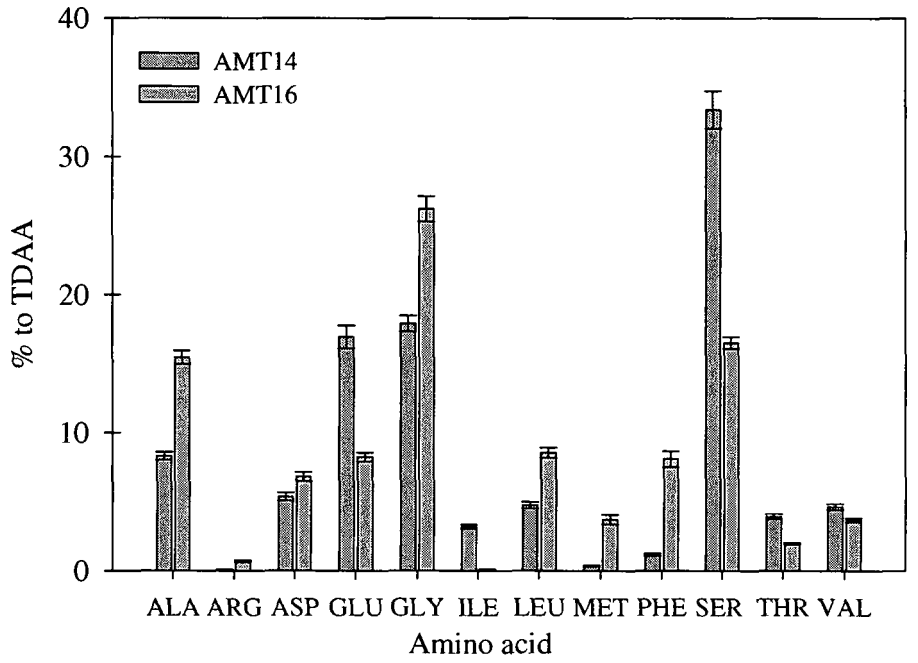

Figure 4.08 Percentage of individual amino acids to the TDAA for the entire data sets for AMT14 (dark gray bars) and AMT16 (light gray bars). Bars represent the mean values, samples run in duplicate. Error bars represent the standard deviation, AMT14 n= 22; AMT16 n= 25.

4.3.1.6 D:L Ratios of DFAA

Very few D-amino acids were detected in samples collected during AMT14; no D:L ratios could be calculated. However, D-Alanine was present at a number of stations in both the DFAA and the THAA collected during AMT16 (Fig. 4.09) and variation in the D:L ratios is apparent, both along the transect and between the two fractions. Higher D:L ratios were observed in the DFAA alanine in the southern and northern gyres. However, at the equator and at the southern flanks of the northern gyre the THAA alanine has greater D:L ratios. In the southern gyre, at the equator and in the northern

gyre, D:L ratios of DFAA alanine remain fairly constant (0.2) but increase dramatically to 1.1 at 29°N and vary between 0.4 – 0.8 elsewhere in the northern gyre. D:L ratios of the THAA alanine exhibit a similar pattern to DFAA, however at the southern flanks of the southern gyre there is a considerable decrease across the flanks (D:L-Ala 1.02) and into the gyre interior (D:L-Ala 0.08). Ratios remain fairly constant across the equatorial region and at the southern flanks of the northern gyre and then subsequently increase in the centre of the northern gyre.

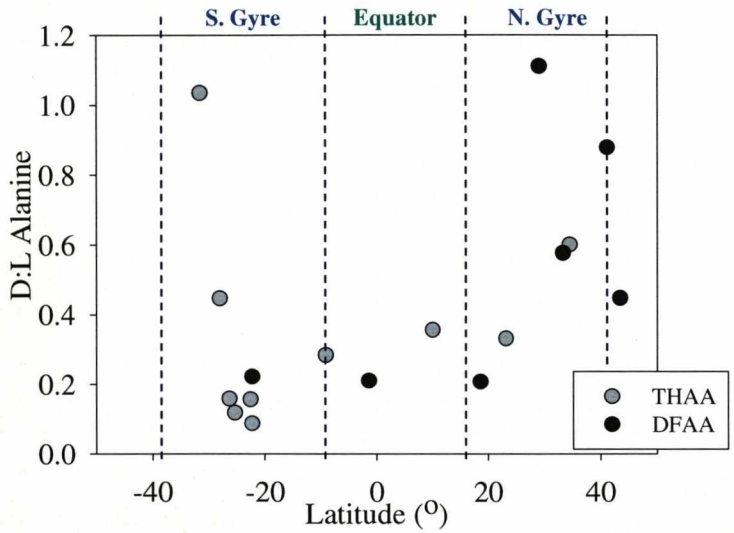

Figure 4.09 D:L ratios for DFAA (black circles) and THAA (gray circles) alanine along the AMT16 transect at the chlorophyll maximum. Biogeochemical regimes labelled.

4.3.2 Particulate Amino Acids

4.3.2.1 Total particulate amino acids

Variations in the concentrations of particulate amino acids (PAA) are apparent along the AMT16 transect and with depth, with concentrations ranging between 9 and 190 nM (Fig. 4.10 a), although no significant trend is apparent between PAA

concentration and depth. At two locations in the southern gyre, PAA concentrations decrease with depth, however this is not the case at the equator and in the northern gyre where concentrations are generally greatest at 100 m. The PAA are lower in the southern gyre (28 – 70 nM) compared with the northern gyre (33 – 190 nM) with a maximum concentration of 190 nM at 30°N (50m).

The molar percentage contribution of PAA to PON also shows variation both along the AMT16 transect and though the water column (Fig. 4.10 b), with values ranging between 0.7 and 9.5%. Whilst there is no particular trend of the molar percentage contribution of PAA to PON in the southern gyre, at the equator and in the deeper northern gyre samples the PAA generally contribute more to the PON compared with the shallower samples. Percentage contributions are lower in the southern gyre (0.6 – 4.7%) than in the northern gyre (3.3 – 9.5%).

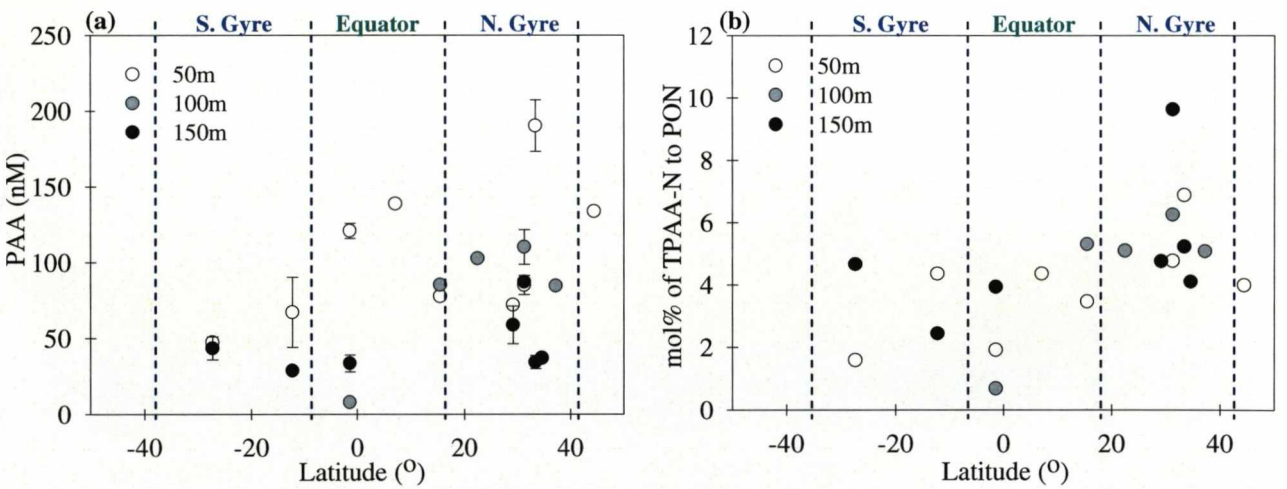

Figure 4.10 (a) Concentrations of total particulate amino acids along the AMT16 transect at 50m (white circles), 100m (gray circles) and 150m (black circles). Bars represent the range of values obtained where the analysis was conducted in duplicate. (b) Molar contribution of TPAA-N to the PON pool along the AMT16 transect at 50m (white circles), 100m (gray circles) and 150m (black circles). Biogeochemical regimes labelled.

4.3.2.2 Individual particulate amino acids

Distributions of individual particulate amino acids along the AMT16 transect (Fig. 4.11) show very little variation with depth, with glutamic acid (18 -22% ±0.9 – 2.5%) being the most abundant component in the total particulate amino acid pool. Other major contributors include alanine, aspartic acid, glycine and serine, each contributing 8 – 13% ± 0.5 -1.3.

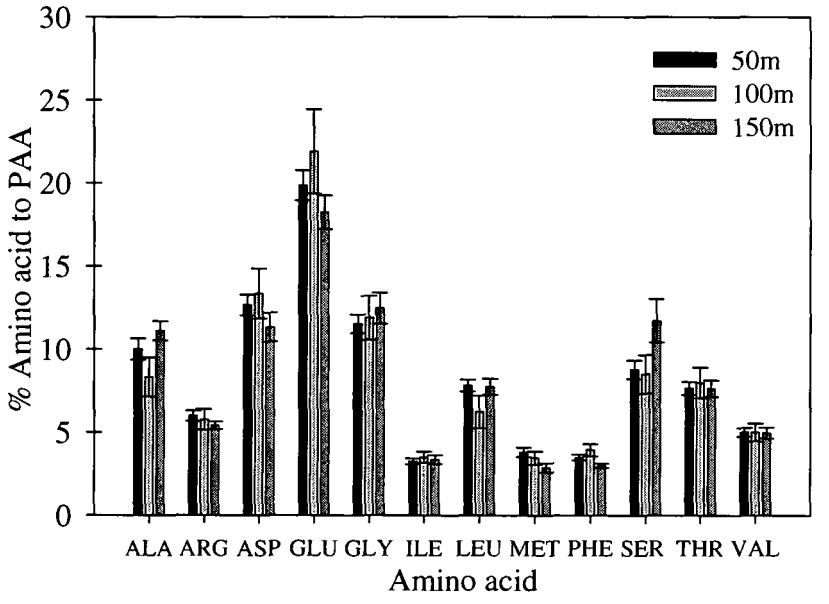

Figure 4.11 Percentage of individual amino acids to the PAA along the AMT16 transect for the data set at 50m (black bars), 100m (light gray bars) and 150m (dark gray bars). Bars represent the mean values, samples run in duplicate. Error bars represent the standard deviation of the mean, 50 m n= 9, 100 m n= 5, 150 m n=7)

4.3.2.3 D:L Ratios of PAA

D-Aapartic acid, D-glutamic acid, D-serine and D-alanine were present in PAA samples along the AMT16 transect at 50m, 100m and 150m. Variations in the ratios are apparent between the individual amino acids, along the transect and with depth. Alanine and glutamic acid have the lowest D:L ratios while aspartic acid exhibits the highest values.

D:L ratios for aspartic acid (Fig.4.12 a) vary between 0.2 and 0.17 with the highest value being found in the 150m sample at the equator. The greatest variation with depth is observed at the equator where the shallowest sample at 50m has a D:L ratio of 0.03 increasing to 0.17 at 150m. In the northern gyre, the difference in D:L ratios between the depths is less than at the equator, however the deeper samples still tend to show highest values. Along the transect, values are fairly constant to the south of the equator whilst to the north they are higher but then subsequently decrease towards the centre of the northern gyre where the lowest ratio (0.02) is observed at 29°N in the 50m sample.

D:L ratios for glutamic acid (Fig.4.12 b) are fairly consistent varying between 0.02 and 0.06. In most cases the deeper samples at 150m have greater D:L ratios, with the exception being at 27°S and just to the north of the equator, where the opposite is observed. Samples in the northern gyre exhibit slightly higher D:L ratios than those observed in the southern gyre.

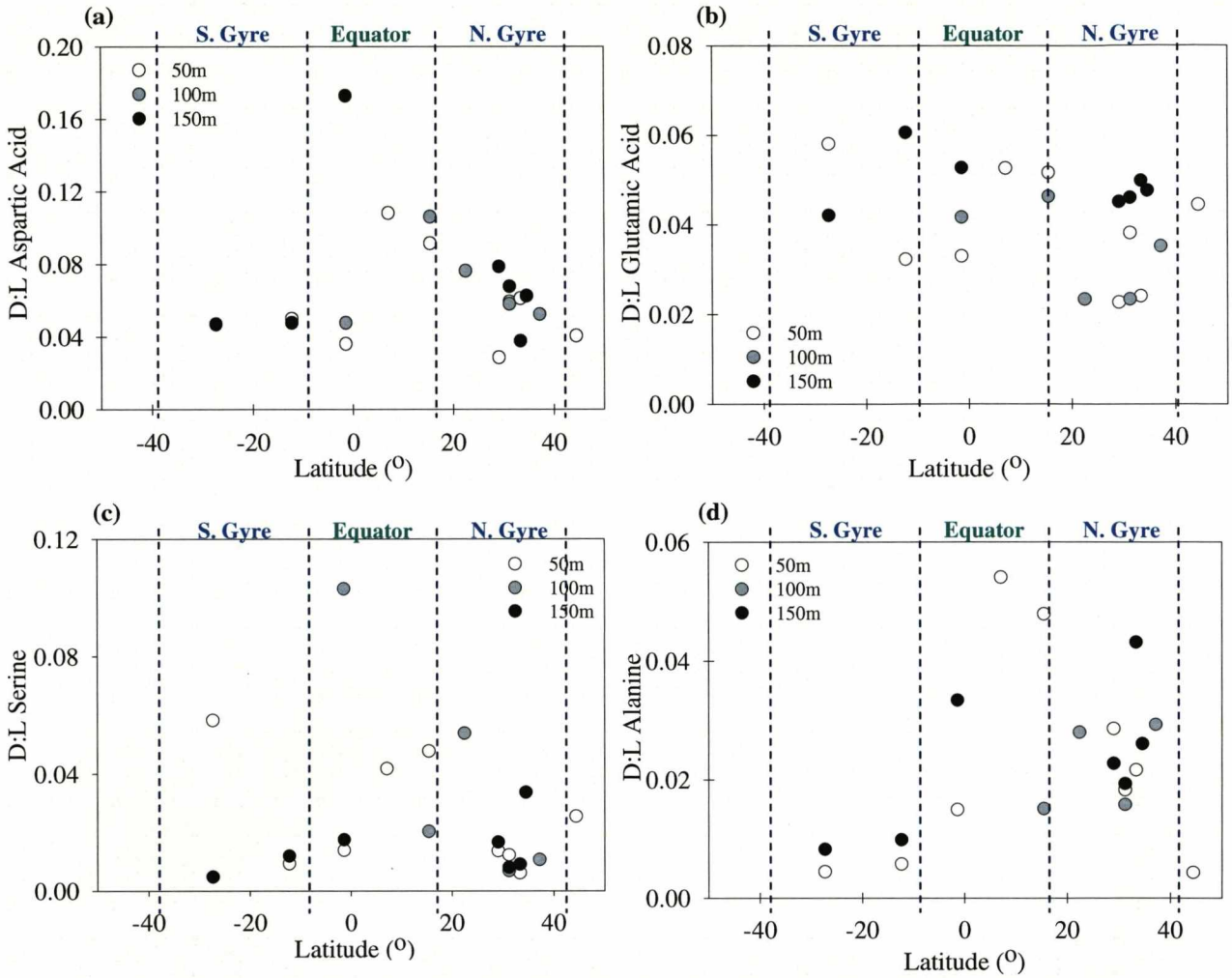

Figure 4.12 D:L ratios of (a) aspartic acid, (b) glutamic acid, (c) serine and (d) alanine in particulate samples along the AMT16 transect at 50m (white circles), 100m (gray circles) and 150m (black circles).

D:L ratios of serine (Fig. 4.12 c), varied between 0.005 – 0.1 with the greatest value at 100m at the equator. Whilst differences were apparent with depth no particular trends are discernable. To the south of the equator, D:L ratios are generally lower than those observed to the north of the equator, however values do decrease in the centre of the northern gyre where there is very little variation with depth.

D:L ratios for alanine (Fig. 4.12 d) are low, varying between 0.004 – 0.05 along the AMT16 transect with the highest value observed just north of the equator (7°N) where the values decrease with depth. To the south of the equator and at the equator the deeper samples have the greatest D:L ratios. Values decrease towards the centre of the northern gyre where variation with depth is minimal, however the ratios are still higher than those observed to the south of the equator.

4.4 Discussion

4.4.1 Amino acid distributions

4.4.1.1 Dissolved amino acids

The concentrations of DFAA and THAA at the chlorophyll maximum are low across the biogeochemical regimes of the AMT in the Atlantic Ocean, where neither fraction dominates the TDAA pool. The low levels of DFAA are not surprising since DFAA's are labile moieties with turnover times of less than ~ 0.5 hours implying a close coupling between their release and uptake [*Fuhrman*, 1987b]. Total DFAA concentrations in the oligotrophic Northern Sargasso Sea were <10 nM in the euphotic zone [*Keil and Kirchman*, 1999], in the same range as the concentrations along the AMT transect. However, the low levels of THAA observed in the present study are unexpected since it has been reported that THAA (or dissolved combined amino acids) are the major contributor to the DON pool with concentrations ranging between 0.15 and 4.20 μM in natural waters (including open ocean, estuaries and streams) [*Bronk*, 2002]. In the Northern Sargasso Sea, THAA concentrations were between 167 and 810 nM in surface waters [*Keil and Kirchman*, 1999] which when compared to 0.2 – 23 nM observed along the AMT transect, suggests that either concentrations of THAA are remarkably low at the chlorophyll maximum or that the method of analysis in the present study leads to lower values being observed. The method employed in this study relies on a hydrolysis time of 6 hours, which according to *Kaufman and Manley* [1998] is sufficient, since amino acid concentrations (with the exception of valine and isoleucine) reach a plateau after 6 to 8 hours of heating (110°C). However, it has also been shown that the acid

hydrolysis method does suffer some restrictions and much longer times >24 hours may be required to enhance the yield of amino acids from hydrophobic peptides [*Tsugita, et al.*, 1987]. Peptide bonds can be cleaved more effectively by the action of HCl/trifluoroacetic acid (TFA) vapour, reducing required reaction times to 22 - 45 minutes at 158°C with a higher recovery of the hydrophobic amino acids [*Tsugita, et al.*, 1987]. Studies conducted on seawater samples also demonstrated that the vapour-phase hydrolysis method significantly increased the THAA concentrations by 1.5 ±0.4 times when compared to the traditional hydrolysis method, suggesting that THAA concentrations in seawater may have been underestimated by as much as 300% [*Keil and Kirchman*, 1991]. In hindsight, experiments into the recovery of the amino acids gained from the hydrolysis method utilised in this study should have been conducted, but since this was not possible we can only presume that the low THAA concentrations observed along the AMT transect are a result of incomplete hydrolysis. Nonetheless since relative trends of THAA exist along the AMT transect remarks can be made on the TDAA pool as a whole.

Concentrations of TDAA are lower for AMT16 than for AMT14, but the general pattern along the AMT transect is similar for the two years. Higher concentrations and variability was observed in the southern gyre and a decreasing trend from the north of the equator followed by a subsequent rise in levels at 20°N. The variability in the southern gyre and the reasonably stable concentrations in the northern gyre could reflect seasonality. The southern gyre was sampled during the autumn following the productivity maximum of the summer months. Therefore, the higher varying levels of TDAA could reflect the decoupling of production and consumption, whereby organic

matter built up over the summer in the euphotic zone decomposes, releasing semi-labile and labile DON which are not rapidly utilised. Since the northern gyre was sampled during the spring, the lower and more stable concentrations observed here could represent a closely coupled system. Production and respiration rates measured along the AMT transect support this hypothesis. During autumn, both the northern and southern gyres are out of metabolic balance in that they appear to show net heterotrophy whilst during the spring, autotrophy and heterotrophy in the gyres are more balanced [*Gist, et al.*, 2007]. The production of DON would also be expected to increase with enhanced productivity; labile moieties such as TDAA could also be utilised as a source of nutrient [*Flynn and Butler*, 1986; *Middelboe, et al.*, 1995; *Palenik and Morel*, 1990a], particularly in the northern oligotrophic gyre where NO_3^- is exhausted.

The decreasing trend in TDAA concentrations to the north of the equator could be result from the lateral advection of equatorial waters rich in DON to the southern flanks of northern gyre [*Williams and Follows*, 2003]. As this water is transported northwards into more nutrient depleted conditions, DON might provide a valuable source of N to the biota. Since the amino acids represent the labile and semi-labile fractions of DON, the turnover times of which are hours to days and weeks to months, respectively [*Fuhrman and Ferguson*, 1986; *Keil and Kirchman*, 1993] they would be utilised quickly and therefore levels would decrease relatively as the water moved away from the source.

The slight increase in TDAA concentrations at 20°N coincides with a region of N_2 fixation (see Chapter 3). Diazotrophs such as *Trichodesmium* spp. have been reported to exude DON rich in dissolved amino acids [*Capone, et al.*, 1994; *Glibert and Bronk*,

1994] and thus could account for the enhanced TDAA concentrations observed in this region of the northern gyre.

4.4.1.2 Particulate amino acids

The PAA exhibited concentrations of 28 to 190 nM along the AMT transect, which is in the same range as measured in the Pacific Ocean (8 – 340 nM) [*Lee and Cronin*, 1984]. Higher concentrations were observed in the northern gyre when compared with to southern gyre. This could be attributed to the process of N_2 fixation between 7°N and 32°N (Chapter 3). N_2 fixation perturbs the N:P stoichiometry in both particulate and dissolved nitrogen pools in that N becomes enriched [*Karl, et al.*, 1997]. A significant relationship ($p>0.05$; product moment correlation. $R = -0.565$) exists between the depleted $\delta^{15}N$ PON_{susp} and the elevated PAA concentrations (Fig.13) implying N_2 fixation is responsible for the amino acid accumulation in the northern gyre.

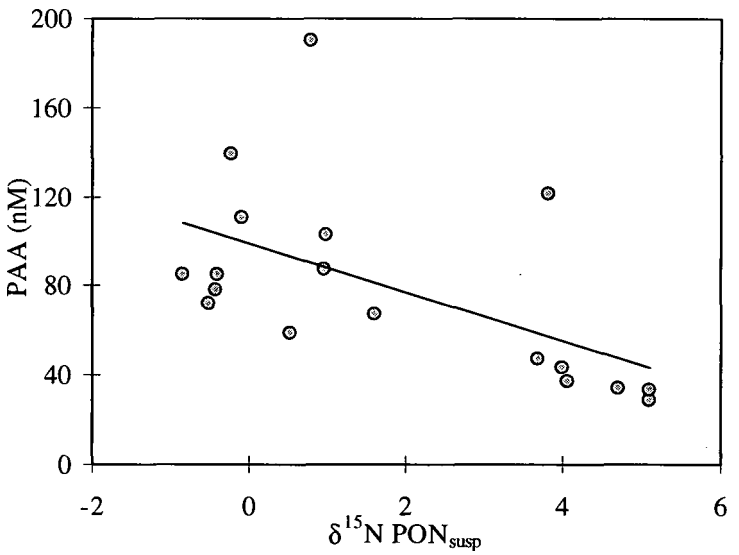

Figure 4.13 Significant relationship ($p>0.05$; product moment correlation. $R = -0.565$) between $\delta^{15}N$ PON_{susp} and the PAA. Depleted isotopic signal implies N_2 fixation (see Chapter 3) which is coincident with elevated PAA concentrations.

4.4.2 *Degradation of dissolved and particulate organic matter*

Whilst the distributions of amino acids can hint at processes involving organic matter cycling in the Atlantic Ocean, they provide little insight in to the quality of the organic matter. The 'age' of organic matter can be assessed by diagnosing positive relationships between the dissolved and particulate amino acids with levels of chlorophyll *a*. Since chlorophyll *a* is a good indicator of phytoplankton biomass [*Platt and Sathyendranath*, 1988], and therefore the primary food source in the marine food web, a dependence of amino acid concentration with chlorophyll *a* might be assumed. However, if the organic matter is degraded or 'older' a significant positive relationship would not be expected between the amino acids and chlorophyll *a* concentrations [*Hubberten, et al.*, 1994]. No significant positive relationship ($p>0.05$; product moment correlation. AMT14: $R = 0.31$, AMT16: $R = -0.38$) between the TDAA and the chlorophyll *a* was apparent for AMT14 and 16 suggesting that the TDAA represent a degraded fraction of TON. The PAA on the other hand did reveal a significant positive relationship with chlorophyll *a* ($p>0.05$; product moment correlation. $R = 0.63$) therefore suggesting that the particulate amino acids are representative of freshly derived organic matter or of the phytoplankton biomass itself.

To further investigate the 'age' of organic matter, principal component analysis was employed. When dealing with large data sets, principal component analysis reduces the complexity of the data by identifying which combinations of variables explain the largest amount of variation. New variables or principle components are created from the linear combinations of the original variables with the first principal component showing the combination of variables which explain the greatest variability, and so on. Using the

mole percent contribution of amino acids, *Dauwe and Middleburg* [1998] used this variance-orientated method to demonstrate that there were systematic variations in amino acid distributions as a consequence of the degradation of organic matter.

In the present study, the *Dauwe and Middleburg* [1998] method (4.03) was applied to the entire AMT data set using the software package XLSTAT.

$$\text{Degradation Index (DI)} = \Sigma_i \left[\frac{\text{var}_i - \text{AVG var}_i}{\text{STD var}_i} \right] \times \text{fac. coef}_i \qquad (4.03)$$

where var_i is the original (nonstandardised) mole percentage of amino acid *i*, AVG var_i and STD var_i are its mean and standard deviation in the entire set and fac. coef_i is the factor coefficient for amino acid *i* (Table 4.03).

The first component of this multivariate analysis explains 34.1% of the variance whilst the second component accounts for 17% of the variance (Table 4.03 and Fig. 4.14). The cross plot of the first and second principal component scores for all the data (Fig. 4.14) demonstrates that the dissolved amino acids behave in a similar way, whilst the particulate fractions cluster separately. AMT14 and AMT16 dissolved amino acids both display analogous first principal component scores between 0.5 and -3.6. However, differences arise between the two years as AMT16 dissolved amino acids exhibit slightly higher second principal component scores (-0.7 to 7) to those obtained for AMT14 (-1.9 to 1). The first principal component scores calculated for the particulate amino acids are much higher (2 to 4) than those gained for the dissolved fractions, whilst very little variation exists in the second principal component score. This difference between the two fractions demonstrates that processes (such as production and

recycling) shaping the properties of the dissolved and particulate organic matter are quite different.

	Factor coefficient	Average	Std. deviation
Alanine	-0.247	12.20	5.90
Arginine	0.935	1.98	2.72
Aspartic Acid	0.741	7.36	4.80
Glutamic Acid	0.478	14.18	8.62
Glycine	-0.681	19.21	9.16
Leucine	-0.036	7.34	9.25
Methionine	0.097	3.36	7.11
Phenylalanine	0.043	4.05	5.21
Serine	-0.662	20.34	11.55
Threonine	0.725	4.61	3.06
Valine	0.325	4.28	2.32
Isoleucine	0.913	1.09	1.72

Table 4.03 Factor scores of the individual amino acids obtained from principal component analyses of the individual amino acid mole percent abundances. Corresponding averages and standard deviations also given.

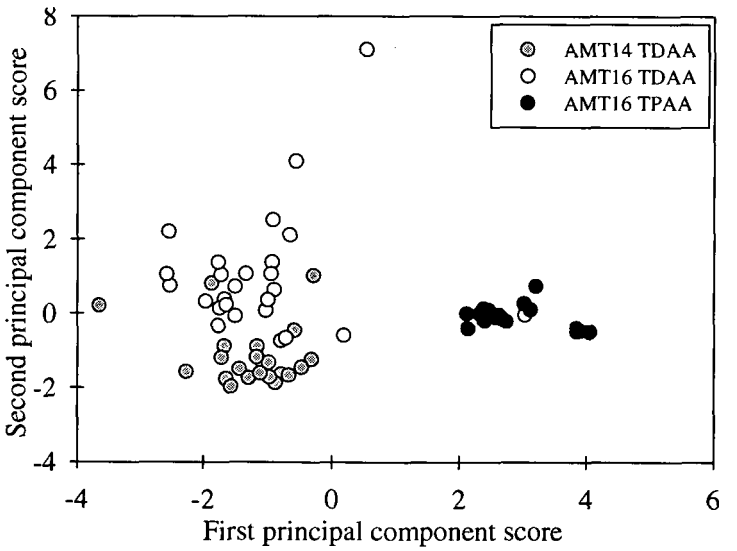

Figure 4.14 Cross plot of the first and second principal component scores obtained using the mole percentage abundances of amino acids.

Dauwe & Middleburg [1998; 1999] derived a quantitative degradation index (DI) where the multivariant analysis was performed on a wide range of organic matter, from source materials such as fresh plankton to much older and more degraded sedimentary materials. In sandy sediments, fresh organic matter and thus labile material the DI score (first principle component score) was high, whilst refractory organic matter present in oxidised deep-sea turbidites had the lowest DI score.

Trends across the various biogeochemical regimes of the Atlantic Ocean (Fig. 4.15) are apparent with dissolved fractions having lower DI values than the particulate matter, confirming the dissolved organic matter has been subjected to a higher degree of degradation than particulate matter. This contrast is not unexpected, since the particulate organic nitrogen sampled and subsequently analysed for amino acids is representative of organic matter primarily derived from autotrophic organisms i.e. phytoplankton (see section 3.3.5). Little variation appears to exist in the particulate DI score from different depths, although slightly fresher PON is observed in the equatorial region, which may reflect the enhanced productivity there.

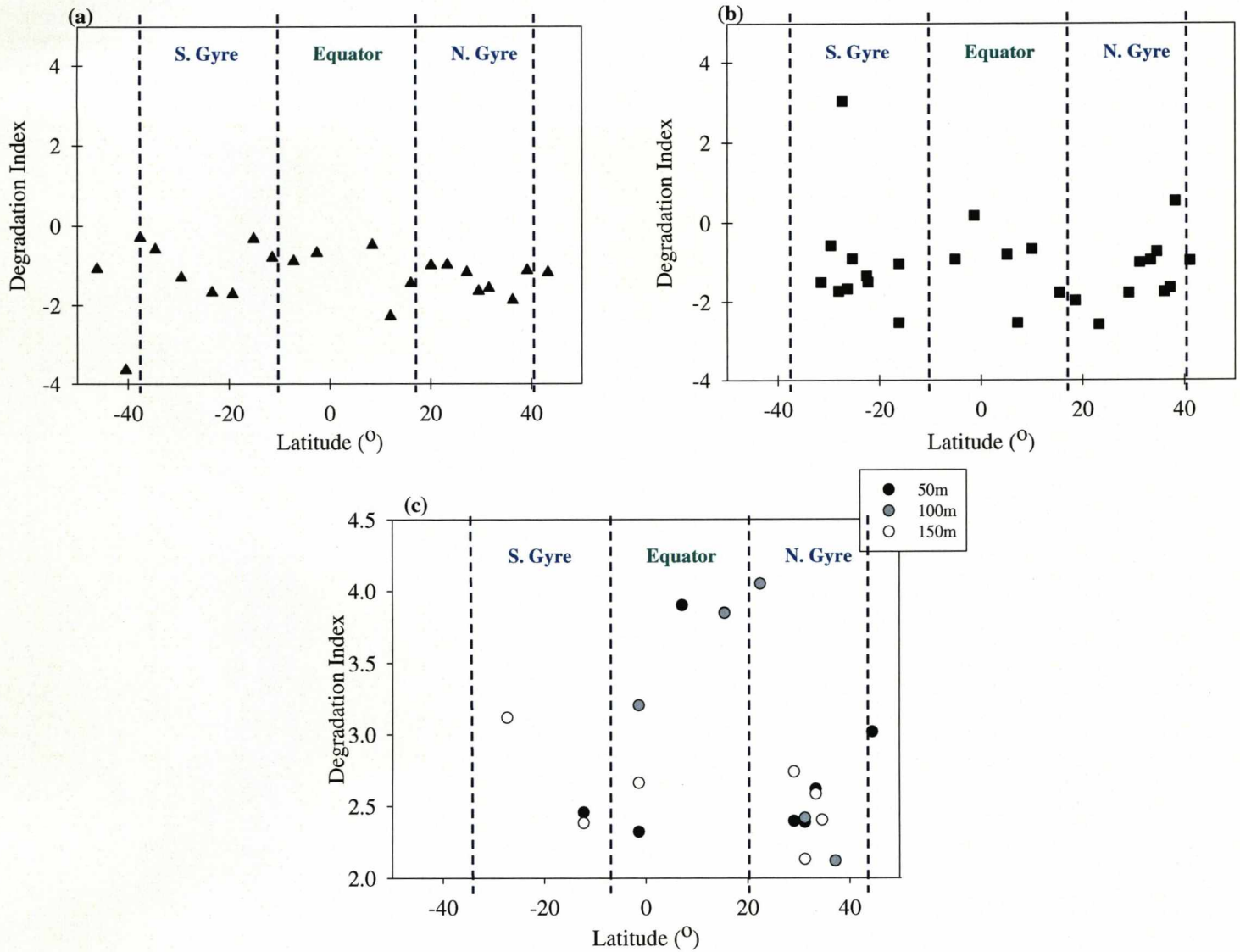

Figure 4.15 Degradation index as a function of latitude (a) AMT14 TDAA; (b) AMT16 TDAA; (c) AMT16 PAA at 50m (black circles), at 100m (gray circles) and at 150m (white circles). Biogeochemical regimes labelled.

The low degradation score for the dissolved organic nitrogen is not surprising, as it has long been understood that both dissolved and hydrolysable amino acids can be an important source of nutrient N to phytoplankton and bacteria [*Flynn and Butler*, 1986; *Middelboe, et al.*, 1995; *Palenik and Morel*, 1990a] and will therefore be subjected to a high degree of degradation particularly in regions where N is limiting. Further evidence of amino acids being utilised as a nutrient source can be observed in differences of the DI as a function of latitude (Fig. 4.15 a & b). A striking difference is observed in the southern gyre particularly for AMT14, where the DI decreases dramatically from the southern flanks towards the centre of the oligotrophic gyre and then subsequently increases in the equatorial region. This implies that at the flanks and in the equatorial region where NO_3^- concentrations are not limiting (i.e. >1 μM), amino acids are not an important source of N to the primary producers. Higher rates of production [*Maranon, et al.*, 2000] and a reduced demand for amino acid-N results in less degraded organic matter. Meanwhile in the centre of the oligotrophic gyres where microorganisms are N-starved, the amino acids represent an available source of nutrient N, and therefore the organic matter appears more degraded since it is under constant microbial [*Fuhrman*, 1987a] and enzymatic [*Palenik and Henson*, 1997; *Palenik and Morel*, 1990a] attack.

Whilst the same trend is apparent in the N-limited waters of the north Atlantic subtropical gyre for AMT16, other processes seem to alter TDAA on AMT14. Just north of the equator (12°N) the DI decreases (-2.2) and then increases (-1.0) to the centre of the oligotrophic gyre. The very low value to the north of the equator could reflect an upwelling signal corresponding to the intertropical convergence zone which is found to the north of the equator at ~10°N (see Chapter 2, Fig. 2.03). The upwelling of deep

water to the surface could introduce old, degraded dissolved organic matter into the euphotic zone and might be responsible for the low DI values found at 12°N. The presence of less degraded dissolved organic matter in the northern gyre during AMT14 suggests that amino acids are not such an important source of nutrient here as compared with the southern gyre. This could well be the case, since other biogeochemical signals suggest that N_2 fixation is occurring in the northern oligotrophic gyre (see Chapter 3) and thus introducing a source of new N into the system.

The occurrence of fresher organic material in the northern gyre could be accounted for by the release of DON by N_2 fixers such as *Trichodesmium* spp [*Karl, et al.*, 1997; *Lenes, et al.*, 2001] whereby the released DON is predominantly rich in dissolved free amino acids [*Capone, et al.*, 1994; *Glibert and Bronk*, 1994]. Examination of the concentrations of TDAA in the northern gyre (Fig. 4.06 a & b) reveals an elevation in levels in the same region where the fresher organic matter is observed, particularly during AMT14. This could be a consequence of net accumulation of DON arising from N_2 fixation. The presence of older or more degraded material in the northern gyre during AMT16 cannot be readily explained since net accumulation of DON occurs during both years. However, it has been reported that whilst N_2 fixers exude DON they are also capable of using this DON as an N source [*Capone, et al.*, 1994]. Therefore the more degraded material found during AMT16 in the northern gyre could arise from a closely coupled system whereby N_2 fixers meet the N cell demand exclusively through the process of N_2 fixation [*Mulholland and Capone*, 1999]. However, the differences between AMT14 and 16 maybe simply explained by the

disparity in the cruise tracks, as AMT16 went further into the northern oligotrophic gyre than did AMT14 (Fig 2.02).

4.4.3 Individual amino acids as degradation indicators

Examination of the mole percent abundances of the individual amino acids as a function of the DI reveals aspects that are characteristic of labile or refractory organic material. Figure 4.16 (a – i) shows cross plots of the mole percent of the individual amino acids against the DI; the respective significant correlation coefficients are given in Table 4.04. The mole percent abundances of glutamic acid, methionine, arginine, threonine, aspartic acid and valine all significantly decrease as the organic matter becomes more degraded, i.e. these amino acids are preferentially removed from the organic material with time. On the other hand serine, glycine and alanine appear to significantly increase as the organic matter becomes more degraded, i.e. these amino acids preferentially accumulate in the organic material with time.

It had been previously reported that levels of glutamic acid are often low relative to source materials [*Cowie and Hedges*, 1992; *Dauwe and Middelburg*, 1998]. Glutamic acid, along with methionine and phenylalanine, found to be concentrated in cell plasma of diatoms, while serine and glycine are dominate in the diatom cell walls [*Hecky, et al.*, 1973]. Diatoms are found along the AMT transect and account for upto 8% of the total primary production in the upper euphotic zone [*Poulton, et al.*, 2006b]. Furthermore diatoms have been reported to account for 15 – 48% of new production at the oligotrophic BATS site in the north Atlantic

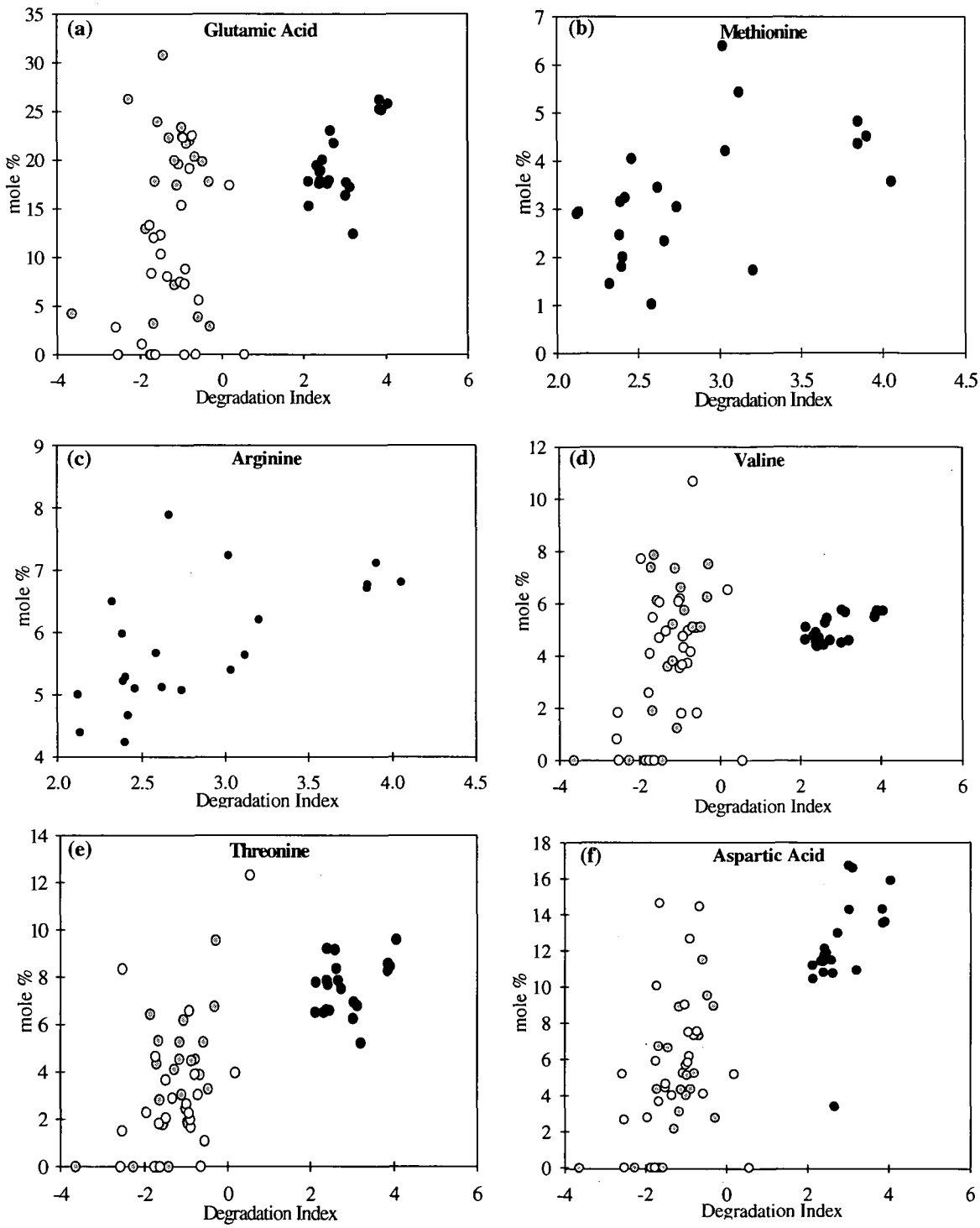

Figure 4.16 Cross plots of degradation index and the mole % abundance of the individual amino acids; AMT14 total dissolved amino acids (gray circle), AMT16 total dissolved amino acids (white circle) and AMT16 total particulate amino acids (black circle). See table 4.04 for further details.

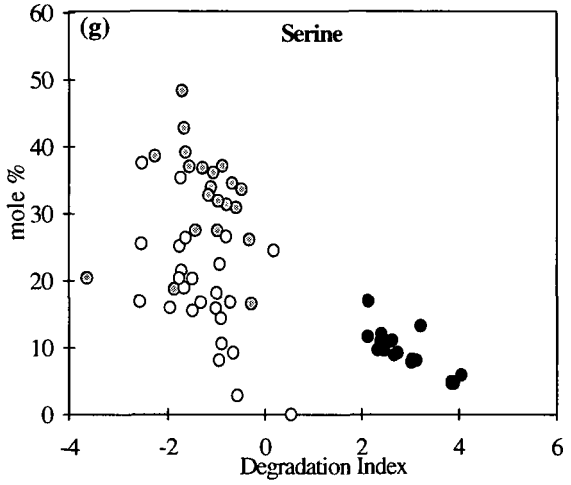

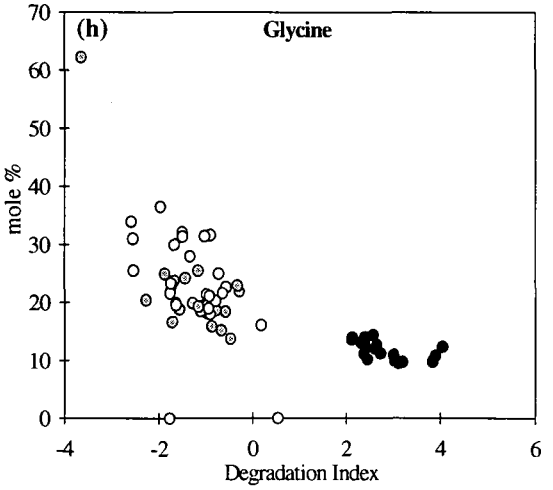

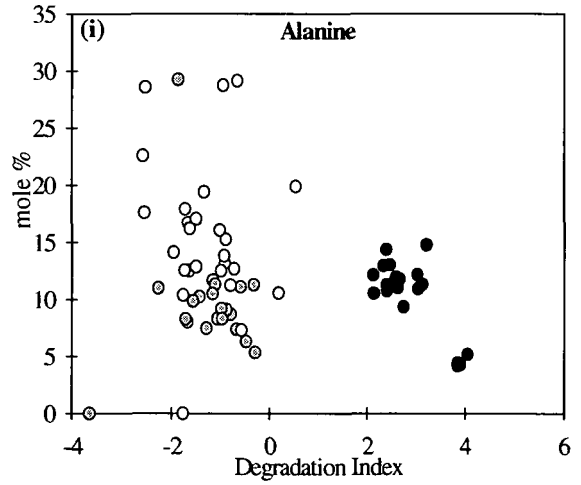

Figure 4.16 continued Cross plots of degradation index and the mole % abundance of the individual amino acids; AMT14 total dissolved amino acids (gray circle), AMT16 total dissolved amino acids (white circle) and AMT16 total particulate amino acids (black circle). See table 4.04 for further details.

Amino acid	n	R value
glutamic acid	68	0.48
methionine*	20	0.52
arginine*	20	0.63
threonine	68	0.73
aspartic acid	68	0.73
valine	68	0.32
serine	68	-0.66
glycine	68	-0.68
alanine	68	-0.25

Table 4.04 Significant correlation coefficients (R values) at a confidence level of 95% ($p>0.05$; product moment correlation) for the individual amino acids (mole percent abundances) vs. the degradation index. *Only for particulate amino acids, as inadequate dissolved amino acid data to test significance.

[*Brzezinski and Nelson*, 1995; *Nelson and Brzezinski*, 1997] and up to 25% of new production at the oligotrophic HOTS site in the North Pacific [*Brzezinski, et al.*, 1998]. *Cowie & Hedges* [1992] suggest that diatoms may undergo selective loss of intracellular amino acids while cell wall components are preserved. This simultaneous loss of glutamic acid and methionine with a preservation of serine and glycine would explain the relationships shown in figure 4.16. *Cowie & Hedges* [1992] go further, by suggesting that protection by the silicious test may result in the cell wall protein being less easily degraded by bacteria and furthermore that the cell protein is less soluble than proteins in the cell plasma. Glycine also has a minor food value to marine organisms; its short chain length allows its synthesis from many other amino acids in heterotrophic metabolism [*Dauwe and Middelburg*, 1998].

Whilst the depletion of methionine with increasing degradation has already been accounted for, it is still to be ascertained why measurable levels of methionine were found only in the particulate phase and not in the dissolved fraction of organic nitrogen. Methionine along with arginine, which was also only found in the particulate fraction, are essential amino acids i.e. they cannot be synthesised by many marine organisms and an external source is required. Thus, the lack of any quantifiable methionine and arginine TDAA in the Atlantic samples must reflect their rapid uptake by marine organisms [*Phillips*, 1984]. Furthermore, it has been reported that in open ocean environments when nutrients are at nanomolar levels, some marine bacteria demonstrate a high affinity for uptake of arginine [*Geesey and Morita*, 1979]. Arginine can also be a N source for diatoms where it can supply upto 30% of the cells requirement of N [*Flynn and Wright*, 1986].

The mole percent abundances of threonine, aspartic acid and valine were also found to decrease with increased degradation. The relationship observed with threonine is somewhat surprising since it has been previously reported to accumulate in the same way as serine and glycine [*Cowie and Hedges*, 1992; *Dauwe and Middelburg*, 1998]. A similar trend was observed in the north western Pacific [*Yamashita and Tanoue*, 2003] for valine which was abundant in relatively bioavailable THAA.

The accumulation of alanine in degraded organic matter has been previously reported in the Artic Ocean [*Dittmar, et al.*, 2001] and in the north western Pacific [*Yamashita and Tanoue*, 2003]. Taken together with the present study, it seems that alanine is somehow protected from remineralisation and high levels of alanine are characteristic of degraded DON.

4.4.4 Microbial inputs to organic matter in the Atlantic Ocean

Along the AMT14 transect very few quantifiable measurements of dissolved D-amino acids were made. However along the AMT16 transect at the chlorophyll maximum, D-alanine, a component of peptidoglycan found in bacteria cell walls [*Schleife.Kh and Kandler*, 1972], was present in both the DFAA and THAA fractions at some of the stations. It was surprising to find very few D-amino acids since it has been reported that peptidoglycan is a major contributor to the DOM pool [*Dittmar, et al.*, 2001; *Jones, et al.*, 2005; *Jorgensen, et al.*, 1999; *McCarthy, et al.*, 1998; *Perez, et al.*, 2003]. However, in those studies samples were of either ultrafiltered DOM (UDOM), concentrating the high molecular weight species present in DOM [*Jones, et al.*, 2005; *McCarthy, et al.*, 1998], or samples were taken from highly productive waters [*Dittmar,*

et al., 2001; *Jorgensen, et al.*, 1999; *Perez, et al.*, 2003]. In both cases the DON concentrations and thus the amino acid levels are much higher than those measured along the AMT transect, which could therefore help explain the presence of very low amounts of D-amino acids. In hindsight, a preconcentration step could have been introduced prior to the analysis of both the DFAA and THAA fractions by HPLC.

Despite the low D-alanine concentrations, the D/L ratios have been calculated along AMT-16 (Fig 4.17 b) and these are similar to previously reported values (Table 4.05) in the oligotrophic regions of the Pacific Ocean and the Gulf of Mexico [*McCarthy, et al.*, 1998]. This is despite methodological differences in the methodology i.e. DOM vs. UDOM [*This study*; *[McCarthy, et al., 1998]*. D/L-alanine ratios in the AMT samples are similar to pure peptidoglycan [*Amon, et al.*, 2001; *McCarthy, et al.*, 1998] this suggests that the D-alanine found in the dissolved fractions along the AMT transect may derive from bacteria.

Location	Environment	Fraction	D/L-alanine	Reference
Atlantic Ocean	Oligotrophic	DON-DFAA	0.53	*This study*
		DON-THAA	0.37	*This study*
	Equatorial	DON-DFAA	0.21	*This study*
		DON-THAA	0.32	*This study*
	Temperate	DON-DFAA	0.66	*This study*
Pacific	Oligotrophic	UDOM-THAA	0.54	*[McCarthy, et al., 1998]*
Gulf of Mexico	Oligotrophic	UDOM-THAA	0.47	*[McCarthy, et al., 1998]*
North Sea	Coastal	UDOM-THAA	0.37	*[McCarthy, et al., 1998]*
Atlantic	Temperate	DON-THAA	0.49	*[Perez, et al., 2003]*
Florida Everglades	Freshwater canal	UDOM-THAA	0.11	*[Jones, et al., 2005]*
	Marsh	UDOM-THAA	0.10	*[Jones, et al., 2005]*
	Coastal	UDOM-THAA	0.20	*[Jones, et al., 2005]*
Roskilde Fjord	Estuarine	DON-DFAA	0.08	*[Jorgensen and Middelboe, 2006]*
		DON-THAA	0.14	*[Jorgensen and Middelboe, 2006]*
Peptidoglycan	*Synechoccus bacillaris*		0.38	*[McCarthy, et al., 1998]*
Peptidoglycan	*Staphyloccus aureus*		0.44	*[Amon, et al., 2001]*

Table 4.05 D/L-alanine ratios from studies in various aquatic environments and from pure peptidoglycan.

In this study the D/L-alanine ratio for DFAA is higher than that for THAA, which, as explained in section 4.4.1.1, could be due to the incomplete hydrolysis of the THAA, which in turn would result in the underestimation of the bacterial contribution to the THAA pool. It has also been suggested that conventional hydrolytic techniques might be substantially less efficient for peptidoglycan residues in an environmental matrix [*McCarthy, et al.*, 1998].

The variations in the D/L-alanine ratios that occur along the AMT transect (Fig. 4.17 b) can be explained by the distribution of bacteria (Fig 4.17 a).

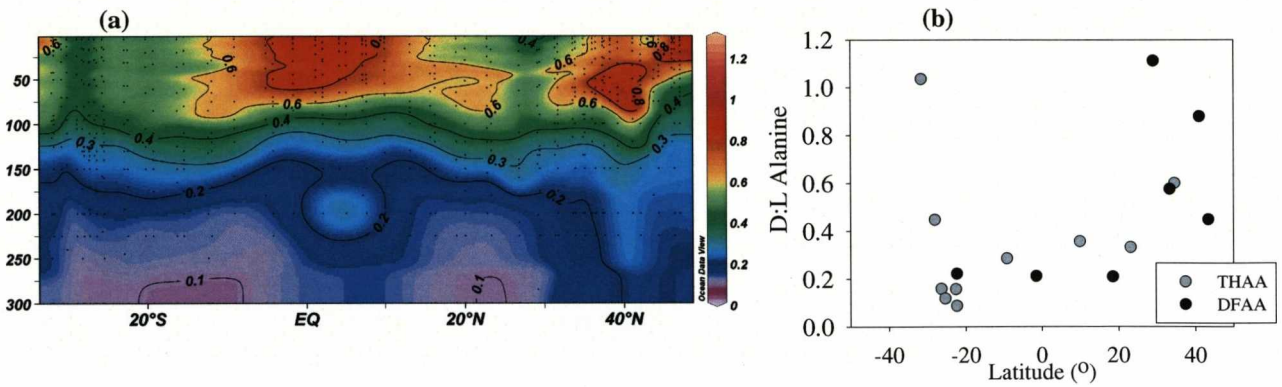

Figure 4.17 (a) Total bacteria numbers (x10^6) for the Atlantic Ocean analysed using flow cytometry. Numbers include both autotrophic and heterotrophic bacteria. Higher abundances exist in the surface waters of the equatorial region and in the more temperate regions at the flanks of the northern gyre. Data kindly supplied by Glen Tarren, Plymouth Marine Laboratory, UK (b) D/L-alanine for DFAA (black circles) and THAA (gray circles) alanine along the AMT16 transect at the chlorophyll maximum, with elevated D/L ratios coincided with the higher bacterial numbers in the temperate regions of the north and south Atlantic.

The high D/L-alanine ratios found on the flanks of both the southern and northern gyre correspond well with the higher abundances of bacteria thus demonstrating that in these regions, the bacterial input to DON is greater than in the oligotrophic Atlantic. However, the low D/L-alanine ratios in the equatorial region, where increased abundances of bacteria are observed, is surprising. Bacterioplankton, can in the absence of other utilizable carbon, utilise D-amino acids as a source of nutrient [*Perez, et al.*, 2003], but since this region is a area where primary production is not nutrient limited, it cannot be assumed that D-alanine is being utilised. Until further investigation into the dynamics of DON in the equatorial region of the Atlantic Ocean is conducted, and improvements made in the recovery of amino acids from DON in the open ocean, little more can be concluded.

The presence of D-amino acids in the particulate fraction is perhaps surprising since one would expect bacteria to pass through a GF/F filter. However, bacteria can be associated with plankton cells and detritus. Studies involving the detection of particulate muramic acid, an amino sugar found in peptidoglycan, reveal that bacterial detritus is an important component of POM [*Benner and Kaiser*, 2003; *Shibata, et al.*, 2006]. Yields of muramic acid were far higher than could be accounted for by bacteria cell abundance, suggesting that a substantial reservoir of particulate bacterial detritus exists throughout the water column [*Benner and Kaiser*, 2003].

The D/L ratios from the PAA along the AMT transect show some variation with latitude (Fig 4.12) in that D/L ratios are slightly higher in the northern gyre than in the southern gyre. This could correspond to higher abundances of bacteria in the northern gyre than the southern gyre (Fig 4.17 a). However, further examination of the actual values acquired from the particulate fractions reveal that the D/L ratios are much lower than those observed for the dissolved fractions. Since D-alanine was the only quantifiable D-amino acid measured in the dissolved fractions in the present study, values from *Perez et al* [2003] are used for comparison as their measurements made were for DON-THAA in the Atlantic Ocean and their values of D/L-alanine were similar to those along the AMT transect. D/L ratios in the PAA along the AMT transect for alanine was 0.02 ±0.01 (mean ± SD; n = 20), for aspartic acid 0.06 ±0.03, for glutamic acid 0.04 ±0.01 and for serine 0.02 ±0.01. The dissolved fractions from *Perez et al* [2003] exhibited much higher D/L ratios, for alanine 0.49 ±0.11 (mean ± SD; n = 54), for aspartic acid 0.42 ±0.2, for glutamic acid 0.15 ±0.11 and for serine 0.09 ±0.04. The low D/L ratios in the PON suggest that bacteria are minor contributors to the PON.

D-amino acids are also present in archaea [*Matsumoto, et al.*, 1999; *Nagata, et al.*, 1998; *Nagata, et al.*, 1999], prokaryotes classified in a separate kingdom to bacteria due to differences between the genetics and physiology of the two groups [*Woese, et al.*, 1990]. Once thought to inhabit extreme environments only, in recent years planktonic archaea have been discovered throughout the worlds oceans [*Delong*, 1992; *Delong, et al.*, 1994; *Fuhrman, et al.*, 1992; *Herndl, et al.*, 2005; *Karner, et al.*, 2001; *Kirchman, et al.*, 2007; *Teira, et al.*, 2006a] and could account for up to one third of all prokaryotic cells in the global ocean [*Karner, et al.*, 2001]. A key difference between bacteria and archaea is that the cell walls of the latter do not contain peptidoglycan [*Kandler and Konig*, 1998]. Instead D-serine, D-alanine, D-proline, D-glutamic acid and D-aspartic acid are found in the archaeal membrane proteins, the soluble proteins and in the free amino acids [*Nagata, et al.*, 1999]. The D/L ratios of these archaeal amino acids are much lower than those reported in DON. D-aspartic acid is dominant in the membrane and soluble proteins, rather than D-alanine as is the case with peptidoglycan [*Schleife.Kh and Kandler*, 1972], while D-serine is most abundant in the free amino acids. Generally in all three fractions and in the three species of archaea analysed to date, D-alanine is the least abundant D-amino acid [*Nagata, et al.*, 1999]. In the present study D-aspartic acid was the predominant D-amino acid followed by D-glutamic acid, whilst D-serine and D-alanine both contributed the least. This suggests that archaeal membrane and soluble proteins may account for the low D/L ratios observed in the PON along the AMT transect.

To investigate this further, [*Jones, et al.*, 2005] derived a peptidoglycan / archaea index (4.04) which could be used as a source indicator for bacterial or archaeal derived organic matter. Since D-alanine is the dominant D-amino acid in peptidoglycan

[*Schleife.Kh and Kandler*, 1972], while D-aspartic acid is dominant in archaeal membranes and soluble proteins [*Nagata, et al.*, 1999], these two D-amino acids are used in the index as follows:

$$\textbf{Peptidoglycan/archaea index} = \textbf{(D/L Ala + 0.1) / (D/L Asp +0.1)} \qquad (4.04)$$

(0.1 is added to both D/L ratios to avoid zero values when either ratio equals one)

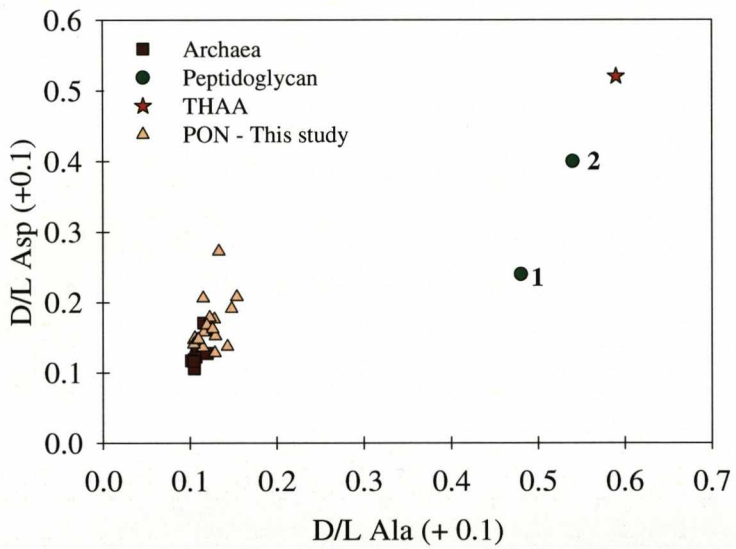

Figure 4.18 Peptidoglycan / archaea index.[*Jones, et al.*, 2005] Values for archaea (dark red squares) represent the D/L ratios of alanine and aspartic acids from the membrane, soluble protein and free amino acids of three archaeal species: *Pyrobalaculum islanicum, Methanosarcina bakeri* and *Halobacterium salinarium* [*Nagata, et al.*, 1999]. Purified peptidoglycan (green circles) from (1) *Synechoccus bacillaris* [*McCarthy, et al.*, 1998] and (2) *Staphylococcus aureus* [*Amon, et al.*, 2001]. DON-THAA (red star) from the North Atlantic (mean, *n*=54) [*Perez, et al.*, 2003]. PON (light pink triangles) from the AMT16 transect at 50m, 100m and 150m.

Figure 4.18 clearly demonstrates that archaeal cells are responsible for the observed D/L ratios found in the PON along the AMT transect.

Previous reports have shown that peptidoglycan can account for 45 to 80% of N found in UDOM which is a similar proportion derived from hydrolysable protein [*McCarthy, et al.*, 1998]. This finding suggested that bacteria are a crucial contributor to the high molecular weight UDOM.

Since very few D-amino acids were quantified in the dissolved amino acids in this study, this calculation cannot be used to provide a peptidoglycan contribution to the dissolved pool. However, since substantial levels of D-amino acids were observed in the PAA, this calculation can be applied to this data set (4.05).

$$\textit{Peptidoglycan N} = 5.7 \times [\text{D-Alanine N}] \qquad (4.05)$$

where 5.7 is the amount of N assuming a common peptidoglycan structure which includes both the amino acid backbone and peptide interbridges [*Rogers*, 1983]. Using the amino acid N calculated from the PON samples the percentage contribution of peptidoglycan N to the amino acid N can be calculated (4.06):

$$\textit{Percentage peptidoglycan N to amino acid N} = \text{peptidoglycan N / amino acid N} \times 100 \qquad (4.06)$$

[*McCarthy, et al.*, 1998]

The amount of N derived from peptidoglycan in the particulate samples ranges from 0.02 – 0.4 nM which results in the percentage contribution of peptidoglycan N to amino acid N ranging from 0.37 to 3.6% (Table 4.06 & Fig 4.19). To further assess this source of N to the N pool of the Atlantic Ocean, the percentage contribution of peptidoglycan to the PON has also been calculated (4.07):

Percentage peptidoglycan N to PON = peptidoglycan N / PON x 100 (4.07)

Values ranged from 0.006 to 0.19%, demonstrating the minor supply of bacterial N to the PON pool.

However, since the D/L ratios obtained in the PON samples collected along the AMT transect suggest that archaea are a more significant contributor to the PON than bacteria, it would be useful to attempt to quantify this supply. Using a similar approach to that of *McCarthy et al* [1998], the archaeal N (4.08) and the percentage contribution to amino acid N (4.09) and subsequently the PON (4.10) has been calculated.

Archaeal N = [D-Aspartic N] x 100 / 3.88 (4.08)

D-Aspartic acid N is used in the calculation since it is the most common D-amino acid found in the archaeal membranes and soluble proteins [*Nagata, et al.*, 1999]. The value 3.88 is the average ratio in molar concentration of D-aspartic acid to the total of the D-amino acid and the corresponding L-amino amino from the membrane and soluble proteins from three species of archaea (*Pyrobalaculum islanicum, Methanosarcina bakeri* and *Halobacterium salinarium* [*Nagata, et al.*, 1999]). Values of archaeal derived N obtained from this calculation range between 0.39 – 5.00 nM (Table 4.06), greater than the peptidoglycan N.

The percentage contribution of archaeal N to amino acid N was calculated as follows (4.09):

Percentage archaeal N to amino acid N = archaeal N / amino acid N x 100 (4.09)

and gave values between 7.07 to 31.89% (Table 4.06 & Fig. 4.19), which is considerably higher than the peptidoglycan contribution to amino acid N. Furthermore the percentage contribution of archaeal N to the PON pool was calculated as follows (4.10):

Percentage archaeal N to PON = archaeal N / PON x 100 (4.10)

and gave values of 0.7 to 1.76% (Table 4.06).

Since a complete data set of PAA does not exist across the entire AMT transect and also with depth it is difficult to comment on any apparent trends. However, it appears that the archaeal contribution to amino acid N is greatest at the equator for samples from 50 and 100 m (Fig 4.19). No distinct trend with depth is apparent, as was found with the actual PAA concentrations (Fig 4.09 a).

Archaea are usually detected in marine waters either through rRNA (e.g. [*Delong*, 1992; *Fuhrman, et al.*, 1992; 1993] or by various forms of fluorescence in-situ hybridisation techniques [*Teira, et al.*, 2004; *Teira, et al.*, 2006b; *Wells, et al.*, 2006]. In POM of oxic and anoxic marine waters, archaea have also been detected by lipid analysis, where C_{40} ether bound lipids which are specific to archaea were found in surface water [*Hoefs, et al.*, 1997]. However, the D/L ratios reported in this study for PON_{susp}, appear to be the first measurements that have revealed the presence of archaea cells in marine waters through the use of enantiomeric amino acids. While no other data exist along the AMT transect to corroborate this conclusion, marine oligotrophic plankton prokaryotic assemblages are known to contain both bacteria and archaea

[*Fuhrman, et al.*, 1993]. The increasing realisation that archaea are extremely abundant in the world's ocean is expanding our knowledge of the role that microbes take in the production of and subsequent recycling of organic N.

Latitude (°)	Depth (m)	PON (nM)	Amino acid N (nM)	D-Alanine N (nM)	D-Aspartic N (nM)	Peptidoglycan N	% contribution of peptidoglycan N to amino acid N	% contribution of peptidoglycan N to PON	Archaeal N	% contribution of archaeal N to amino acid N	% contribution of archaeal N to PON
27.3180°S	50	353.48	5.60	0.004	0.032	0.02	0.368	0.006	0.820	14.64	0.23
	150	109.75	5.12	0.006	0.034	0.04	0.702	0.033	0.880	17.19	0.80
12.2479°S	50	184.18	8.02	0.008	0.040	0.04	0.558	0.024	1.030	12.84	0.56
	150	143.23	3.49	0.006	0.016	0.04	1.033	0.025	0.404	11.56	0.28
1.3762°S	50	766.14	14.67	0.036	0.050	0.21	1.404	0.027	1.301	8.87	0.17
	150	101.92	4.01	0.020	0.018	0.11	2.848	0.112	0.452	11.29	0.44
7.14894°N	50	360.32	15.70	0.048	0.194	0.27	1.740	0.076	5.007	31.89	1.39
15.4775°N	50	252.37	8.74	0.025	0.093	0.14	1.611	0.056	2.389	27.35	0.95
	100	180.24	9.56	0.008	0.123	0.05	0.498	0.026	3.173	33.21	1.76
22.4833°N	100	232.15	11.82	0.023	0.122	0.13	1.098	0.056	3.140	26.56	1.35
29.0948°N	50	185.07	8.81	0.034	0.024	0.19	2.182	0.104	0.623	7.07	0.34
	150	146.05	6.95	0.019	0.058	0.11	1.572	0.075	1.507	21.67	1.03
31.2299°N	50	216.31	10.32	0.027	0.054	0.15	1.490	0.071	1.393	13.50	0.64
	100	213.19	13.33	0.030	0.077	0.17	1.276	0.080	1.986	14.90	0.93
	150	113.06	10.88	0.027	0.061	0.16	1.433	0.138	1.565	14.38	1.38
33.3468°N	50	334.44	23.00	0.070	0.124	0.40	1.729	0.119	3.194	13.89	0.96
	150	80.83	4.23	0.027	0.015	0.15	3.584	0.187	0.386	9.14	0.48
34.5717°N	150	110.90	4.55	0.017	0.027	0.10	2.092	0.086	0.693	15.25	0.63
37.2092°N	100	204.34	10.38	0.046	0.050	0.26	2.523	0.128	1.276	12.29	0.62
44.4411°N	50	396.65	15.85	0.011	0.092	0.06	0.395	0.016	2.359	14.88	0.59

Table 4.06 Station positions with depths and corresponding peptidoglycan N and archaeal N and their contributions to the total amino acid N and the PON. See text for information regarding calculations.

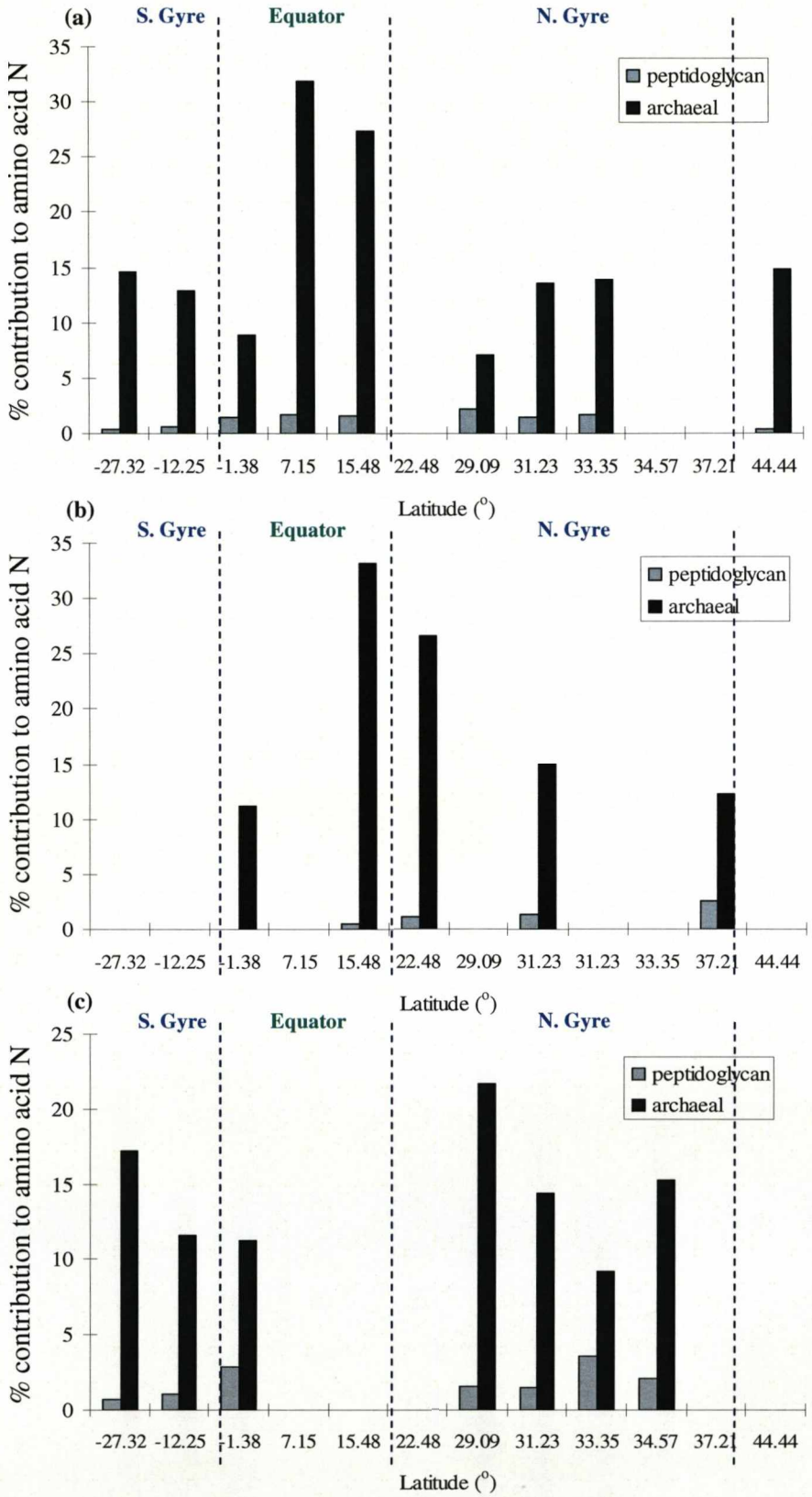

Figure 4.19 Percentage contribution from peptidoglycan (gray bars) and archaea (black bars) to the amino acid N at (a) 50m, (b) 100m and (c) 150m along the AMT16 transect.

4.5 Conclusions

Particulate and dissolved amino acids have been determined along the AMT transect at the chlorophyll maximum. The relative concentrations of TDAA along the transect reveal a depletion towards the centre of the oligotrophic gyres with elevated concentrations in the neighbouring upwelling regions. This could reflect a decrease in the production of amino acids in the low productivity regions of the oligotrophic gyres or could be signify the utilisation of amino acids as source of N by autotrophs/heterotrophs.

To assess the relative 'age' of the organic nitrogen in the surface waters of the Atlantic Ocean, the *Dauwe and Middelburg* [1998] degradation index was applied to the entire data set. Trends observed in the dissolved amino acids along the AMT transect demonstrated that organic matter in the centre of the oligotrophic gyres is older/more degraded than in the more productive waters of the temperate and equatorial regions. This evidence further corroborates that amino acids are a valuable source of N to the biota in the oligotrophic regions of the Atlantic Ocean.

The microbial role in the production and recycling of organic N has been assessed though examination of the D/L amino acids ratios of the samples. The bacterial contribution to the DON pool could not be quantified due to the virtual absence of D-amino acids, which was surprising since previous studies have indicated that bacteria are a major contributor to UDOM [*McCarthy, et al.*, 1998]. This finding suggests that bacteria appear to exude primarily high molecular weight organic N. The few quantified D/L ratios of alanine correspond well with those measured previously in open ocean samples and in pure peptidoglycan. This suggests that D-alanine in the dissolved

fractions of the Atlantic surface values can be attributed to bacteria. Elevated bacterial numbers in the temperate regions of the AMT transect coincide with highest D/L-alanine values.

The D/L ratios of the PAA samples are consistent with a very important contribution of archaea to PON when compared with bacteria. However, the contribution of archaeal N to the total PON is small which raises the question 'where does the remaining amino acid N derive from?' At present it can be assumed that the phytoplankton is the primary contributor since the PON_{susp} is thought to mainly originate from autotrophic phytoplankton (see section 3.3.5). The enantiomeric evidence of archaea in marine PON appears to be the first of its kind, but is consistent with other independent observations.

This study has demonstrated through the evaluation of the distributions of dissolved and particulate amino acids and the employment of a degradation index that amino acids are indeed an important source of labile N in the oligotrophic gyres of the Atlantic Ocean. The bacterial role in the production and recycling of organic N is of little significance when compared with other literature highlighting, the need for further work in this area.

CHAPTER 5

Conclusions, implications and future work

5.1 Overview

Our understanding of the marine chemistry of nitrogen is fundamentally important since nitrogen plays a crucial role in the primary production of the world's oceans and thus controls the drawdown of carbon from the atmosphere to the deep ocean [*Falkowski*, 1997]. Our view of the marine N cycle has changed considerably over the past twenty years due to discoveries which have identified new processes and pathways by which N enters, leaves and is transported through the marine system.

One major problem that still remains unresolved is the mismatch that exists between the observed export production and known inputs of N in the vast oligotrophic gyres of the Atlantic Ocean. In the first chapter of this thesis, various means by which N can be supplied to the euphotic zone are reviewed. *McGillicuddy et al* [1998] claim that this imbalance can be answered by deep ocean NO_3^- injections from eddies. However, whilst this may certainly be the case at the western flanks of the north Atlantic subtropical gyre, model estimates suggest that this supply of N is of less significance towards the central oligotrophic gyre [*Oschlies*, 2002; *Oschlies and Garcon*, 1998]. Therefore, further consideration into the potential role that N_2 fixation and DON as sources of N to the primary producers is required. Numerous direct and indirect studies have demonstrated that N_2 fixation is taking place in the oligotrophic regions of the North Atlantic [*Capone, et al.*, 2005; *Gruber and Sarmiento*, 1997; *Hansell, et al.*, 2004; *Hood, et al.*, 2001; *Lipschultz and Owens*, 1996a; *Montoya, et al.*, 2002]. However, large discrepancies exist between estimates of new N that is supplied to the Atlantic euphotic zone via this process [*Capone, et al.*, 2005; *Mahaffey, et al.*, 2005], since areal estimates made assume temporal and spatial uniformity when N_2 fixation occurs during stochastic, heterogeneous blooms that are not easily predicted or resolved by marine expeditionary field work [*Karl, et al.*, 2002].

One of two major objectives of this study was to assess the spatial extent of N_2 fixation in the Atlantic Ocean and attempt to quantify this input of new N to the euphotic zone. This issue was addressed in Chapter Three, where direct evidence was provided demonstrating that N_2 fixation occurs consistently over the subtropical northern gyre. Stable N isotopic analysis of PON_{susp} samples collected along the AMT transect over three years showed a consistently depleted signal in the northern oligotrophic gyre. This

region overlaps with a region where the tracer N* increases westward following the gyre circulation. This non-conservative behaviour of N* implies that N_2 fixation is responsible for the depleted $\delta^{15}N$ PON_{susp}. A mixing model suggests that N_2 fixation over parts of the northern gyre provides a significant amount of new N (up to 74%) to the euphotic zone that is utilised by the phytoplankton. However, the PON_{susp} represents only a small fraction of the total N pool and therefore N_2 fixation appears to play a minor role in fuelling export production from the euphotic zone to deeper waters over the northern subtropical gyre. It therefore remains to be ascertained what happens to this new N supplied through N_2 fixation? Stable N isotopic data from sediment traps below the euphotic zone in regions of N_2 fixation reveal that PON_{sink} has a fairly enriched signal (3.7‰) [*Altabet*, 1988], suggesting that the isotopically depleted PON does not leave the euphotic zone. It could then be assumed that the depleted N could be exuded from the phytoplankton through DON and NO_3^-. However, isotopic studies at BATS have demonstrated that this is not the case [*Knapp, et al.*, 2005]. Whether the DON measured in that study was refractory, and irrelevant is an open question. If so, then the process of N_2 fixation must be a closely coupled system whereby the diazotrophs provide regenerated and isotopically depleted N to the phytoplankton community. This would imply that N_2 fixation is crucial in supplying N to the northern oligotrophic gyre of the Atlantic not only as introducing a new source of N to the euphotic zone but also providing an invaluable regenerated source of N to other phytoplankton.

The second major objective of this thesis was to gain further understanding into the composition, production and subsequent recycling of organic nitrogen along the AMT transect. This objective was broad and has been met through a variety of means.

Primarily DFAA, THAA and PAA concentrations were determined from surface waters of the Atlantic Ocean. The distributions alone proved a powerful tool in identifying regions of organic N production and consumption. Higher concentrations were found not only in the more productive waters of the equator and temperate regions but also in the region of the North Atlantic subtropical gyre where N_2 fixation was occurring. The employment of a degradation index [*Dauwe and Middelburg*, 1998] demonstrates that fresher organic matter is present at the equator and temperate regions along the AMT transect, while more degraded material is observed towards the centre of the oligotrophic gyres, indicating that DON is utilised as a source of nutrient. Furthermore in the region of N_2 fixation in the northern gyre, slightly fresher organic matter was present, consistent with the release of DON by N_2 fixers such as *Trichodesmium* spp [*Karl, et al.*, 1997; *Lenes, et al.*, 2001], the released DON being enriched in dissolved free amino acids [*Capone, et al.*, 1994; *Glibert and Bronk*, 1994]. Whilst this study suggests that DON provides a source of N to the phytoplankton and previous studies have demonstrated that both phytoplankton and bacteria possess the ability to utilise this source [*Flynn and Butler*, 1986; *Middelboe, et al.*, 1995; *Palenik and Morel*, 1990a], the measure of primary production and ultimately export production fuelled through this means is still unclear. Model studies have demonstrated that horizontal advection of semi-labile DON to the north Atlantic oligotrophic gyre from neighbouring upwelling regions fuels 0.05 mol N m^{-2} y^{-1} of export production [*Roussenov, et al.*, 2006]. This contribution is still not large enough to account for the discrepancies that exist between the N supply and observed export production in the North Atlantic.

As described in Chapter One of this thesis, DON is a complex mixture of labile, semi-labile and refractory moieties with the refractory molecules being dominant. Many

labile and semi-labile N compounds have been identified and quantified in the marine environment whilst the large remainder of the bulk DON pool remains unknown (see review by *Bronk*, 2002). Amino acid analyses along the AMT transect have revealed that the labile and semi-labile components of the DON pool are very small (0.001 – 0.07%). Other N-compounds have also been identified in the DON pool such as purines, pyrimidines and nucleic acids and have also been proven to be utilised as an N source by primary producers (see review by *Bronk*, 2002). One could argue that greater insight is required into the composition of the DON pool, in particular the refractory molecules, to enable better justification in DON being used as a nutrient source. However, since the refractory N molecules dominate the bulk DON pool, is there really any need researching this component of the DON pool when turnover rates are of the order of hundreds of years and therefore irrelevant in fuelling export production? One major step that has advanced our understanding of the DON pool is the realisation that microbial organisms are not only responsible for the remineralisation of organic N but also produce and utilise DON as a nutrient source. Examination of the enantiomeric ratios of TDAA along the AMT transect revealed that the bacterial inputs to the DON pool are much lower (cannot be quantified) than observed in the UDOM, conflicting with previous statements that bacteria can produce 45 to 80% of the total DON pool [*McCarthy, et al.*, 1998]. Whilst this conflict could arise through methodological differences, it does highlight the requirement for a closer examination of the production of DON. Another major discovery in the microbial world has been the growing acknowledgement that archaea could account for up to one third of all prokaryotic cells in the global ocean [*Karner, et al.*, 2001]. This is consistent with the present study of the AMT where archaea were found to contribute ~7 to 32% to the total particulate amino

acid N suggesting that archaea are fundamentally important in the production and recycling of organic N in the worlds oceans.

Whilst DON is an important source of N to primary producers, dissolved organic phosphorus (DOP) could play a more vital role in sustaining particle export. Latitudinal DOP concentrations vary far more than DON concentrations along the AMT transect [*Mahaffey, et al.*, 2004], suggesting that DOP is being depleted in the centre of the oligotrophic gyres. Since DOP is more reactive than DON, with turnover times between 60-300 days [*Bjorkman, et al.*, 2000], it can be an extremely valuable source of P to primary producers, particularly in the oligotrophic gyres of the Atlantic Ocean. Model studies suggest assuming that 95% of DOP is semi-labile then the transport of DOP from neighbouring upwelling regions of the north Atlantic subtropical gyre could supply 12 mmol P m^{-2} yr^{-1} which is equal to half of the P requirements for particle export [*Roussenov, et al.*, 2006].

It is apparent that the northern and southern oligotrophic gyres of the Atlantic Ocean behave differently. Both stable N isotopes and dissolved amino acids demonstrate that while N_2 fixation is a consistent feature of the North Atlantic it is absent from the southern gyre. This could be a seasonal feature since both AMT14 and AMT16 sailed during the northern hemisphere spring. However, during the previous phase of AMT (AMT 1 -8), *Trichodesmium* sp. filaments were counted along the transect during both seasons and colonies were consistently most abundant to the north of the equator [*Tyrrell, et al.*, 2003]. The question than arises regarding the influencing factors in play affecting the North Atlantic that are minimal or even absent from the South Atlantic? In Chapter Three of this thesis, aeolian inputs of dust to the north Atlantic were mentioned. The Saharan Desert in North Africa represents one of the world's largest sources of dust

that can be transported across the North Atlantic basin [*Prospero, et al.*, 1996].This dust is a significant source of soluble aerosol iron (Fe), silica (Si) and phosphorus (P) to the surface waters of the North Atlantic [*Baker, et al.*, 2006]. As described in Chapter Three, the process of N_2 fixation is limited by both Fe and P [*Mills, et al.*, 2004; *Mulholland and Bernhardt*, 2005; *Sanudo-Wilhelmy, et al.*, 2001; *Wu, et al.*, 2000]. Therefore, N_2 fixation is stimulated in the northern gyre but presumably limited by Fe and P in the southern gyre. However, P concentrations (see Appendix F) along the AMT transect reveal higher concentrations in the southern gyre when compared with the northern gyre. This distribution not only demonstrates the depletion of P by N_2 fixation in the northern gyre but also suggests that in the southern gyre N_2 fixation is limited by Fe. Therefore one of the major governing factors controlling the differences in the productivity dynamics between the northern and southern gyres of the Atlantic Ocean is the magnitude of atmospheric inputs to the surface euphotic zones.

5.2 Future work

This thesis throughout, has highlighted areas in the biogeochemical dynamics of the Atlantic Ocean that have yet to be resolved and thus requires further research. These include:

1. Determining the $\delta^{15}N$ of PON_{susp}, PON_{sink}, DON and NO_3^- at one site/station at one particular time. At present, the N isotopic data that exist for the various components of the total N pool are from different sites/stations, seasons and years. Therefore in attempting to close the N isotopic budget for the North

Atlantic too many assumptions are being made and the estimates of the sources and sinks of N made cannot be seen as wholly reliable.

2. To assess the turnover rates of labile DON and DOP in surface waters, fluorogenic substrates can be utilised to determine the amino peptidase and phosphatase enzyme activities respectively (see Appendix F).
3. Through the use of radiolabelled N and P compounds in culture incubations, the rates of uptake and subsequent production of organic compounds could be assessed.
4. To examine further the amino acid dynamics, culture experiments could be conducted whereby amino acid concentrations are monitored throughout the growth and stationary phase of phytoplankton. To the data collected, the Dauwe degradation index could be applied to gain understanding of the production and consumption of amino acids.
5. Identification of C_{40} ether bound lipids in PON_{susp} from the surface waters could help quantify the archaeal contribution to the biomass of the Atlantic Ocean.

5.3 Broader implications

This present study has formed part of the AMT programme which began in 1995 involving bi-annual latitudinal transects of the Atlantic Ocean. The most recent phase (2003-2005) involved measurements of ecosystem structure and elemental cycling, contributing to a decadal data set. This has enabled validation of current models and provided further data for future biogeochemical models [*Robinson, et al.*, 2006]. The AMT programme has advantages compared to other time series such as the Bermuda

Atlantic Time Series (BATS) since the bi-annual transects provide excellent spatial coverage of the various biogeochemical regimes of the Atlantic Ocean for two seasons (spring and autumn). This provides a strong data set that enables the collection of accurate parameters that can be utilised in model studies. However, a drawback of this type of time series is that the biannual sampling along the transect only provides a 'snapshot' of the biogeochemical dynamics. The BATS programme (www.bbsr.edu/cintoo/bats/bats.html) on the other hand samples hydrographic, biological and chemical parameters throughout the water column at a few sites in the Sargasso Sea on a monthly basis. BATS began in 1988, where this rigorous sampling enabled major discoveries to be made regarding the importance of biological diversity in understanding biological and chemical cycles and also quantifying carbon removal pathways in this region. Whilst this style of time-series is beneficial in providing a high resolution data set, it is for only a small region of the western Atlantic Ocean. Several publications using the data collected from the BATS site have involved extrapolating these data to provide estimates for the entire northern Atlantic Ocean (e.g. [*Bates and Hansell*, 2004; *Gruber, et al.*, 2002]. Despite the fact that these estimates provide insight to the dynamics of processes occurring in the Atlantic, the conclusions drawn from these estimates cannot be seen as robust. Therefore future oceanographic research involving time-series should attempt to involve both types of sampling of the two styles of time-series.

The next AMT phase (funded through Oceans 2025; National Environmental Research Council) aims to maintain the programme as a long-term multidisciplinary open-ocean observation system as well as improving the physical measurements and deploying sediment traps in the centre of the oligotrophic gyres [*Robinson, et al.*, 2006].

However, it still lacks the higher time resolution monitoring. The use of novel approaches such as the proposed Esonet (www.oceanlab.addn.ac.uk) observatory network, where single site observatories will be stationed in various oceanic locations around Europe and data is sent back to land via fibre optic sub-sea cables, would compliment the AMT programme, enabling further validation of processes occurring in the open ocean.

REFERENCES

Abell, J., S. Emerson, and P. Renaud (2000), Distributions of TOP, TON and TOC in the North Pacific subtropical gyre: Implications for nutrient supply in the surface ocean and remineralization in the upper thermocline, *Journal of Marine Research, 58*, 203-222.

Achilles, K. M., T. M. Church, S. W. Luther, and D. A. Hutchins (2003), Bioavailability of iron to *Trichodesmium* colonies in the western subtropical Atlantic Ocean, *Limnology and Oceanography, 48*, 2250-2255.

Aiken, J., N. Rees, S. Hooker, P. Holligan, A. Bale, D. Robins, G. Moore, R. Harris, and D. Pilgrim (2000), The Atlantic Meridional Transect: overview and synthesis of data, *Progress in Oceanography, 45*, 257-312.

Altabet, M. A. (1988), Variations in nitrogen isotopic composition between sinking and suspended particles: implications for nitrogen cycling and particle transformation in the open ocean, *Deep Sea Research, 35*, 535-554.

Altabet, M. A. (1996), Nitrogen and carbon isotopic tracers of the source and transformation of particles in the deep sea, *In: Particle Flux in the Ocean*, 155-184.

Altabet, M. A., W. G. Deuser, S. Honjo, and C. Stienen (1991), Seasonal And Depth-Related Changes In The Source Of Sinking Particles In The North-Atlantic, *Nature, 354*, 136-139.

Altabet, M. A., and J. J. McCarthy (1985), Temporal And Spatial Variations In The Natural Abundance Of ^{15}N In PON From A Warm-Core Ring, *Deep-Sea Research Part A-Oceanographic Research Papers, 32*, 755-772.

Amon, R. M. W., H. Fitznar, and R. Benner (2001), Linkages among the bioreactivity, chemical composition, and diagenetic state of marine dissolved organic matter, *Limnology and Oceanography, 46*, 287-297.

Anderson, T. R., and P. Pondaven (2003), Non-redfield carbon and nitrogen cycling in the Sargasso Sea: pelagic imbalances and export flux, *Deep Sea Research I, 50*, 573-591.

Andersson, A., C. Lee, F. Azam, and A. Hagstrom (1985), Release of Amino-Acids and Inorganic Nutrients by Heterotrophic Marine Microflagellates, *Marine Ecology-Progress Series, 23*, 99-106.

Arrigo, K. R. (2005), Marine microorganisms and global nutrient cycles, *Nature, 437*, 349-355.

Azam, F., T. Fenchel, J. G. Field, J. S. Gray, L. A. Meyerreil, and F. Thingstad (1983), The Ecological Role Of Water-Column Microbes In The Sea, *Marine Ecology-Progress Series, 10*, 257-263.

Baker, A. R., T. D. Jickells, K. F. Biswas, K. Weston, and M. French (2006), Nutrients in atmospheric aerosol particles along the Atlantic Meridional Transect, *Deep-Sea Research Part Ii-Topical Studies in Oceanography, 53*, 1706-1719.

Baker, A. R., S. D. Kelly, K. F. Biswas, M. Witt, and T. D. Jickells (2003), Atmospheric deposition of nutrients to the Atlantic Ocean, *Geophysical Research Letters, 30*.

Bale, T., A. Poulton, N. Gist, G. Tarran, K. Chamberlain, I. Cook, T. Frickers, X. Pan, S. Reynolds, M. Schattenhofer, S. Ussher, D. Raitos, S. Lavender, E. Mawji, M. Koblizek, J. Kaiser, M. Hale, D. Drapeau, and M. Frada (2005), Atlantic Meridional Transect: AMT16 Cruise Report, RRS Discovery, 20 May - 29 June 2005.

Bates, N. R., and D. A. Hansell (2004), Temporal variability of excess nitrate in the subtropical mode water of the North Atlantic Ocean, *Marine Chemistry*, *84*, 225-241.

Bell, T. G., G. Malin, C. M. McKee, and P. S. Liss (2006), A comparison of dimethylsulphide (DMS) data from the Atlantic Meridional Transect (AMT) programme with proposed algorithms for global surface DMS concentrations, *Deep-Sea Research Part Ii-Topical Studies in Oceanography*, *53*, 1720-1735.

Benner, R., and K. Kaiser (2003), Abundance of amino sugars and peptidoglycan in marine particulate and dissolved organic matter, *Limnology and Oceanography*, *48*, 118-128.

Bergman, B., and E. J. Carpenter (1991), Nitrogenase confined to randomly distributed trichomes in the marine cyanobacterium *Trichodesmium theibautii*, *Journal of Phycology*, *27*, 158-165.

Berman-Frank, I., J. T. Cullen, Y. Shaked, R. M. Sherrell, and P. G. Falkowski (2001), Iron availability, cellular iron quotas, and nitrogen fixation in *Trichodesmium*, *Limnology and Oceanography*, *46*, 1249-1260.

Berman, T., and D. A. Bronk (2003), Dissolved organic nitrogen: a dynamic participant in aquatic ecosystems, *Aquatic Microbial Ecology*, *31*, 279-305.

Berman, T., and S. Chava (1999), Algal growth on organic compounds as nitrogen sources, *Journal of Plankton Research*, *21*, 1423-1437.

Biggs, D. C. (1977), Respiration And Ammonium Excretion By Open Ocean Gelatinous Zooplankton, *Limnology And Oceanography*, *22*, 108-117.

Bjorkman, K., A. L. Thomas-Bulldis, and D. M. Karl (2000), Phosphorus dynamics in the North Pacific subtropical gyre, *Aquatic Microbial Ecology*, *22*, 185-198.

Bjorkman, K. M., and D. M. Karl (2003), Bioavailability of dissolved organic phosphorus in the euphotic zone at Station ALOHA, North Pacific Subtropical Gyre, *Limnology and Oceanography*, *48*, 1049-1057.

Brandes, J. A., A. H. Devol, and C. Deutsch (2007), New developments in the marine nitrogen cycle, *Chemical Reviews*, *107*, 577-589.

Bronk, D. A. (2002), Dynamics of DON, *In: Biogeochemistry of Marine Dissolved Matter. Academic Press. Eds. Hansell & Carlson*, 159-247.

Brzezinski, M. A., and D. M. Nelson (1995), The Annual Silica Cycle in the Sargasso Sea near Bermuda, *Deep-Sea Research Part I-Oceanographic Research Papers*, *42*, 1215-1237.

Brzezinski, M. A., T. A. Villareal, and F. Lipschultz (1998), Silica production and the contribution of diatoms to new and primary production in the central North Pacific, *Marine Ecology-Progress Series, 167*, 89-104.

Capone, D. G., J. A. Burns, J. P. Montoya, A. Subramaniam, C. Mahaffey, T. Gunderson, A. F. Michaels, and E. J. Capenter (2005), Nitrogen fixation by *Trichodesmium* spp.: An important source of new nitrogen to the tropical and subtropical North Atlantic Ocean, *Global Biogeochemical Cycles, 19*, doi:10.1029/2004GB002331.

Capone, D. G., and E. J. Carpenter (1982), Nitrogen-Fixation in the Marine-Environment, *Science, 217*, 1140-1142.

Capone, D. G., M. D. Ferrier, and E. J. Carpenter (1994), Amino-Acid Cycling in Colonies of the Planktonic Marine Cyanobacterium Trichodesmium-Thiebautii, *Applied and Environmental Microbiology, 60*, 3989-3995.

Capone, D. G., J. P. Zehr, H. W. Paerl, B. Bergman, and E. J. Carpenter (1997), *Trichodesmium*, a globally significant marine cyanobacterium, *Science, 276*, 1221-1229.

Carlson, C. A. (2002), Production and Removal Processes, *In: Biogeochemistry of Marine Dissolved Organic Matter. Academic Press. Eds. Hansell & Carlson*, 91-151.

Carlucci, A. F., D. B. Craven, and S. M. Henrichs (1984), Diel Production and Microheterotrophic Utilization of Dissolved Free Amino Acids in Waters Off Southern California, edited, pp. 165-170.

Carpenter, E. J., H. R. Harvey, B. Fry, and D. G. Capone (1997), Biogeochemical tracers of the marine cyanobacterium *Trichodesmium*, *Deep Sea Research I, 44*, 27-38.

Carpenter, E. J., and K. Romans (1991), Major role of the cyanobacterium *Trichodesmium* in nutrient cycling in the North Atlantic Ocean, *Science, 254*, 1356-1358.

Charette, M. A., S. Bradley Moran, and J. K. B. Bishop (1999), 234Th as a tracer of particulate organic carbon export in the subarctic northeast Pacific Ocean, *Deep Sea Research Part II: Topical Studies in Oceanography, 46*, 2833.

Checkley, D. M., and C. A. Miller (1989), Nitrogen isotopic fractionation by oceanic zooplankton, *Deep Sea Research 36*, 1449-1456.

Codispoti, L. A., J. A. Brandes, J. P. Christensen, A. H. Devol, S. W. A. Naqvi, H. W. Paerl, and T. Yoshinari (2001), The oceanic fixed nitrogen and nitrous oxide budgets: Moving targets as we enter the anthropocene?, *Scientia Marina, 65*, 85-105.

Corner, E. D. S., and A. G. Davies (1971), Plankton As A Factor In Nitrogen And Phosphorus Cycles In Sea, *Advances In Marine Biology, 9*, 101-&.

Cowie, G. L., and J. I. Hedges (1992), Sources and reactivities of amino acids in a coastal marine environment, *Limnology and Oceanography, 37*, 703-724.

Dalsgaard, T., B. Thamdrup, and D. E. Canfield (2005), Anaerobic ammonium oxidation (anammox) in the marine environment, *Research in Microbiology, 156*, 457-464.

Dauwe, B., and J. J. Middelburg (1998), Amino acids and hexosamines as indicators of organic matter degradation state in North Sea sediments, *Limnology and Oceanography*, *43*, 782-798.

Delong, E. F. (1992), Archaea in Coastal Marine Environments, *Proceedings of the National Academy of Sciences of the United States of America*, *89*, 5685-5689.

Delong, E. F., K. Y. Wu, B. B. Prezelin, and R. V. M. Jovine (1994), High Abundance of Archaea in Antarctic Marine Picoplankton, *Nature*, *371*, 695-697.

Dentener, F., J. Drevet, J. F. Lamarque, I. Bey, B. Eickhout, A. M. Fiore, D. Hauglustaine, L. W. Horowitz, M. Krol, U. C. Kulshrestha, M. Lawrence, C. Galy-Lacaux, S. Rast, D. Shindell, D. Stevenson, T. Van Noije, C. Atherton, N. Bell, D. Bergman, T. Butler, J. Cofala, B. Collins, R. Doherty, K. Ellingsen, J. Galloway, M. Gauss, V. Montanaro, J. F. Muller, G. Pitari, J. Rodriguez, M. Sanderson, F. Solmon, S. Strahan, M. Schultz, K. Sudo, S. Szopa, and O. Wild (2006), Nitrogen and sulfur deposition on regional and global scales: A multimodel evaluation, *Global Biogeochemical Cycles*, *20*.

Deutsch, C., N. Gruber, R. M. Key, J. L. Sarmiento, and A. Ganachaud (2001), Denitrification and N-2 fixation in the Pacific Ocean, *Global Biogeochemical Cycles*, *15*, 483-506.

Dittmar, T., H. P. Fitznar, and G. Kattner (2001), Origin and biogeochemical cycling of organic nitrogen in the eastern Arctic Ocean as evident form D- and L-amino acids, *Geochimica et Cosmochimica Acta*, *65*, 4103-4114.

Dore, J. E., and D. M. Karl (1996), Nitrification in the euphotic zone as a source for nitrite, nitrate, and nitrous oxide at Station ALOHA, *Limnology and Oceanography*, *41*, 1619-1628.

Duce, R. A., and N. W. Tindale (1991), Atmospheric transport of iron and its deposition in the ocean, *Limnology and Oceanography*, *36*, 1715-1726.

Dugdale, R. C., and J. J. Goering (1967), Uptake of new and regenerated forms of nitrogen in primary production, *Limnology and Oceanography*, *12*, 196-206.

Emerson, S., P. Quay, D. Karl, C. Winn, L. Tupas, and M. Landry (1997), Experimental determination of the organic carbon flux from open ocean surface waters, *Nature*, *389*, 951-954.

Eppley, R. W., and B. J. Peterson (1979), Particulate Organic-Matter Flux and Planktonic New Production in the Deep Ocean, *Nature*, *282*, 677-680.

Falcon, L. I., E. J. Carpenter, F. Cipriano, B. Bergman, and D. G. Capone (2004), N_2 fixation by unicellular bacterioplankton from the Atlantic and Pacific Oceans: Phylogeny and In Situ Rates, *Applied and Environmental Microbiology*, *70*, 765-770.

Falkowski, P. G. (1997), Evolution of the nitrogen cycle and its influence on the biological sequestration of CO_2 in the ocean, *Nature*, *387*, 272-275.

Flynn, K. J., and I. Butler (1986), Nitrogen sources for the growth of marine microalgae: role of dissolved free amino acids, *Marine Ecology Progress Series*, *34*, 281-304.

Flynn, K. J., and C. R. N. Wright (1986), The Simultaneous Assimilation of Ammonium and L-Arginine by the Marine Diatom Phaeodactylum-Tricornutum Bohlin, *Journal of Experimental Marine Biology and Ecology, 95*, 257-269.

Fogel, M. L., and L. A. Cifuentes (1993), Isotope fractionation during primary production, *In: Organic Geochemistry - Principles and Applications. Edited by M. H. Engel & S. A. Macko. PLENUM Publishing Corporation*, 73-98.

Fuhrman, J. (1987a), Close Coupling between Release and Uptake of Dissolved Free Amino-Acids in Seawater Studied by an Isotope-Dilution Approach, *Marine Ecology-Progress Series, 37*, 45-52.

Fuhrman, J. (1987b), Close coupling between release and uptake of dissolved free amino acids in seawater studied by an isotope dilution approach, *Marine Ecology Progress Series, 37*, 45-52.

Fuhrman, J. A., and R. L. Ferguson (1986), Nanomolar Concentrations and Rapid Turnover of Dissolved Free Amino-Acids in Seawater - Agreement between Chemical and Microbiological Measurements, *Marine Ecology-Progress Series, 33*, 237-242.

Fuhrman, J. A., K. McCallum, and A. A. Davis (1992), Novel Major Archaebacterial Group from Marine Plankton, *Nature, 356*, 148-149.

Fuhrman, J. A., K. McCallum, and A. A. Davis (1993), Phylogenetic Diversity of Subsurface Marine Microbial Communities from the Atlantic and Pacific Oceans, *Applied and Environmental Microbiology, 59*, 1294-1302.

Gallon, J. R. (1992), Reconciling the incompatible: N_2 fixation and O_2, *Tansley Review No. 44: New Phytologist, 122*, 571-609.

Galloway, J. N., F. J. Dentener, D. G. Capone, E. W. Boyer, R. W. Howarth, S. P. Seitzinger, G. P. Asner, C. C. Cleveland, P. A. Green, E. A. Holland, D. M. Karl, A. F. Michaels, J. H. Porter, A. R. Townsend, and C. J. Vorosmarty (2004), Nitrogen cycles: past, present, and future, *Biogeochemistry, 70*, 153-226.

Garcon, V. C., A. Oschilies, S. C. Doney, D. McGillicuddy, and J. Waniek (2001), The role of mesoscale variability on plankton dynamics in the North Atlantic, *Deep-Sea Research II, 48*, 2199-2226.

Geesey, G. G., and R. Y. Morita (1979), Capture of Arginine at Low Concentrations by a Marine Psychrophilic Bacterium, *Applied and Environmental Microbiology, 38*, 1092-1097.

Gist, N., P. Serret, E. M. S. Woodward, K. Chamberlain, and C. Robinson (2007), Seasonal, interannual and spatial variability in plankton production and respiration in the Atlantic Ocean, *Deep-Sea Research II*, Submitted.

Glibert, P. M., and D. A. Bronk (1994), Release of Dissolved Organic Nitrogen by Marine Diazotrophic Cyanobacteria, Trichodesmium Spp, *Applied and Environmental Microbiology, 60*, 3996-4000.

Gruber, N., C. D. Keeling, and N. R. Bates (2002), Interannual variability in the North Atlantic Ocean carbon sink, *Science, 298*, 2374-2378.

Gruber, N., C. D. Keeling, and T. F. Stocker (1998), Carbon-13 constraints on the seasonal inorganic carbon budget at the BATS site in the northwestern Sargasso Sea, *Deep Sea Research Part I - Oceanographic Research Papers*, *45*, 673-717.

Gruber, N., and J. L. Sarmiento (1997), Global patterns of nitrogen fixation and denitrification, *Global Biogeochemical Cycles*, *11*, 235-266.

Grutters, M., W. v. Raaphorst, E. Epping, W. Helder, and J. W. d. Leeuw (2002), Preservation of amino acids from in situ-produced bacterial cell wall peptidoglycans in northeastern Atlantic continental margin sediments, *Limnology and Oceanography*, *47*, 1521-1524.

Hammer, K. D., and U. H. Brockmann (1983), Rhythmic Release of Dissolved Free Amino-Acids from Partly Synchronized Thalassiosira-Rotula under Nearly Natural Conditions, *Marine Biology*, *74*, 305-312.

Hansell, D. A., N. R. Bates, and D. B. Olson (2004), Excess nitrate and nitrogen fixation in the North Atlantic Ocean, *Marine Chemistry*, *84*, 243-265.

Hastings, M. G., D. M. Sigman, and F. Lipschultz (2003), Isotopic evidence for source changes of nitrate in rain at Bermuda, *Journal Of Geophysical Research-Atmospheres*, *108*.

Hecky, R. E., K. Mopper, P. Kilham, and E. T. Degens (1973), Amino-Acid and Sugar Composition of Diatom Cell-Walls, *Marine Biology*, *19*, 323-331.

Hellebust, J. A. (1965), Excretion of some organic compounds by marine phytoplankton, *Limnology and Oceanography*, *10*, 192-206.

Herndl, G. J., T. Reinthaler, E. Teira, H. van Aken, C. Veth, A. Pernthaler, and J. Pernthaler (2005), Contribution of Archaea to total prokaryotic production in the deep Atlantic Ocean, *Applied and Environmental Microbiology*, *71*, 2303-2309.

Heywood, J. L., M. V. Zubkov, G. A. Tarran, B. M. Fuchs, and P. M. Holligan (2006), Prokaryoplankton standing stocks in oligotrophic gyre and equatorial provinces of the Atlantic Ocean: Evaluation of inter-annual variability, *Deep Sea Research Part II: Topical Studies in Oceanography*, *53*, 1530.

Hoefs, M. J. L., S. Schouten, J. W. deLeeuw, L. L. King, S. G. Wakeham, and J. S. S. Damste (1997), Ether lipids of planktonic archaea in the marine water column, *Applied and Environmental Microbiology*, *63*, 3090-3095.

Holligan, P., M. Zubkov, A. Poulton, S. Painter, Y. N. Kim, T. Adey, J. Heywood, M. Stinchcombe, A. Harvey, N. Gist, C. Lowe, E. S. Martin, P. Hampton, N. Millward, K. Chamberlain, T. Bell, A. Hind, B. K. Farhana, S. Reynolds, J. Robinson, and S. Thomalla (2004), Atlantic Meridional Transect: AMT14 Cruise Report, RRS James Clark Ross, 28 April - 1 June, 6.

Hood, R. R., N. R. Hood, D. G. Capone, and D. B. Olson (2001), Modeling the effect of nitrogen fixation on carbon and nitrogen fluxes at BATS, *Deep Sea Research II*, *48*, 1609-1648.

Hoppe, H. (1993), Use of fluorogenic model substrates for extracellular enzyme activity (EAA) measurment of bacteria, *In: Handbook of methods in aquatic microbial ecology. Lewis Publisherd. Eds. Kemp, Sherr, Cole.*, 423-431.

Howard, J. B., and D. C. Rees (1996), Structural basis of biological nitrogen fixation, *Chemistry Reviews, 96*, 2965-2982.

Hubberten, U., R. J. Lara, and G. Kattner (1994), Amino acid composition of seawater and dissolved humic substances in the Greenland Sea, *Marine Chemistry, 45*, 121-128.

Hulth, S., R. C. Aller, D. E. Canfield, T. Dalsgaard, P. Engstrom, F. Gilbert, K. Sundback, and B. Thamdrup (2005), Nitrogen removal in marine environments: recent findings and future research challenges, *Marine Chemistry, 94*, 125-145.

Jackson, G. A., and P. M. Williams (1985), Importance of dissolved organic nitrogen and phosphorus to biological nutrient cycling, *Deep-Sea Research, 32*, 223-235.

Janson, S., E. J. Carpenter, and B. Bergman (1994), Compartmentalization of nitrogenase in a non-heterocystous cyanobacterium *Trichodesmium contortum*, *FEMS Microbiology Letters, 118*, 9-14.

Jenkins, W. J. (1988), Nitrite flux into the euphotic zone near Bermuda, *Nature, 311*, 521-523.

Jenkins, W. J., and C. Goldman (1985), Seasonal oxygen cycling and primary production in the Sargasso Sea, *Journal of Marine Research, 43*, 465-491.

Jickells, T., C. Robinson, A. Poulton, N. Gist, T. Bell, A. Hickman, M. Lucas, F. Nedelec, S. Painter, S. Root, P. Statham, S. Thomalla, K. Chamberlain, C. Lowe, N. Millward, G. Moore, E. S. Martin, M. Woodward, C. Hodge, G. Foster, J. Robinson, and G. Hargreaves (2003a), Atlantic Meridional Transect: AMT12 Cruise Report, RRS James Clark Ross, 12 May - 17 June, 2003.

Jickells, T. D., Z. S. An, K. K. Anderson, A. R. Baker, G. Bergametti, N. Brooks, J. J. Cao, P. N. Boyd, R. A. Duce, C. A. Hunter, H. Kawahata, N. Kubilay, J. laRoche, P. S. Liss, N. Mahowald, J. M. Prospero, A. J. Ridgewell, I. Tegen, and T. Torres (2005), Global iron connections between desert dust, ocean biogeochemistry and climate, *Science, 308*, 67-71.

Jickells, T. D., S. D. Kelly, A. R. Baker, K. Biswas, P. F. Dennis, L. J. Spokes, M. Witt, and S. G. Yeatman (2003b), Isotopic evidence for a marine ammonia source, *Geophysical Research Letters, 30*.

Jones, V., M. J. Collins, K. E. H. Penkman, R. Jaffe, and G. A. Wolff (2005), An assessment of the microbial contribution to aquatic dissolved organic nitrogen using amino acid enantiomeric ratios, *Organic Geochemistry, 36*, 1099-1107.

Jorgensen, N. O. G., and M. Middelboe (2006), Occurrence and bacterial cycling of D amino acid isomers in an estuarine environment, *Biogeochemistry, 81*, 77-94.

Jorgensen, N. O. G., L. J. Tranvik, and G. M. Berg (1999), Occurrence and bacterial cycling of dissolved nitrogen in the Gulf of Riga, the Baltic Sea, *Marine Ecology-Progress Series, 191*, 1-18.

Kandler, O., and H. Konig (1998), Cell wall polymers in Archaea (Archaebacteria), *Cellular and Molecular Life Sciences, 54*, 305-308.

Karl, D., A. Michaels, B. Bergman, D. Capone, E. Carpenter, R. Letelier, F. Lipschultz, H. Paerl, D. Sigman, and L. Stal (2002), Dinitrogen fixation in the world's oceans, *Biogeochemistry, 57/58*, 47-98.

Karl, D., L. Tupas, J. Dore, J. Christian, and D. Hebel (1997), The role of nitrogen fixation in biogeochemical cycling un the subtropical North Pacific Ocean, *Nature, 388*, 533-538.

Karl, D. M., and K. M. Bjorkman (2002), Dynamics of DOP, *In: Biogeochemistry of Marine Dissolved Matter. Academic Press. Eds. Hansell & Carlson*, 249-366.

Karner, M. B., E. F. DeLong, and D. M. Karl (2001), Archaeal dominance in the mesopelagic zone of the Pacific Ocean, *Nature, 409*, 507-510.

Keil, R. G., and D. L. Kirchman (1991), Dissolved combined amino acids in marine waters as determined by a vapor-phase hydrolysis method, *Marine Chemistry, 33*, 243-259.

Keil, R. G., and D. L. Kirchman (1993), Dissolved Combined Amino-Acids - Chemical Form and Utilization by Marine-Bacteria, *Limnology and Oceanography, 38*, 1256-1270.

Keil, R. G., and D. L. Kirchman (1999), Utilization of dissolved protein and amino acids in the northern Sagasso Sea, *Aquatic Microbial Ecology, 18*, 293-300.

Kirchman, D. L. (1994), The Uptake of Inorganic Nutrients by Heterotrophic Bacteria, *Microbial Ecology, 28*, 255-271.

Kirchman, D. L., H. Elifantz, A. I. Dittel, R. R. Malmstrom, and M. T. Cottrell (2007), Standing stocks and activity of Archaea and Bacteria in the western Arctic Ocean, *Limnology and Oceanography, 52*, 495-507.

Kiriakoulakis, K., B. J. Bett, M. White, and G. A. Wolff (2004), Organic biogeochemistry of the Darwin Mounds, a deep-water coral ecosystem, of the NE Atlantic, *Deep-Sea Research Part I-Oceanographic Research Papers, 51*, 1937-1954.

Knap, A., T. Jickells, A. Pszenny, and J. Galloway (1986), Significance of Atmospheric-Derived Fixed Nitrogen on Productivity of the Sargasso Sea, *Nature, 320*, 158-160.

Knapp, A. N., D. M. Sigman, and F. Lipschultz (2005), N isotopic composition of dissolved organic nitrogen and nitrate and the Bermuda Atlantic Time Series, *Global Biogeochemical Cycles, 19*, doi: 10.1029/2004GB002320.

Kuypers, M. M. M., G. Lavik, D. Woebken, M. Schmid, B. M. Fuchs, R. Amann, B. B. Jorgensen, and M. S. M. Jetten (2005), Massive nitrogen loss from the Benguela upwelling system through anaerobic ammonium oxidation, *Proceedings of the National Academy of Sciences of the United States of America, 102*, 6478-6483.

Kuypers, M. M. M., A. O. Sliekers, G. Lavik, M. Schmid, B. B. Jorgensen, J. G. Kuenen, J. S. S. Damste, M. Strous, and M. S. M. Jetten (2003), Anaerobic ammonium oxidation by anammox bacteria in the Black Sea, *Nature, 422*, 608-611.

Ledwell, J. R., A. J. Watson, and C. S. Law (1993), Evidence for Slow Mixing across the Pycnocline from an Open-Ocean Tracer-Release Experiment, *Nature, 364*, 701-703.

Lee, C. (1988), Amino Acid and Amine Biogeochemistry in Marine Particulate Material and Sediments, *In: Nitrogen Cycling in Coastal Marine Environments. John Wiley & Sons. Eds. T.H. Blackburn & J. Sorensen*, 125-141.

Lee, C., and J. L. Bada (1977), Dissolved Amino-Acids in Equatorial Pacific, Sargasso Sea, and Biscayne Bay, *Limnology and Oceanography, 22*, 502-510.

Lee, C., and C. Cronin (1984), Particulate amino acids in the sea: Effects of primary productivity and biological decomposition, *Journal of Marine Research, 42*, 1075-1097.

Lee, K., D. Karl, R. Wannikhof, and J. Z. Zhang (2002), Global estimate of net carbon production in the nitrate-depleted tropical and sub-tropical ocean, *Journal of Geophysical Research - Oceans, 29*, 10.1029/2001GL014198.

Lenes, J. M., B. P. Darrow, C. Cattrall, C. A. Heil, M. Callahan, G. A. Vargo, R. H. Byrne, J. M. Prospero, D. E. Bates, K. A. Fanning, and J. J. Walsh (2001), Iron fertilization and the Trichodesmium response on the West Florida shelf, *Limnology And Oceanography, 46*, 1261-1277.

Lewis, M. R., W. G. Harrison, N. S. Oakey, D. Hebert, and T. Platt (1986), Vertical Nitrate Fluxes in the Oligotrophic Ocean, *Science, 234*, 870-873.

Libes, S. M. (1992), The Marine Nitrogen Cycle, *In: An introduction to Marine Biogeochemistry. John Wiley & Sons Inc.*, 423-446.

Lipschultz, F., and N. J. P. Owens (1996a), An assessment of nitrogen fixation as a source of nitrogen to the North Atlantic Ocean, *Biogeochemistry, 35*, 261-274.

Lipschultz, F., and N. J. P. Owens (1996b), An assessment of nitrogen fixation as a source of nitrogen to the North Atlantic Ocean, *Biogeochemistry, 35*, 261-274.

Liu, K.-K., and I. R. Kaplan (1989), The eastern tropical Pacific as a source of ^{15}N-enriched nitrate in seawater off southern California, *Limnology and Oceanography, 34*, 820-830.

Lumpkin, R., and M. Pazos (2006), Measuring surface currents with Surface Velocity Program drifters: the instrument, its data, and some recent results. Chapter two of Lagrangian Analysis and Prediction of Coastal and Ocean Dynamics (LAPCOD) ed. A. Griffa, A. D. Kirwan, A. J. Mariano, T. Ozgokmen, and T. Rossby.

Mahaffey, C., A. F. Michaels, and D. G. Capone (2005), The conundrum of marine N-2 fixation, *American Journal Of Science, 305*, 546-595.

Mahaffey, C., R. G. Williams, and G. A. Wolff (2004), Physical supply of nitrogen to phytoplankton in the Atlantic Ocean, *Global Biogeochemical Cycles, 18*, doi:10.1029/2003GB002129.

Mahaffey, C., R. G. Williams, G. A. Wolff, N. Mahowald, W. Anderson, and M. Woodward (2003), Biogeochemical signatures of nitrogen fixation in the eastern North Atlantic, *Geophysical Research Letters, 30*.

Mahowald, N. M., A. R. Baker, G. Bergametti, N. Brooks, R. A. Duce, T. D. Jickells, N. Kubilay, J. M. Prospero, and I. Tegen (2005), Atmospheric global dust cycle and iron inputs to the ocean, *Global Biogeochemical Cycles, 19.*

Maranon, E., P. M. Holligan, R. Barciela, N. Gonzalez, B. Mourino, M. J. Pazo, and M. Varela (2001), Patterns of phytoplankton size structure and productivity in contrasting open-ocean environments, *Marine Ecology-Progress Series, 216,* 43-56.

Maranon, E., P. M. Holligan, M. Varela, B. Mourino, and A. J. Bale (2000), Basin-scale variability of phytoplankton biomass, production and growth in the Atlantic Ocean, *Deep Sea Research Part I: Oceanographic Research Papers, 47,* 825-857.

Martin, J. H., and S. E. Fitzwater (1988), Iron deficiency limits phytoplankton growth in the north-east Pacific sub-arctic, *Nature, 331,* 341-343.

Matsumoto, M., H. Homma, Z. Long, K. Imai, R. Iida, T. Maruyama, Y. Aikawa, I. Endo, and M. Yahda (1999), Occurrence of free D-amino acids and aspartate racemases in hyperthermophillic archaea *Journal of Bacteriology, 181,* 6560-6563.

McCarthy, M. D., J.I.Hedges, and R. Benner (1998), Major bacterial contribution to marine dissolved organic nitrogen, *Science, 281,* 231-234.

McGillicuddy, D. J., and A. R. Robinson (1997), Eddy-induced nutrient supply and new production in the Sargasso Sea, *Deep Sea Research I, 44,* 1427-1450.

McGillicuddy, D. J., A. R. Robinson, D. A. Siegel, H. W. Jannasch, R. Johnson, T. D. Dickey, J. McNeil, A. F. Micheals, and A. H. Knap (1998), Influence of mesoscale eddies on new production in the Sargasso Sea, *Nature, 394,* 263-265.

Michaels, A. F., D. Olson, J. L. Sarmiento, J. W. Ammerman, K. Fanning, R. Jahnke, A. H. Knap, F. Lipschultz, and J. M. Prospero (1996), Inputs, losses and transformations of nitrogen and phosphorus in the pelagic north Atlantic ocean, *Biogeochemistry, 25,* 181-226.

Middelboe, M., N. Borch, and D. L. Kirchman (1995), Bacterial utilization of dissolved free amino acids, dissolved combined amino acids and ammonium in the Delaware Bay estuary: effects of carbon and nitrogen limitation, *Marine Ecology Progress Series, 128.*

Middelboe, M., and N. O. G. Jorgensen (2006), Viral lysis of bacteria: an important source of dissolved amino acids and cell wall compounds, *Journal of the Marine Biological Association of the United Kingdom, 86,* 605-612.

Mills, M. M., C. Ridame, M. Davey, J. L. Roche, and R. J. Geider (2004), Iron and phosphorus co-limit nitrogen fixation in the eastern tropical North Atlantic, *Nature, 429,* 292-432.

Minagawa, M., and E. Wada (1986), Nitrogen isotope ratios of red tide organisms in the East China Sea: a characterisation of biological nitrogen fixation, *Marine Chemistry, 19,* 245-259.

Montoya, J. P., E. J. Carpenter, and D. G. Capone (2002), Nitrogen fixation and nitrogen isotope abundances in zooplankton of the oligotrophic North Atlantic, *Limnology and Oceanography*, *47*, 1617-1628.

Montoya, J. P., and J. J. McCarthy (1995), Isotopic fractionation during nitrate uptake by phytoplankton grown in continuous culture, *Journal of Plankton Research*, *17*, 439-464.

Moore, L. R., A. F. Post, G. Rocap, and S. W. Chisholm (2002), Utilization of different nitrogen sources by the marine cyanobacteria Prochlorococcus and Synechococcus, *Limnology and Oceanography*, *47*, 989-996.

Mulder, A., A. A. Vandegraaf, L. A. Robertson, and J. G. Kuenen (1995), Anaerobic Ammonium Oxidation Discovered in a Denitrifying Fluidized-Bed Reactor, *Fems Microbiology Ecology*, *16*, 177-183.

Mulholland, M. R., and P. W. Bernhardt (2005), The effect of growth rate, phosphorus concentration, and temperature on N_2 fixation, and nitrogen release in continuous cultures of *Trichodesmium* IMS101, *Limnology and Oceanography*, *50*, 839-849.

Mulholland, M. R., and D. G. Capone (1999), Nitrogen fixation, uptake and metabolism in natural and cultured populations of Trichodesmium spp, *Marine Ecology-Progress Series*, *188*, 33-49.

Nagata, T., and D. L. Kirchman (1991), Release of Dissolved Free and Combined Amino-Acids by Bacterivorous Marine Flagellates, *Limnology and Oceanography*, *36*, 433-443.

Nagata, Y., T. Fujiwara, K. Kawaguchi-Nagata, Y. Fukumori, and T. Yamanaka (1998), Occurrence of peptidyl D-amino acids in soluble fractions of several eubacteria, archaea and eukaryotes, *Biochimica et Biophysica Acta*, *1379*, 76-82.

Nagata, Y., K. Tanaka, T. Iida, Y. Kera, R. Yamada, Y. Nakajima, T. Fujiwara, Y. Fukumori, T. Yamanaka, Y. Koga, S. Tsuji, and K. Kawaguchi-Nagata (1999), Occurrence of D-amino acids in a few archaea and dehydrogenase activities in hyperthermophile *Pyrobaculum islandicum*, *Biochimica et Biophysica Acta*, *1435*, 160-166.

Nakatsuka, T., N. Handa, N. Harada, T. Sugimoto, and S. Imaizumi (1997), Origin and decomposition of sinking particulate organic matter in the deep water column inferred form the vertical distributions of its $\delta^{15}N$, $\delta^{13}C$ and $\delta^{14}C$, *Deep-Sea Research I*, *44*, 1957-1979.

Naqvi, S. (2006), Marine nitrogen cycle, *In: Encyclopedia of Earth. Eds. Cutler J. Cleveland (Washington, D.C.: Environmental Information Coalition, National Council for Science and the Environment). http://www.eoearth.org/article/Marine_nitrogen_cycle (02/07/2007).*

Nelson, D. M., and M. A. Brzezinski (1997), Diatom growth and productivity in an oligotrophic midocean gyre: A 3-yr record from the Sargasso Sea near Bermuda, *Limnology and Oceanography*, *42*, 473-486.

Nguyen, R. T., and H. R. Harvey (1997), Protein and amino acid cycling during phytoplankton decomposition in oxic and anoxic waters, *Organic Geochemistry*, *27*, 115-128.

Nielsen, E. S. (1951), Measurement Of The Production Of Organic Matter In The Sea By Means Of Carbon-14, *Nature*, *167*, 684-685.

Nielsen, L. P., and R. N. Glud (1996), Denitrification in a coastal sediment measured in situ by the nitrogen isotope pairing technique applied to a benthic flux chamber, *Marine Ecology-Progress Series*, *137*, 181-186.

Ogawa, H., Y. Amagai, I. Koike, K. Kaiser, and R. Benner (2001), Production of refractory dissolved organic matter by bacteria, *Science*, *292*, 917-920.

Orcutt, K. M., F. Lipschultz, K. Gundersen, R. Arimoto, A. F. Micheals, A. H. Knap, and J. R. Gallon (2001), A seasonal study of the significance of N_2 fixation by *Trichodesmium* spp. at the Bermuda Atlantic Time-series Study (BATS) site, *Deep Sea Research II*, *48*, 1583-1608.

Oschlies, A., and V. Garcon (1998), Eddy-induced enhancement of primary production in a model of the North Atlantic Ocean, *Nature*, *394*, 266-269.

Oschlies, A. (2002), Can eddies make ocean deserts bloom?, *Global Biogeochemical Cycles*, *16*.

Oschlies, A., and V. Garcon (1998), Eddy-induced enhancement of primary production in a model of the North Atlantic Ocean, *Nature*, *394*, 266-269.

Owens, N. J. P. (1987), Natural Variations in ^{15}N in the Marine Environment, *Advances in Marine Biology*, *24*, 389-451.

Paerl, H. W., and J. P. Zehr (2000), Marine nitrogen fixation, *In: Kirchman (Ed) Microbial Ecology of the Oceans*, 387-426.

Palenik, B., and S. E. Henson (1997), The use of amides and other organic nitrogen sources by the phytoplankton *Emiliania huxleyi*, *Limnology and Oceanography*, *42*, 1544-1551.

Palenik, B., and F. M. M. Morel (1990a), Amino acid utilization by marine phytoplankton: a novel mechanism, *Limnology and Oceanography*, *35*, 260-269.

Palenik, B., and F. M. M. Morel (1990b), Comparison of cell surface L-amino acid oxidases from several marine phytoplankton, *Marine Ecology Progress Series*, *59*, 195-201.

Panosso, R., and E. Graneli (2000), Effects of dissolved organic matter on the growth of *Nodularia spumigena* (Cyanophyceae) cultivated under N or P deficiancy, *Marine Biology*, *136*, 331-336.

Perez, M. T., C. Pausz, and G. J. Herndl (2003), Major shift in bacterioplankton utilization of enantiomeric amino acids between surface waters and the ocean's interior, *Limnology and Oceanography*, *48*, 755-763.

Phillips, N. W. (1984), Role of Different Microbes and Substrates as Potential Suppliers of Specific, Essential Nutrients to Marine Detritivores, *Bulletin of Marine Science*, *35*, 283-298.

Platt, T., and S. Sathyendranath (1988), Oceanic Primary Production - Estimation by Remote-Sensing at Local and Regional Scales, *Science*, *241*, 1613-1620.

Poulton, A. J., P. M. Holligan, A. Hickman, Y.-N. Kim, T. R. Adey, M. C. Stinchcombe, C. Holeton, S. Root, and E. M. S. Woodward (2006a), Phytoplankton carbon fixation, chlorophyll-biomass and diagnostic pigments in the Atlantic Ocean, *Deep Sea Research Part II: Topical Studies in Oceanography*, *53*, 1593.

Poulton, A. J., R. Sanders, P. M. Holligan, M. C. Stinchcombe, T. R. Adey, L. Brown, and K. Chamberlain (2006b), Phytoplankton mineralization in the tropical and subtropical Atlantic Ocean, *Global Biogeochemical Cycles*, *20*.

Prospero, J. M., K. Barrett, T. Church, F. Dentener, R. A. Duce, J. N. Galloway, H. Levy, J. Moody, and P. Quinn (1996), Atmospheric deposition of nutrients to the North Atlantic Basin, *Biogeochemistry*, *35*, 27-73.

Redfield, A. C. (1958), The Biological Control Of Chemical Factors In The Environment, *American Scientist*, *46*, 205-221.

Redifeld, A. C. (1934), On the proportions of organic derivations in seawater and their relation to the composition of plankton *In: James Memorial Volume (ed. R.J. Daniel) University Press of Liverpool*, 177-192.

Robinson, C., A. J. Poulton, P. M. Holligan, A. R. Baker, G. Forster, N. Gist, T. D. Jickells, G. Malin, R. Upstill-Goddard, and R. G. Williams (2006), The Atlantic Meridional Transect (AMT) Programme: A contextual view 1995-2005, *Deep Sea Research Part II: Topical Studies in Oceanography*, *53*, 1485.

Robinson, C., and P. J. L. Williams (1999), Plankton net community production and dark respiration in the Arabian Sea during September 1994, *Deep-Sea Research Part Ii-Topical Studies in Oceanography*, *46*, 745-765.

Rogers, H. J. (1983), Aspects of Microbiology, Vol. 6: Bacterial Cell Wall Structure. Van Nostrand Reinhold Co. Ltd., Berkshire, England., 1-27.

Roussenov, V., R. G. Williams, C. Mahaffey, and G. A. Wolff (2006), Does the transport of dissolved organic nutrients affect export production in the Atlantic Ocean?, *Global Biogeochemical Cycles*, *20*.

Rysgaard, S., and R. N. Glud (2004), Anaerobic N-2 production in Arctic sea ice, *Limnology and Oceanography*, *49*, 86-94.

Sanders, R., and T. Jickells (2000), Total organic nutrients in Drake Passage, *Deep Sea Research I*, *47*, 997-1014.

Sanudo-Wilhelmy, S. A., A. B. Kustka, C. J. Gobler, D. A. Hutchins, M. Yang, K. Lwiza, J. Burns, D. G. Capone, J. A. Raven, and E. J. Carpenter (2001), Phosphorus limitation of nitrogen fixation by *Trichodesmium* in the central Atlantic Ocean, *Nature*, *411*, 66-69.

Schleife.Kh, and O. Kandler (1972), Peptidoglycan Types of Bacterial Cell-Walls and Their Taxonomic Implications, *Bacteriological Reviews*, *36*, 407-477.

Serret, P., C. Robinson, E. Fernandez, E. Teira, and G. Tilstone (2001), Latitudinal variation of the balance between plankton photosynthesis and respiration in the eastern Atlantic Ocean, *Limnology and Oceanography*, *46*, 1642-1652.

Shibata, A., K. Ohwada, M. Tsuchiya, and K. Kogure (2006), Particulate peptidoglycan in seawater determined by the silkworm larvae plasma (SLP) assay, *Journal of Oceanography*, *62*, 91-97.

Sigman, D. M., M. A. Altabet, R. Michener, D. C. McCorkle, B. Fry, and R. M. Holmes (1997), Natural abundance-level measurement of the nitrogen isotopic composition of oceanic nitrate: an adaptation of the ammonia diffusion method, *Marine Chemistry*, *57*, 227-242.

Spokes, L. J., S. G. Yeatman, S. E. Cornell, and T. D. Jickells (2000), Nitrogen deposition to the eastern Atlantic Ocean. The importance of south-easterly flow, *Tellus*, *52B*, 37-49.

Strass, V. H. (1992), Chlorophyll patchiness caused by mesoscale upwelling at fronts, *Deep-Sea Research*, *39*, 75-96.

Stryer, L. (1995), *In: Biochemistry, Fourth Edition. W. H. Freeman and Company, New York*, 193-195.

Tarran, G. A., J. L. Heywood, and M. V. Zubkov (2006), Latitudinal changes in the standing stocks of nano- and picoeukaryotic phytoplankton in the Atlantic Ocean, *Deep Sea Research Part II: Topical Studies in Oceanography*, *53*, 1516.

Teira, E., P. Lebaron, H. van Aken, and G. J. Herndl (2006a), Distribution and activity of Bacteria and Archaea in the deep water masses of the North Atlantic, *Limnology and Oceanography*, *51*, 2131-2144.

Teira, E., T. Reinthaler, A. Pernthaler, J. Pernthaler, and G. J. Herndl (2004), Combining catalyzed reporter deposition-fluorescence in situ hybridization and microautoradiography to detect substrate utilization by bacteria and archaea in the deep ocean, *Applied and Environmental Microbiology*, *70*, 4411-4414.

Teira, E., H. van Aken, C. Veth, and G. J. Herndl (2006b), Archaeal uptake of enantiomeric amino acids in the meso- and bathypelagic waters of the North Atlantic, *Limnology and Oceanography*, *51*, 60-69.

Thamdrup, B., and T. Dalsgaard (2002), Production of N-2 through anaerobic ammonium oxidation coupled to nitrate reduction in marine sediments, *Applied and Environmental Microbiology*, *68*, 1312-1318.

Thompson, P. A., M. E. Levasseur, and P. J. Harrison (1989), Light-Limited Growth on Ammonium Vs Nitrate - What Is the Advantage for Marine-Phytoplankton, *Limnology and Oceanography*, *34*, 1014-1024.

Tsugita, A., T. Uchida, H. W. Mewes, and T. Ataka (1987), A Rapid Vapor-Phase Acid (Hydrochloric-Acid and Trifluoroacetic-Acid) Hydrolysis of Peptide and Protein, *Journal of Biochemistry*, *102*, 1593-1597.

Tyrrell, T. (1999), The relative influences of nitrogen and phosphorus on oceanic primary production, *Nature*, *400*, 525-531.

Tyrrell, T., E. Maranon, A. J. Poulton, A. R. Bowie, D. S. Harbour, and E. M. S. Woodward (2003), Large-scale latitudinal distribution of Trichodesmium spp. in the Atlantic Ocean, *Journal of Plankton Research, 25*, 405-416.

Vandegraaf, A. A., A. Mulder, P. Debruijn, M. S. M. Jetten, L. A. Robertson, and J. G. Kuenen (1995), Anaerobic Oxidation of Ammonium Is a Biologically Mediated Process, *Applied and Environmental Microbiology, 61*, 1246-1251.

Villareal, T. A., and E. J. Carpenter (1989), Nitrogen fixation, suspension characteristics, and chemical composition of Rhizosolenia mats in the central North Pacific gyre. , *Biological Oceanography 6*, 387-405.

Voss, M., M. A. Altabet, and B. v. Bodungen (1996), $\delta^{15}N$ in sedimenting particles as indicator of euphotic zone processes, *Deep-Sea Research I, 43*, 33-46.

Wakeham, S. G., and C. Lee (1989), Organic Geochemistry of Particulate Matter in the Ocean - the Role of Particles in Oceanic Sedimentary Cycles, *Organic Geochemistry, 14*, 83-96.

Wankel, S. D., C. Kendall, J. T. Pennington, F. P. Chavez, and A. Paytan (2007), Nitrification in the euphotic zone as evidenced by nitrate dual isotopic composition: Observations from Monterey Bay, California, *Global Biogeochemical Cycles, 21*.

Ward, B. B., K. A. Kilpatrick, E. H. Renger, and R. W. Epply (1989), Biological nitrogen cycling in the nitracline, *Limnology and Oceanography, 34*, 493-513.

Waser, N. A. D., W. G. Harrison, E. J. H. Head, B. Nielsen, V. A. Lutz, and S. A. Calvert (2000), Geographic variations in the nitrogen isotope composition of surface particulate nitrogen and new production across the North Atlantic Ocean, *Deep-Sea Research I, 47*, 1207-1226.

Wells, L. E., M. Cordray, S. Bowerman, L. A. Miller, W. F. Vincent, and J. W. Deming (2006), Archaea in particle-rich waters of the Beaufort Shelf and Franklin Bay, Canadian Arctic: Clues to an allochthonous origin?, *Limnology and Oceanography, 51*, 47-59.

Welschmeyer, N. A. (1994), Fluorometric Analysis Of Chlorophyll-A In The Presence Of Chlorophyll-B And Pheopigments, *Limnology And Oceanography, 39*, 1985-1992.

Williams, P. J. L. (1998), The balance of plankton respiration and photosynthesis in the open oceans, *Nature, 394*, 55-57.

Williams, R. G., and M. J. Follows (1998), The Ekman transfer of nutrients and maintenance of new production over the North Atlantic, *Deep-Sea Research I, 45*, 461-489.

Williams, R. G., and M. J. Follows (2003), Physical Transport of Nutrients and the Maintenance of Biological Production, *In: Ocean Biogeochemistry: the role of the ocean carbon cycle in global change. Edited by M. Fasham. Springer.*

Woese, C. R., O. Kandler, and M. L. Wheelis (1990), Towards a Natural System of Organisms - Proposal for the Domains Archaea, Bacteria, and Eucarya, *Proceedings of the National Academy of Sciences of the United States of America, 87*, 4576-4579.

Woodward, E. M. S., and A. P. Rees (2001), Nutrient Distributions in an anticyclonic gyre in the northeast Atlantic Ocean, with reference to nanomolar ammonium concentrations, *Deep Sea Research II*, *48*, 775-793.

Wu, J., W. Sunda, E. A. Boyle, and D. M. Karl (2000), Phosphate depletion in the western North Atlantic Ocean, *Science*, *289*, 759-762.

Yamashita, Y., and E. Tanoue (2003), Distribution and alteration of amino acids in bulk DOM along a transect from bay to oceanic waters, *Marine Chemistry*, *82*, 145-160.

Yool, A., A. P. Martin, C. Fernandez, and D. R. Clark (2007), The significance of nitrification for oceanic new production, *Nature*, *447*, 999-1002.

Zehr, J. P., M. T. Mellon, and S. Zani (1998), New nitrogen fixing microorganisms detected in oligotrophic oceans by amplification of nitrogenase (*nifH*) genes, *Applied and Environmental Microbiology*, *64*, 3444-3450.

Zehr, J. P., and B. B. Ward (2002), Nitrogen cycling in the ocean: New perspectives on processes and paradigms, *Applied and Environmental Microbiology*, *68*, 1015-1024.

Zehr, J. P., J. B. Waterbury, P. J. Turner, J. P. Montoya, E. Omoregie, G. F. Steward, A. Hansen, and D. M. Karl (2001), Unicellular cyanobacteria fix N_2 in the subtropical North Pacific Ocean, *Nature*, *412*, 635-638.

APPENDIX A

The three scientific objectives of the AMT programme with the corresponding hypotheses

Objective One

To determine how the structure, functional properties and trophic status of the major planktonic ecosystems vary in space and time.

Hypothesis 1*: The size spectra, and mineralisation capacity of planktonic organisms are major determinants of CO2 and organic matter export to the atmosphere and deep water.*

Hypothesis 2: *Growth rates of phytoplankton in tropical and subtropical waters are correlated with the* f *ratio and, for the surface layer, with the relative contribution of nanophytoplankton.*

Hypothesis 3: *The biodiversity of the microbial planktonic community significantly influences C, N and P recycling and ecosystem trophic state.*

Hypothesis 4: *Basin scale variability in photosynthetic growth rates and pCO_2 flux can be derived from remotely sensed data.*

Objective Two

To determine the role of physical processes in controlling the rates of nutrient supply, including DOM, to the planktonic ecosystem.

Hypothesis 5: *Net heterotrophy and export production in the subtropical gyre are partly sustained by lateral inputs of dissolved organic nutrients from neighbouring upwelling regions.*

Hypothesis 6: *Interannual variations in the nutrient supply to the euphotic zone of the N and S Atlantic sub-tropical gyres are related to atmospheric-induced changes in convection and gyre-scale circulation.*

Objective 3

To determine the role of atmosphere-ocean exchange and photo-degradation in the formation and fate of organic matter.

Hypothesis 7: *Spatial variability in atmospheric deposition over the N and S Atlantic sub-tropical gyres leads to significant variations in the relative importance of N and P as limiting nutrients and leads to short term imbalances in the assimilation of C and N by phytoplankton.*

Hypothesis 8: *pCO_2 and trace gas exchange are a function of phytoplankton community structure and biomass and significantly influence aerosol formation over the remote oceans.*

Hypothesis 9: *Absorbance bleaching is the major control of DOM degradation and photoreactivity, and significantly influences plankton community structure, the recycling and export of organic matter and photochemical trace gas production and removal.*

APPENDIX B

SAP stations for AMT12, 14 & 16

Latitude	Longitude	Depth (m)	$\delta^{15}N$ PON_{susp}
43.1249°S	45.1925°W	50	5.61
		150	7.51
31.4711°S	29.4256°W	50	0.16
		100	-0.14
		150	4.64
13.5557°S	24.5985°W	50	2.90
		100	2.82
		150	5.13
2.1416°S	24.5994°W	50	4.55
		100	4.50
12.1406°N	32.1717°W	50	0.08
		100	3.81
24.1972°N	32.3442°W	50	-1.38
		150	1.01
36.4415°N	20.4884°W	50	2.48
		100	0.91
		150	3.65

Table B1 SAP stations and corresponding $\delta^{15}N$ PON_{susp} for AMT12

Latitude	Longitude	Depth (m)	$\delta^{15}N$ PON_{susp}
41.2000°S	41.3300°W	50	5.10
32.5900°S	31.1000°W	50	-1.25
		100	1.27
		150	2.49
12.1655°S	24.5966°W	50	2.68
		150	3.88
0.0560°S	24.5987°W	50	2.62
		150	4.82
11.2403°N	29.2207°W	50	1.30
		150	5.02
22.1991°N	33.4410°W	50	-1.04
		100	-1.69
		150	0.27
29.1827°N	36.4184°W	50	0.28
		100	0.35
38.3998°N	19.5763°W	50	6.07
48.5999°N	16.2368°W	50	-0.83
		100	0.25

Table B2 SAP stations and corresponding $\delta^{15}N$ PON_{susp} for AMT14

Latitude	Longitude	Depth (m)	$\delta^{15}N$ PON_{susp}
-27.3180°S	13.2657°W	50	3.69
		100	2.70
		150	4.00
-22.5281°S	25.0003°W	50	1.30
		150	2.84
-12.2479°S	24.5979°W	50	1.61
		150	5.09
-1.3762°S	24.5966°W	50	3.81
		150	5.10
7.1494°N	28.2726°W	50	-0.21
		100	3.13
15.4775°N	32.3610°W	50	-0.41
		100	-0.40
		150	2.92
22.4833°N	36.0985°W	50	-0.62
		100	1.01
		150	3.31
29.0948°N	39.3253°W	50	-0.50
		100	-0.72
		150	0.54
31.2299°N	42.0865°W	50	-0.84
		100	-0.09
		150	0.97
33.3468°N	45.3240°W	50	0.81
		100	1.74
		150	4.71
34.5717°N	42.3357°W	50	1.10
		100	2.22
		150	4.06
37.2092°N	33.3963°W	50	2.99
		100	3.31
		150	5.32
44.4411°N	22.5240°W	50	4.37
		100	4.86
		150	4.28

Table B3 SAP stations and corresponding $\delta^{15}N$ PON_{susp} for AMT16

APPENDIX C

Structures of amino acids analysed in this study

ALANINE

Formula: $C_3H_7NO_2$

Molecular weight: **89.1**

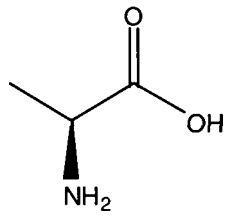

ASPARGININE

Formula: $C_6H_{14}N_4O_2$

Molecular weight: **174.2**

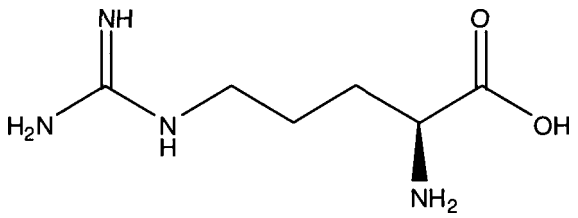

ASPARTIC ACID

Formula: $C_4H_7NO_0$

Molecular weight: **133.10**

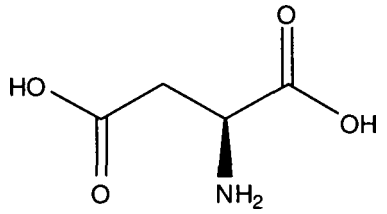

GLUTAMIC ACID

Formula: $C_5H_9NO_4$

Molecular weight: **147.13**

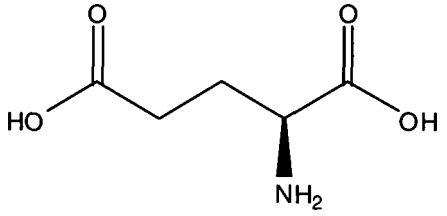

GLYCINE

Formula: $C_2H_5NO_2$

Molecular weight: **75.07**

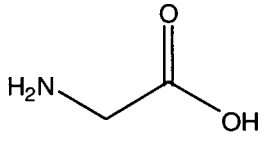

ISOLEUCINE

Formula: $C_6H_{13}NO_2$

Molecular weight: **131.18**

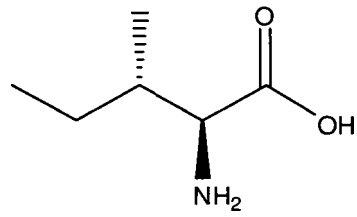

LEUCINE

Formula: $C_6H_{13}NO_2$

Molecular weight: 131.18

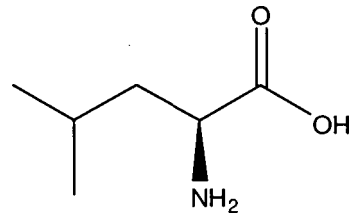

METHIONINE

Formula: $C_5H_{11}NO_2S$

Molecular weight: **149.21**

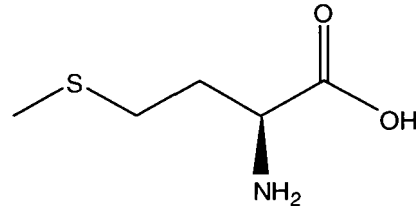

PHENYLALANINE

Formula: $C_9H_{11}NO_2$

Molecular weight: **165.19**

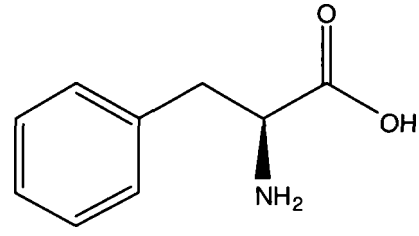

SERINE

Formula: $C_3H_7NO_3$

Molecular weight: **105.09**

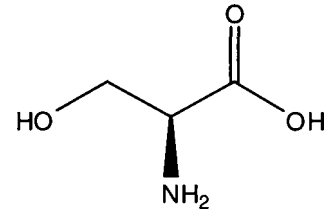

THREONINE

Formula: $C_4H_9NO_3$

Molecular weight: **119.12**

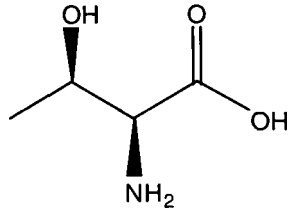

VALINE

Formula: $C_5H_{11}NO_2$

Molecular weight: 117.15

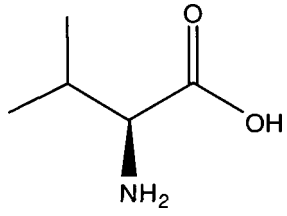

L-HOMOARGININE (non-protein; internal standard)

Formula: $C_7H_{16}N_4O_2$

Molecular weight: **188.23**

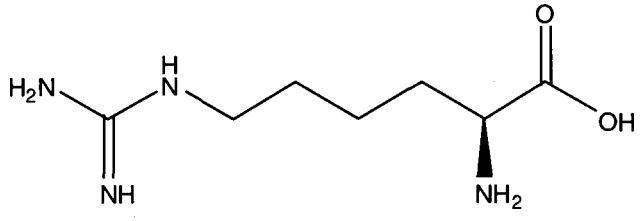

APPENDIX D

Response factors for amino acids

Amino acid	Response Factor
L-Asparctic Acid	1.13596
D-Asparctic Acid	1.18417
L-Glutamic Acid	1.13752
D-Glutamic Acid	1.12158
L-Serine	1.24810
D-Serine	1.39356
L-Threonine	1.19010
Glycine	1.60418
L-Arginine	1.36417
D-Arginine	1.20010
L-Alanine	1.41778
D-Alanine	1.58993
L-Valine	1.32355
L-Methionine	1.15487
D-Methionine	1.30142
D-Valine	1.48670
L-Phenylalanine	1.00690
D-Phenylalanine	1.28832
L-Isoleucine	1.39386
L-Leucine	1.03303
D-Isoleucine	1.28456
D-Leucine	1.13118

Table D1 Typical response factors for amino acids.

APPENDIX E

Latitudinal sections of phosphate concentrations for AMT12, 14 & 16

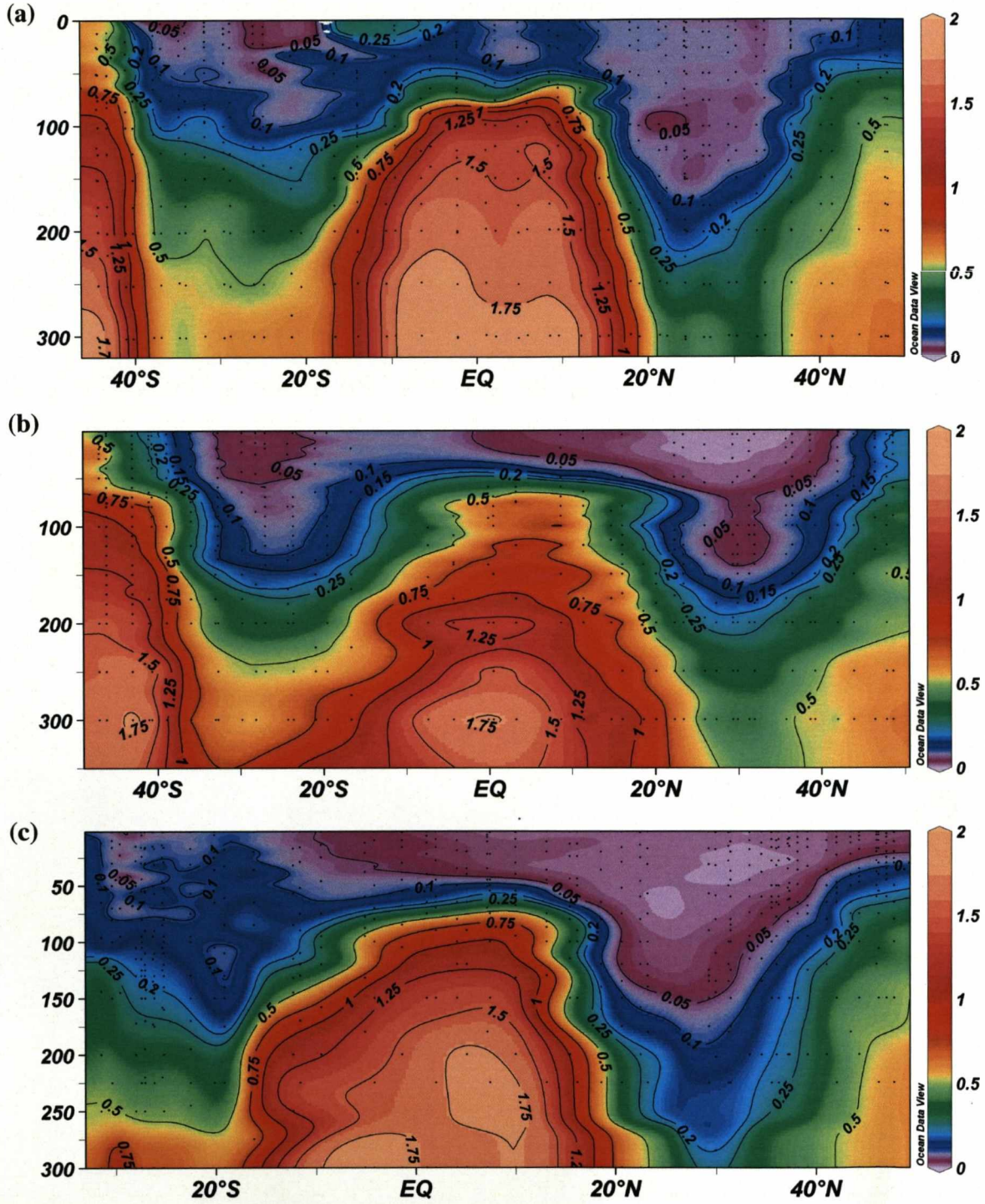

Figure E1 Phosphate concentrations (μM) for (a) AMT12, (b) AMT14 and (c) AMT16. Sections show lower concentrations in the northern gyre compared with the southern gyre, probably due to N_2 fixation driving down levels in the northern gyre.

APPENDIX F

Enzyme activities in surface waters along the AMT16 transect

Determining ecto-enzyme activities in an attempt to obtain an estimate in the turnover rate of labile organic nitrogen and phosphorus compounds

F1 Introduction

Dissolved organic species make up a large proportion of the marine nitrogen and phosphorus pools; they are heterogeneous mixtures of compounds including biologically labile moieties, which likely turn over from days to hours and refractory components, which persist for months to thousands of years [*Bronk*, 2002]. Examples of identified organic nitrogen compounds include urea, amino acids, proteins and nucleic acids [*Berman and Bronk*, 2003]. Organic P fractions include primarily monomeric and polymeric phosphate esters (C-O-P bonded compounds), phosphonates (C-P compounds) and organic condensed phosphates [*Karl and Bjorkman*, 2002]. There is evidence that when inorganic nutrients are limiting the system dissolved organic nitrogen and phosphorus compounds can be a direct or indirect sources of nutrient to marine microorganisms [*Berman and Chava*, 1999; *Bjorkman and Karl*, 2003; *Jackson and Williams*, 1985].

The mechanisms responsible for the release of nitrogen and phosphorus from organic matter for use by phytoplankton are poorly understood [*Panosso and Graneli*, 2000], however the importance of cell-surface enzymes or cell-surface catalysed mechanisms are now being recognised [*Palenik and Morel*, 1990b] . Extracellular enzymes hydrolyse peptide or ester bonds within the organic matter to release the organically bound nitrogen or phosphate (respectively), providing essential nutrients required for growth.

Following methods described by Hoppe (1993), overall extracellular enzyme activities can be determined by utilising fluorogenic model substrates. These model substrates (i) contain an artificial fluorescent molecule and one or more natural molecules (e.g. amino acids), linked by a specific binding site (e.g. peptide bond); (ii) fluorescence is observed after enzymatic splitting of the complex molecule (Fig G1); (iii) hydrolysis of model substrates follows first order enzyme kinetics; and (iv) application of those model substrates allows enzyme activity measurements under natural (*in situ*) conditions within short incubation periods [*Hoppe*, 1993]. Rate kinetics can be applied the data obtained from incubation experiments to determine the rate of catalysis of the fluorogenic compounds. Michaelis-Menten kinetics demonstrates that the rate of catalysis is directly proportional to substrate concentration [*Stryer*, 1995]. The Michaelis-Menten constant (K_M) can be utilized to provide an estimate of the turnover rate of the labile component of dissolved organic nitrogen and phosphorus.

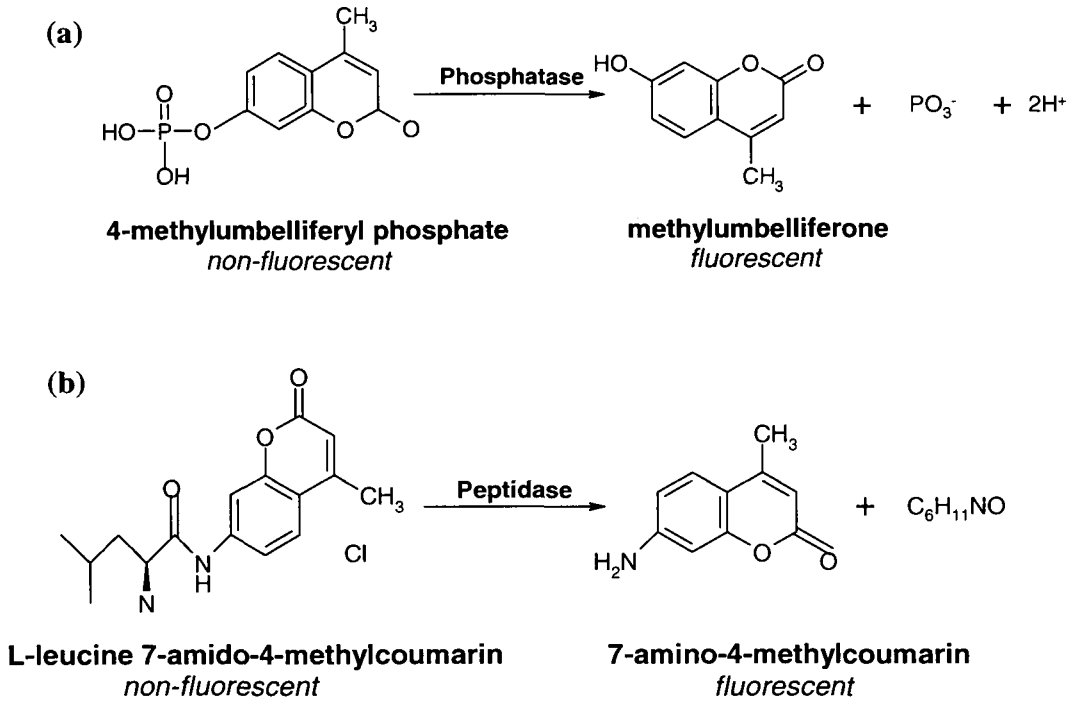

Figure G1 Structures and reactions of (a) 4-methylumbelliferyl phosphate which fluoresces once undergone hydrolysis by the enzyme phosphatase; (b) L-leucine 7 amido-4-methylcoumarine which fluoresces once undergone hydrolysis by the enzyme amino peptidase.

F 2 Methodology

To determine the leucine aminopeptidase and alkaline phosphatase activities in seawater the fluorogenic substrates L-leucine-7-amido-methylcoumarin hydrochloride (Leu-AMC) and 4-methylumbelliferyl phosphate (4-MUP) were employed respectively following a method described by [*Hoppe*, 1993]. Seawater was sampled from surface waters off the pre-dawn casts on AMT16 into a 1 L Pyrex bottle (pre cleaned in a 10% HCl acid bath and rinsed three times in milli-q water). Briefly seawater was inoculated with the respective fluorogenic substrates to give resultant concentrations of 100, 200, 400, 500 and 750 μM in 10 mL. The initial fluorescence was measured (T_0) using a

Turner Designs TD-700 Laboratory Fluorometer and then incubated at 16°C for 48 hours in the dark, after which the fluorescence was re-measured (T_1).

To convert the observed change in fluorescence into a rate of hydrolyses a calibration was conducted using the flourophores of the fluorogenic substrates. For Leu-AMC, 7-amino-4-methylcoumarin (AMC) was used and 4-methylumbelliferone (MUF) was used for 4-MUP using a range of concentrations between 0.5 and 300 μM.

Michaelis-Menten kinetics were applied to the data to gain the V_{max} which corresponds to the maximum turnover i.e. when the catalytic sites on the enzyme are saturated with substrate.

F 3 Results

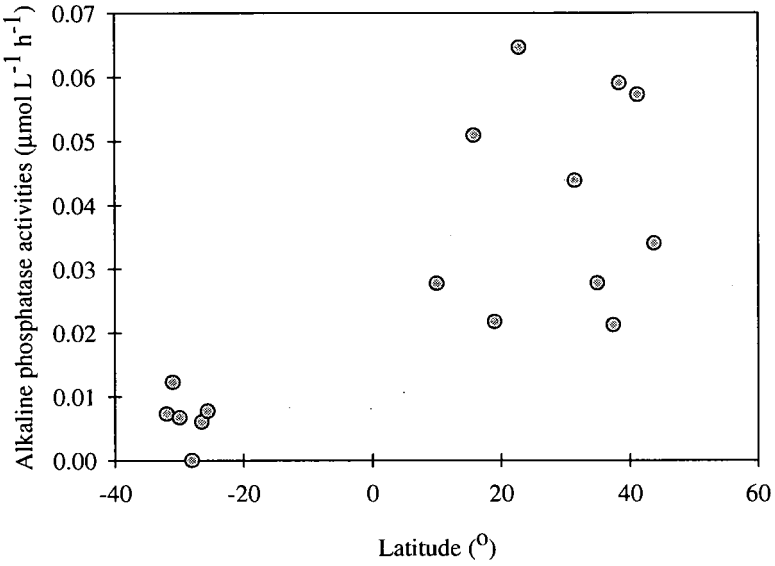

Figure F1 Alkaline phosphatase activites in surface waters along the AMT16 transect.

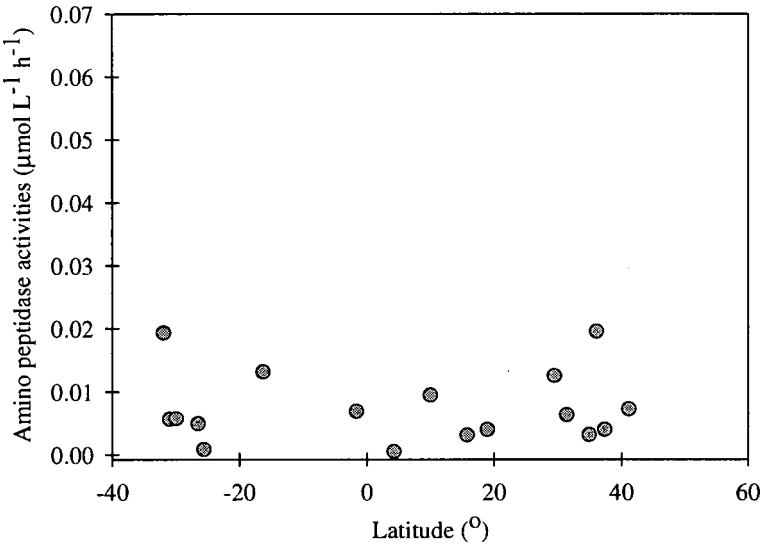

Figure F2 Leucine amino peptidase activities in surface waters along the AMT16 transect.

Higher phosphatase activities are observed in the northern gyre which coincide with the region of N_2 fixation as inferred from stable N isotopes (see Chapter 3). Much lower turnover rates are observed for the labile DON compared with the labile DOP.

APPENDIX G

Lipid Analysis of suspended particulate organic matter along the AMT16 transect

G 1 Phospholipid methodology

G 1.1 Sampling protocol

Suspended particulate organic matter samples for phospholipid analysis were collected using Stand Alone Pumps (SAPs; Challenger Oceanic) on AMT16 (see Chapter 2 for cruise details and Fig. 2.02 for cruise track).Two GF/F filters (293 mm diameter; Whatman; pre-combusted at 400°C, >4 hours) were placed on the filter bed with the top filter being used for the analysis. The SAPs were deployed to depths of 50, 100 and 150 m and pumped ~1000 L seawater in 90 minutes. The filters were removed and wrapped in pre-combusted (400°C >4 hours) aluminium foil and frozen (-20°C) until further analysis in the laboratory. Prior to analysis, filters were lypholised (-60°C; 10^{-2} Torr, 24 h).

G 1.2 Determination of POC

Concentrations of particulate organic carbon (POC) collected on the GF/F filters were determined as described by Kiriakoulakis et al [2004]. This was to ensure a sufficient quantity of filter was extracted and enable accurate quantification. Briefly, analyses of freeze-dried SAPS filters were carried out in duplicate (analytical error < 10 %; CEInstruments NC 2500 CHN analyser), on aliquots of known area (~130 mm^2), using the HCl vapour method of Yamamuro and Keyanne [1995].

G 1.3 Procedure for lipid analysis

G 1.3.1Preparation of glassware

Unless otherwise stated all glassware used for the lipid analysis was prepared by soaking in 10% Decon 90 overnight, rinsed thoroughly with tap water followed by rinsing with copious amounts of fresh milli-q water. The glassware was then wrapped in aluminium foil and placed into a drying oven (~100°C) overnight and then pre-combusted at 400°C for no less than four hours.

G 1.3.2Extraction

From each filter, four aliquots (314 mm^2) were cut using an aluminium puncher (rinsed with DCM). Using clean scissors (rinsed with DCM) the aliquots of filter were cut into smaller pieces and placed into a glass centrifuge tube. 25 μL additions of internal standards cholestane (100 ng/g) and cholanic acid (100 ng/g) were made (final mass of 2500 ng). 4 ml of methanol (MeOH; HiPerSolv; redistilled), 2 ml dichloromethane (DCM; HiPerSolv; redistilled) and 1.6 ml phosphate buffer (AnalaR; pH adjusted to 7.4 with 1 M HCl) were added to the centrifuge tube. This gave a final ratio of MeOH:DCM:phosphate buffer of 2:1:0.8). The centrifuge tube containing the POM sample and solvent mixture was sonicated for 30 minutes. A further 2 ml of DCM and 2 ml phosphate buffer was added to the centrifuge tube to give a final ratio of MeOH:DCM:phosphate buffer of 1:1:09). This mixture was centrifuged for 5 minutes (2500 rpm; 15°C) and the upper aqueous fraction was removed using a glass Pasteur pipette (pre-combusted; 400°C > 4 hours) and discarded. The lower organic fraction was

transferred to a 25 ml round bottom flask and the solvent was removed under vacuum (35°C). The sample was re-dissolved in a small amount of DCM and transferred to a 7 ml glass vial (pre-combusted; 400°C >4 hours). The DCM was removed under a stream of N_2 gas and a further 1 ml of DCM was added and subsequently removed under N_2 gas. This was repeated once more.

A 230mm Pasteur pipette was plugged with cotton wool (24 hour Soxhlet extracted, DCM:MeOH 9:1) and filled with sodium sulphate (24 hour Soxhlet extracted, DCM:MeOH 9:1) which was rinsed through with a few ml of DCM. The extract was re-dissolved in ~0.5 ml of DCM and transferred to the prepared pipette, followed by a 1 ml addition of DCM. The extract and DCM was collected into a 2ml glass vial (pre-combusted; 400°C >4 hours) whereby the DCM was subsequently removed under a stream of N_2 gas.

G 1.3.3Fractionation

Fractionation of the extracted samples was carried out on Varian bonded phase aminopropyl SPE cartridges (500 mg; 6 ml). Cartridges were placed into a CEREX Varian SPE processor and washed with 4 ml hexane, where the vacuum was immediately released once the hexane had passed through to ensure that the cartridges did not dry out. The extracted sample was re-dissolved in 200 µL of DCM and transferred to the cartridge whereby sufficient pressure was applied to pull the sample through. Glass collection tubes were placed into the processor underneath the cartridges which were firstly eluted under pressure with 4 ml of a 2:1 DCM to isopropanol (IPA) mixture. This first elution is the neutral lipid fraction. The second elution which

involved an addition of 4 ml of diethyl ether with 2% acetic acid to the cartridges is the fatty acid fraction which was collected separately into new collection tubes. The third and final fraction, phospholipids, is eluted with 100% MeOH and was also collected in new collection tubes. The solvent was removed from all fractions under a stream of N_2 gas. All fractions were then dissolved in a small amount of DCM. The neutral lipid fraction (fraction 1) was transferred to a 2 ml glass vial; the DCM was removed under N_2 gas and was stored at -20°C until further analysis. The fatty acid (fraction 2) and the phospholipid fraction (fraction 3) were transferred to 5 ml reaction vials and the DCM was removed under a stream of N_2 gas.

G 1.3.4Trans-methylation

Trans-methylation was only applied to the fatty acid and the phospholipid fraction. 10 ml of MeOH was cooled in an ice bath for 20 minutes. Once cooled, 300 µL of acetyl chloride was added to the MeOH drop wise. ~1 ml of this solution was then added to the fatty acid and phospholipid fraction in the reaction vials. The vial were sealed with Teflon seal and cap and placed on a heating block at 40°C overnight.

All solvent was removed from the sample fractions under N_2 gas and were subsequently rinsed with DCM by making ~1 ml additions of DCM which was then dried under N_2 gas. This was repeated at least four times to ensure all methananolic acetyl chloride was removed.

In order to clean up any contaminants that may be present in the acetyl chloride the now trans-methylated fractions, Pasteur pipettes were prepared with a plug of cotton wool, filled with potassium carbonate and rinsed with a few ml of DCM. The fractions

of sample were transferred to the prepared pipettes in a small amount of DCM by which a further 1 ml of DCM was added to the pipette. The sample and DCM were collected in a 2 ml glass vial; the solvent was removed under N_2 gas and stored at -20°C until further analysis.

G 1.3.5Derivatisation

Prior to analysis of all the fractions using gas chromatography – mass spectrometry (GCMS), 50 µL of *bis*-trimethylsilyltrifluoroacetamide (BSTFA) was added to the fractions and heated at 40°C for 45 minutes. The BSTFA was removed under N_2 gas.

G 1.3.6Analysis of lipid by Gas Chromatography-mass spectrometry (GCMS)

The derivatised samples were analysed using a Trace 2000 series gas chromatograph equipped with an on-column injector and a fused high temperature silica column (60m x 0.25mm i.d.; 5% phenyl/95% methyl polysiloxane equivalent phase, 0.1 µm film thickness, DB5-HT, J & W; carrier gas helium at 1.6 mL min^{-1}). The column was fed directly into the EI source of a Thermoquest Finnigan TSQ700 MS and data was process using the software Xcaliber. Please see [*Kiriakoulakis, et al.*, 2004] for further details.

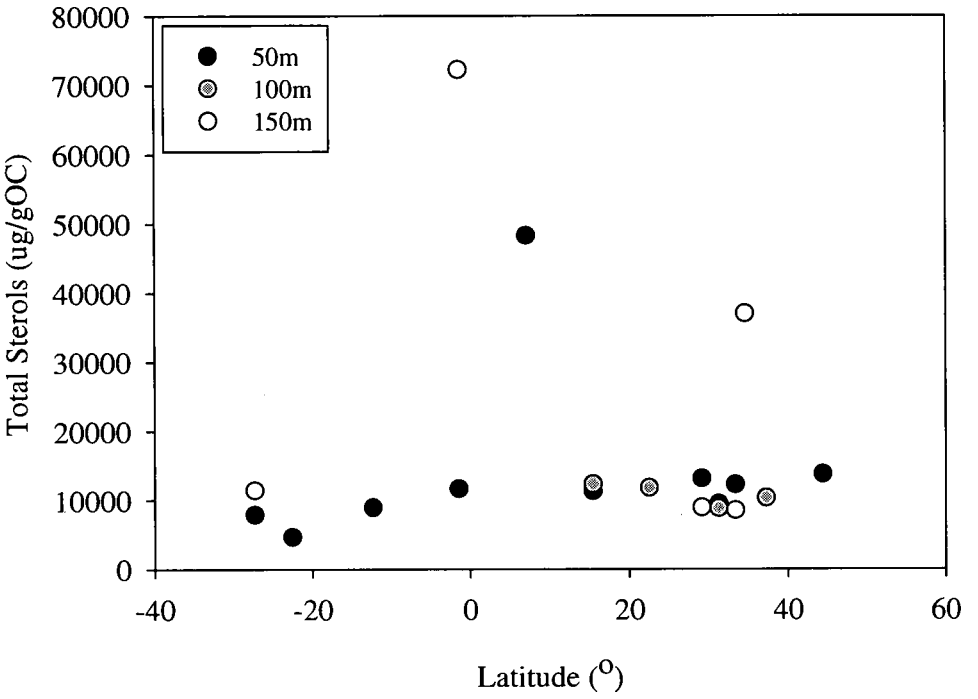

Figure G1 Latitudinal section of total sterols (ug/g organic carbon) along the AMT16 transect at depths of 50m, 100m and 150m.

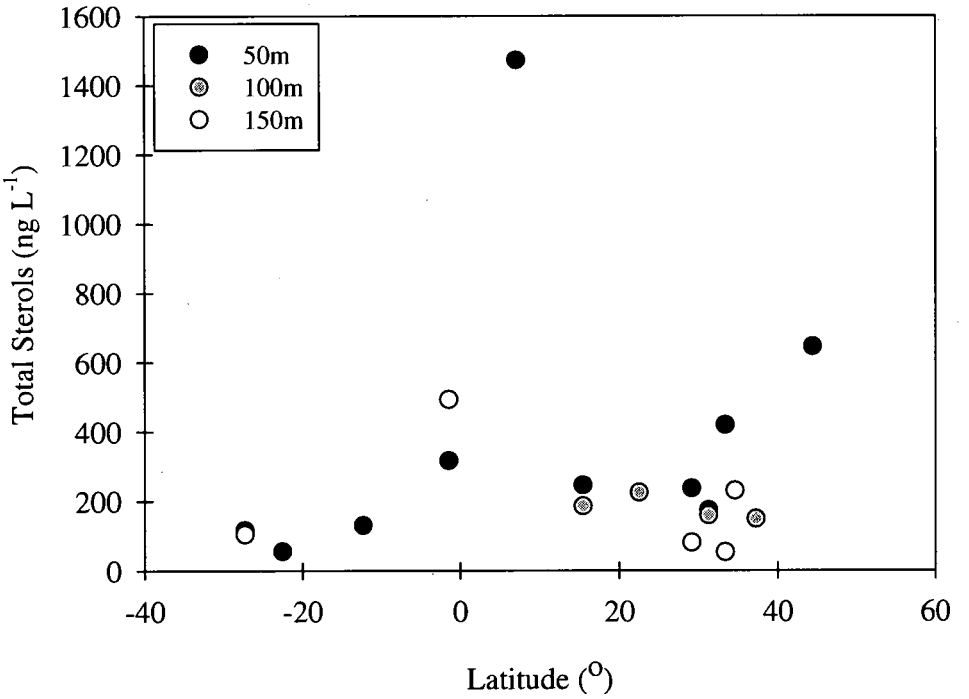

Figure G2 Latitudinal section of total sterols (ng/L) along the AMT16 transect at depths of 50m, 100m and 150m.

APPENDIX H

Total organic phosphate concentrations for AMT16

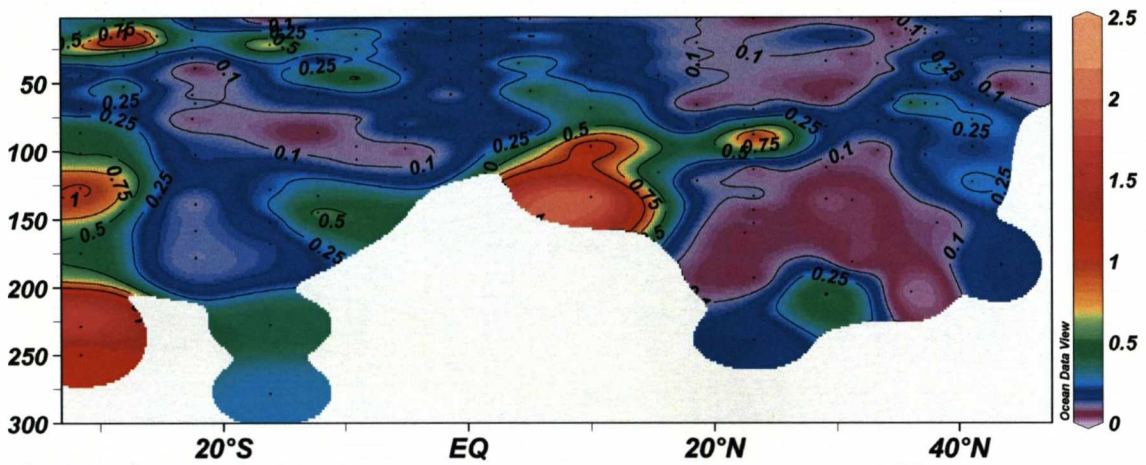

Figure H1 Total Organic Phosphate (TOP) concentrations along the AMT16 transect. For details of analysis see [*Sanders and Jickells*, 2000].